MOVEMENT BEHAVIOR OF WILD BOAR WITHIN THE FUKUSHIMA EXCLUSION ZONE AND CONSEQUENCES FOR RADIATION EXPOSURE ASSESSMENTS

by

HELEN LOUISE BONTRAGER

(Under the Direction of James Beasley)

ABSTRACT

Understanding the impacts of contamination events on wildlife is important for both remediation efforts and the generation of risk assessments. In this thesis, I used GPS and dosimetry data collected for wild boar (*Sus scrofa leucomystax*) living in and around the Fukushima Exclusion Zone (FEZ) to study the impact of the Fukushima Dai-ichi accident on the movement behavior and radiation exposure of wildlife. I found wild boar within the FEZ were more diurnal compared to those outside the zone and they utilized abandoned anthropogenic areas in addition to natural areas. I also found methods of estimating contaminant exposure using conservative inputs (i.e., assumed maximal exposures) consistently generated conservative estimates whereas methods incorporating finer-scale contaminant surveys and animal movement data produced the most realistic estimates. Collectively, my results contribute to our understanding of the impacts of nuclear accidents on wildlife and provide improved guidelines for conducting risk assessments in these areas.

INDEX WORDS: Wild Boar, Radioactive, Contamination, Risk assessment, Resource Selection, Human-wildlife conflict, Radiation

MOVEMENT BEHAVIOR OF WILD BOAR WITHIN THE FUKUSHIMA EXCLUSION ZONE AND CONSEQUENCES FOR RADIATION EXPOSURE ASSESSMENTS

by

HELEN BONTRAGER

B.S., The University of Kansas, 2017

A Thesis Submitted to the Graduate Faculty of The University of Georgia in Partial Fulfillment of the Requirements for the Degree

MASTER OF SCIENCE

ATHENS, GEORGIA

2023

MOVEMENT BEHAVIOR OF WILD BOAR WITHIN THE FUKUSHIMA EXCLUSION ZONE AND CONSEQUENCES FOR RADIATION EXPOSURE ASSESSMENTS

by

HELEN LOUISE BONTRAGER

Major Professor:	James Beasley
Committee:	Jeffrey Hepinstall-Cymerman
	George Wittemyer

Electronic Version Approved:

Ron Walcott
Vice Provost for Graduate Education and Dean of the Graduate School
The University of Georgia
May 2023

ACKNOWLEDGEMENTS

This thesis was only made possible by the combined effort of many different people.

To start, I have to acknowledge my advisor Jim Beasley. Not only has he provided me with the chance to explore and analyze interesting questions, but he has also been a constant source of support throughout my master's. He is one of the main reasons for me finishing this thesis and I cannot adequately express my gratitude for his help, guidance, and patience. Thank you so much Jim, I know that my master's was more than a little bumpy, and I am so grateful that you were my advisor throughout it.

This master's thesis made use of previously collected boar tracking data. Therefore, I would like to thank all of those involved with collecting the movement data used throughout this thesis. This includes, but is not limited to, T. Hinton, K. Okuda, Uno, D. Anderson, S. Chinn, K. Cunningham, J. Hayes, H. Ishiniwa, M. LiPuma, H. Nagata, Y. Nemoto, S. Pederson, members of Japanese hunting associations, and various towns who gave permission to conduct research.

I would like to give a special thanks to Tom Hinton. I knew virtually nothing about radioecology when I started my master's. This thesis would not have been possible without your willingness to share and discuss your expertise. Thank you for providing useful insight, especially for chapter 3.

Finally, I want to thank my family for their love and support. Love you lots.

TABLE OF CONTENTS

Page

LIST OF TABLES

Page

LIST OF FIGURES

Page

CHAPTER 1

INTRODUCTION & LITERATURE REVIEW

Like many other forms of pollution, radioactive contamination has the potential to be harmful to wildlife. The consequences of radioactive pollution can transcend biological scales, from molecular impacts to ecosystem level changes (IAEA 2001, Hinton et al. 2007). Molecularly, ionizing radiation can lead to oxidation of DNA and other bio-molecules like proteins and lipids (Reisz et al. 2014). At higher doses, the resulting damage can lead to reduced fitness or even death (Arkhipov et al. 1994, Whicker 1997, Ellegren et al. 1997, Hinton et al. 2007). Provided enough radiation, entire groups of radiosensitive individuals may be directly impacted (IAEA 1992, Arkhipov et al. 1994, Hinton et al. 2007). This impact may then indirectly propagate to non-radiosensitive species to have broader community or ecosystem-level impacts. For example, in the months following the Chernobyl disaster, entire patches of radiosensitive pine trees in the Red Forest died after receiving large doses of radiation (Arkhipov et al. 1994) and the area has subsequently undergone a community shift to favor less sensitive species (Geras'kin 2016).

Deciding which biological scale (i.e., molecular, individual, population, or ecosystem) to use when assessing impacts following a contamination event is important because it can change our viewpoint of how harmful the event was. This is especially true because impacts at finer biological scales (e.g., DNA mutations) may be effectively neutral in impact at coarser (e.g., population) scales (Ohta 1992, Loewe and Hill 2010). Typically, when concerned with human exposure, one focuses on the potential harm to an individual (i.e., counts of cancers or other

health effects; Lei et al. 2015). However, for wildlife, managers are often most concerned with maintaining viable populations rather than individual health (ICRP 1977, DOE 2019). Historically, it was assumed that: “the level of safety required for protection of all human individuals is thought likely to be adequate to protect other species, although not necessarily individual members of those species” (ICRP 1977). However, this statement assumes that humans and wildlife inhabit the same area and ingest, or otherwise come into contact to, contaminants in identical ways (DOE 2019). Thus, this statement is inadequate in protecting wildlife inhabiting contaminated environments in which human access is controlled (DOE 2019). An example of such a scenario is the formation of exclusion zones following the Chernobyl and the Fukushima nuclear disasters, where humans were evacuated but wildlife was allowed to persist.

In 2011, following a large earthquake and tsunami, reactors at the Fukushima Dai-ichi Nuclear Power Plant (FDNPP) melted down and released large amounts of radionuclides onto the surrounding environment (Tanaka 2012). This radioactive fallout resulted in the evacuation of approximately 164,000 humans from a 1,150 km^2 area referred to as the Fukushima Exclusion Zone (FEZ) (Ministry of the Environment 2018, Do 2019). Once the reactors were stabilized, a massive decontamination effort was undertaken (Ministry of the Environment 2018). Following these remediation efforts and due to the natural decay of radionuclides deposited on the landscape, radiation levels have since fallen (Ministry of the Environment 2018). Beginning in 2016, some areas of the FEZ were reopened to human settlement, but only some of the residents have returned (Ministry of the Environment 2018, Do 2019, Nagamatsu et al. 2020). However, a large portion of the FEZ to the northwest of the FDNPP remains restricted from human

resettlement (Ministry of the Environment 2018). At least for now, the FEZ has become a rewilding experiment, where wildlife live with minimal human contact (Lyons et al. 2020).

Current research on the health of wildlife within the FEZ, and analogous areas such as Chernobyl, is conflicting. In the weeks and months following the Chernobyl disaster, wildlife inhabiting areas near the plant were exposed to extremely high radiation exposure rates (~20 Gy/d; IAEA 2001). Several studies have reported negative impacts from this radiation exposure: radiosensitive pine trees died in areas of highest radiation (Arkhipov et al. 1994) and barn swallows were reported to have a higher frequency of partial albinism and reduced fitness (Ellegren et al. 1997, Møller and Mousseau 2001). Similarly, some studies observed negative effects following the FDNPP disaster, including physical abnormalities in pale grass blue butterflies (*Zizeeria maha*) (Hiyama et al. 2012) and decreased reproduction among goshawks (*Accipiter gentilis fujiyamae*) (Murase et al. 2015). Still other studies were unable to find correlations between exposure and known markers of radiation exposure like frequency of dicentric chromosomes or telomere length (Cunningham et al. 2021), abnormal germ cell morphology or defective spermatogenesis (Yamashiro et al. 2013, 2015), or occurrence of cataracts (Pederson et al. 2020). Nonetheless, as time has passed and radiation levels have dropped, many species of wildlife within both Chernobyl and Fukushima seem to be thriving – with some research suggesting several wildlife species such as wild boar (*Sus scrofa leucomystax*), roe deer (*Capreolus capreolus*), and moose (*Alces alces*) have increased in population size in Fukushima or Chernobyl following the evacuation of humans (Deryabina et al. 2015, Lyons et al. 2020).

The debate about the true impacts of the Chernobyl and Fukushima disaster are made especially difficult by the questionable dosimetry that has been used in several studies reporting

negative effects (Strand et al. 2014, 2017). Many wildlife are highly mobile, and thus estimating exact radiation dose rates can be challenging or often impractical. As a result, many studies rely on simple metrics like air dose rate at the trap site (Møller and Mousseau 2009, Lehmann et al. 2016). However, due to the inability to track true exposure, these methods of estimating exposure have not been verified and may lead to spurious conclusions (Hinton et al. 2019). Further, it is questionable whether a simple metric could realistically capture the complexity of contaminant distribution and of an organism's interaction with and exposure to the contaminant.

The radioactive fallout following the FDNPP disaster included large quantities of Cesium-137 (^{137}Cs), Cesium-134 (^{134}Cs), and Iodine-131 (^{131}I), which were subsequently deposited onto the surrounding landscape and into the Pacific Ocean (Ministry of the Environment 2018). Researchers today often focus on ^{134}Cs and ^{137}Cs (Koarashi et al. 2012, Oshita 2013, Koizumi et al. 2013, Nakanishi et al. 2014, Suchara et al. 2016, Kurihara et al. 2018, Hayes et al. 2020, Nemoto et al. 2020) because, unlike ^{131}I, these radionuclides did not quickly decay after initial release due to their long half-lives (Povinec et al. 2013). This is especially true for ^{137}Cs whose half-life of 30.17 years means that instead of rapidly decaying, it has time to migrate through the system and be washed through canopy and vegetation layers into the litter layer, soil, and eventually, waterways (Onda et al. 2020). However, vertical migration through the soil is often slow, due in part to the fixation of Cesium cations to negatively charged clay minerals within the soil column (Sato et al. 2013, Fujii et al. 2014). The speed at which Cesium migrates through the landscape is also dependent on the landcover upon which it was deposited. For example, ^{137}Cs migrates downward faster through paddy fields than through forest soil columns (Takahashi et al. 2018, 2019, Onda et al. 2020).

The initial contaminant deposition combined with subsequent migration patterns have resulted in the landscape within the FEZ becoming a heterogeneous patchwork of radiation levels. Historically, it was acceptable to ignore the impact of fine-scale heterogeneity on external exposure in favor of using average contamination levels across the contaminated area because this was assumed to produce conservative (i.e., higher than actual) estimates for external exposure (USEPA 1996, DOE 2019). However, recent research has shown that these estimates are not always conservative and that fine-scale heterogeneity may play a bigger role than previously expected (Hinton et al. 2019). This fine-scale patchiness likely has biological consequences because small changes in an animal's location, direction, or speed across the landscape may significantly alter the amount of radiation an individual is exposed to. It is difficult, therefore, to accurately estimate radiation exposure without a good understanding of both the characteristic movement patterns of an organism and a fine-scale external radiation model of the areas in which they live. These estimates are made even more difficult by the possibility that wildlife may have shifted their home ranges and behaviors following the accident to select for previously unfavored areas, including areas formerly occupied by humans.

One species suspected of occupying abandoned anthropogenic areas in the FEZ is the Japanese wild boar (*Sus scrofa leucomystax*), which have been observed wandering down streets and into backyards within the FEZ (J. Beasley, personal communication, May 2020). Japanese wild boar are a subspecies of *S. scrofa* native to Japan and are distributed throughout Honshu, Shikoku, and Kyushu islands (Watanobe et al. 1999). *S. scrofa* are globally known to be opportunistic generalists (Schley and Roper 2003, Barrios-Garcia and Ballari 2012) and are a known nuisance species in Japan (Honda and Sugita 2007, 2007, Matsumura et al. 2019). Within the FEZ, wild boar have been used extensively as study organisms because their wide

distribution across the FEZ makes them ideal for studying topics such as whether chronic low radiation exposure is associated with DNA damage (Cunningham et al. 2021, Anderson et al. 2022) or cataracts (Pederson et al. 2020) in wildlife, whether human activity reduction is associated with changes in population size or diurnal activity (Lyons et al. 2020), and whether consumption of boar from within the zone would lead to unsafe radiation doses in humans (Anderson et al. 2022). Their wide distribution across areas of both high and low contamination levels also makes them the ideal species to use to study the impact which contaminant heterogeneity, such as the contaminant heterogeneity observed within the FEZ, has on exposure estimates.

If fine-scale heterogeneity does play a significant role in determining external exposure, then it should be included in exposure prediction models. However, capturing such fine-scale contaminant heterogeneity likely requires extensive contaminant surveys, surveys which are often beyond the capabilities of those conducting them. In the case of large-scale contamination events, such as the FDNPP disaster, capturing fine-scale heterogeneity is even more difficult because surveys would not only have to be fine-scale but also cover a large spatial extent.

In terrestrial systems, soil radionuclide levels can be transformed into external exposure estimates (Larsson 2008, Brown et al. 2016, Hinton et al. 2019, Gerke et al. 2020). For small contamination events, conducting an extensive soil survey to capture fine-scale heterogeneity may be feasible. However, for larger contamination events, such as the Fukushima Dai-ichi Nuclear Disaster, the manpower required to conduct comprehensive soil surveys would be enormous. Flyover surveys utilizing aircraft equipped with scintillation detectors return radiation levels from the entire FEZ at a finer scale and require less manpower than comprehensive soil surveys (Sanada et al. 2014, Sanada and Torii 2015). Therefore, it is possible that flyover

surveys could be used instead of soil surveys when approximating radiation exposure of widespread species. However, flyover surveys provide estimates for external exposure at 1 meter above the surface (i.e., the height of a human). Thus, these surveys may not be suitable for estimating radiation exposure of smaller terrestrial or burrowing animals. Comparing the accuracy of models based on both flyover and soil samples will help researchers determine the viability of flyover surveys in estimating the amount of radiation wildlife encounter. Further, by comparing these models to actual exposure rates captured by contaminant monitors worn by individual boar, we can help determine the best way to use these surveys to conservatively estimate exposure.

Understanding how wild animals, such as wild boar, have altered their movements in response to the creation of the FEZ and how best to estimate their radiation exposure are important components of developing appropriate management plans and ecosystem risk assessments following radioactive contamination. In this thesis, I will specifically focus on how the scale of sampling contaminant levels and the scale of tracking an individual influences the realism and conservativeness of exposure estimates. In Chapter 2, I use GPS tracking data to conduct and 2nd and 3rd order resource selection analysis on wild boar in and around the FEZ. In addition, I analyze and compare the temporal behavioral activity patterns of wild boar inside and outside the zone. Together, results derived from Chapter 2 can be used by those interested in managing wild boar populations in preparation for resettlement and will expand upon previous literature asking the question of how human presence impacts wildlife behavior. In Chapter 3, I compare varying methods for estimating radiation exposure in both conservative and realistic ways. In addition, I explore the impact that accounting for fine scale contaminant heterogeneity and increasing the complexity with which an organism's movements are estimated have on

deriving contaminant exposure estimates. My Chapter 3 results will assist both individuals interested in generating conservative estimates for risk assessments, as well as those interested in realistic estimates for dose-effect studies. Collectively, this thesis explores the intersection of spatial and radioecology and demonstrates how this intersection can be used for both management and risk assessment processes.

References

Anderson, D., S. Kaneko, A. Harshman, K. Okuda, T. Takagi, S. Chinn, J. C. Beasley, K. Nanba, H. Ishiniwa, and T. G. Hinton. 2022. Radiocesium accumulation and germline mutations in chronically exposed wild boar from Fukushima, with radiation doses to human consumers of contaminated meat. Environmental Pollution 306:119359.

Arkhipov, N. P., N. D. Kuchma, S. Askbrant, P. S. Pasternak, and V. V. Musica. 1994. Acute and long-term effects of irradiation on pine (Pinus silvestris) strands post-Chernobyl. The Science of the Total Environment 157:383–386.

Barrios-Garcia, M. N., and S. A. Ballari. 2012. Impact of wild boar (Sus scrofa) in its introduced and native range: a review. Biological Invasions 14:2283–2300.

Brown, J. E., B. Alfonso, R. Avila, N. A. Beresford, D. Copplestone, and A. Hosseini. 2016. A new version of the ERICA tool to facilitate impact assessments of radioactivity on wild plants and animals. Journal of Environmental Radioactivity 153:141–148.

Cunningham, K., T. G. Hinton, J. J. Luxton, A. Bordman, K. Okuda, L. E. Taylor, J. Hayes, H. C. Gerke, S. M. Chinn, D. Anderson, M. L. Laudenslager, T. Takase, Y. Nemoto, H. Ishiniwa, J. C. Beasley, and S. M. Bailey. 2021. Evaluation of DNA damage and stress in wildlife chronically exposed to low-dose, low-dose rate radiation from the Fukushima Dai-ichi Nuclear Power Plant accident. Environment International 155:106675.

Deryabina, T. G., S. V. Kuchmel, L. L. Nagorskaya, T. G. Hinton, J. C. Beasley, A. Lerebours, and J. T. Smith. 2015. Long-term census data reveal abundant wildlife populations at Chernobyl. Current Biology 25:R824–R826.

Do, X. B. 2019. Fukushima Nuclear Disaster displacement: How far people moved and determinants of evacuation destinations. International Journal of Disaster Risk Reduction 33:235–252.

DOE (U.S. Department of Energy). 2019. A Graded Approach for Evaluating Radiation Doses to Aquatic and Terrestrial Biota. DOE-STD-1153-2019. U.S. Department of Energy, Washington, DC 20585.

Ellegren, H., G. Lindgren, C. R. Primmer, and A. P. Møller. 1997. Fitness loss and germline mutations in barn swallows breeding in Chernobyl. Nature 389:593–596.

Fujii, K., S. Ikeda, A. Akama, M. Komatsu, M. Takahashi, and S. Kaneko. 2014. Vertical migration of radiocesium and clay mineral composition in five forest soils contaminated by the Fukushima nuclear accident. Soil Science and Plant Nutrition 60:751–764.

Geras'kin, S. A. 2016. Ecological effects of exposure to enhanced levels of ionizing radiation. Journal of Environmental Radioactivity 162–163:347–357.

Gerke, H. C., T. G. Hinton, T. Takase, D. Anderson, K. Nanba, and J. C. Beasley. 2020. Radiocesium concentrations and GPS-coupled dosimetry in Fukushima snakes. Science of The Total Environment 734:139389.

Hayes, J. M., T. E. Johnson, D. Anderson, and K. Nanba. 2020. Effective Half-life of 134Cs and 137Cs in Fukushima Prefecture When Compared to Theoretical Decay Models. Health Physics 118:60–64.

Hinton, T. G., R. Alexakhin, M. Balonov, N. Gentner, J. Hendry, B. Prister, P. Strand, and D. Woodhead. 2007. RADIATION-INDUCED EFFECTS ON PLANTS AND ANIMALS: FINDINGS OF THE UNITED NATIONS CHERNOBYL FORUM. Health Physics 93:427–440.

Hinton, T. G., M. E. Byrne, S. C. Webster, C. N. Love, D. Broggio, F. Trompier, D. Shamovich, S. Horloogin, S. L. Lance, J. Brown, M. Dowdall, and J. C. Beasley. 2019. GPS-coupled contaminant monitors on free-ranging Chernobyl wolves challenge a fundamental assumption in exposure assessments. Environment International 133:105152.

Hiyama, A., C. Nohara, S. Kinjo, W. Taira, S. Gima, A. Tanahara, and J. M. Otaki. 2012. The biological impacts of the Fukushima nuclear accident on the pale grass blue butterfly. Scientific Reports 2:570.

Honda, T., and M. Sugita. 2007. Environmental factors affecting damage by wild boars (Sus scrofa) to rice fields in Yamanashi Prefecture, central Japan. Mammal Study 32:173–176.

IAEA (International Atomic Energy Agency). 1992. Effects of Ionizing Radiation on Plants and Animals at Levels Implied by Current Radiation Protection Standards. International Atomic Energy Agency, Vienna, Austria.

IAEA (International Atomic Energy Agency). 2001. Present and Future Environmental Impact of the Chernobyl Accident. International Atomic Energy, Vienna, Austria.

ICRP (International Commission on Radiological Protection). 1977. Recommendations of the ICRP. Pergamon Press, Elmsford, NY 10523.

Koarashi, J., M. Atarashi-Andoh, T. Matsunaga, T. Sato, S. Nagao, and H. Nagai. 2012. Factors affecting vertical distribution of Fukushima accident-derived radiocesium in soil under different land-use conditions. Science of The Total Environment 431:392–401.

Koizumi, A., T. Niisoe, K. H. Harada, Y. Fujii, A. Adachi, T. Hitomi, and H. Ishikawa. 2013. 137Cs Trapped by Biomass within 20 km of the Fukushima Daiichi Nuclear Power Plant. Environmental Science & Technology 47:9612–9618.

Kurihara, M., Y. Onda, H. Suzuki, Y. Iwasaki, and T. Yasutaka. 2018. Spatial and temporal variation in vertical migration of dissolved 137Cs passed through the litter layer in Fukushima forests. Journal of Environmental Radioactivity 192:1–9.

Larsson, C.-M. 2008. An overview of the ERICA Integrated Approach to the assessment and management of environmental risks from ionising contaminants. Journal of environmental radioactivity 99:1364–70.

Lehmann, P., Z. Boratyński, T. Mappes, T. A. Mousseau, and A. P. Møller. 2016. Fitness costs of increased cataract frequency and cumulative radiation dose in natural mammalian populations from Chernobyl. Scientific Reports 6:19974.

Lei, M., L. Zhang, J. Lei, L. Zong, J. Li, Z. Wu, and Z. Wang. 2015. Overview of Emerging Contaminants and Associated Human Health Effects. BioMed Research International 2015:404796.

Lyons, P. C., K. Okuda, M. T. Hamilton, T. G. Hinton, and J. C. Beasley. 2020. Rewilding of Fukushima's human evacuation zone. Frontiers in Ecology and the Environment 18:127–134.

Matsumura, H., T. Kawana, K. Sekiyama, T. Otani, S. Uematsu, M. Saito, and M. Hiroshi. 2019. Extension of protective fencing is not connected to reduction of paddy damage by wild boars. Wildlife and Human Society 7:23–31.

Ministry of the Environment. 2018. Decontamination Projects for Radioactive Contamination Discharged by Tokyo Electric Power Company Fukushima Daiichi Nuclear Power Station Accident. Editorial Committee for the Paper on Decontamination Projects http://josen.env.go.jp/en/policy_document/pdf/decontamination_report1807_01.pdf

Møller, A. P., and T. A. Mousseau. 2001. Albinism and phenotype of barn swallows (Hirundo rustica) from Chernobyl. Evolution; International Journal of Organic Evolution 55:2097–2104.

Møller, A. P., and T. A. Mousseau. 2009. Reduced abundance of insects and spiders linked to radiation at Chernobyl 20 years after the accident. Biology Letters 5:356–359.

Murase, K., J. Murase, R. Horie, and K. Endo. 2015. Effects of the Fukushima Daiichi nuclear accident on goshawk reproduction. Scientific Reports 5:9405.

Nagamatsu, S., A. Rose, and J. Eyer. 2020. Return Migration and Decontamination After the 2011 Fukushima Nuclear Power Plant Disaster. Risk Analysis 40:800–817.

Nakanishi, T., T. Matsunaga, J. Koarashi, and M. Atarashi-Andoh. 2014. 137Cs vertical migration in a deciduous forest soil following the Fukushima Dai-ichi Nuclear Power Plant accident. Journal of Environmental Radioactivity 128:9–14.

Nemoto, Y., H. Oomachi, R. Saito, R. Kumada, M. Sasaki, and S. Takatsuki. 2020. Effects of 137Cs contamination after the TEPCO Fukushima Dai-ichi Nuclear Power Station accident on food and habitat of wild boar in Fukushima Prefecture. Journal of Environmental Radioactivity 225:106342.

Onda, Y., K. Taniguchi, K. Yoshimura, H. Kato, J. Takahashi, Y. Wakiyama, F. Coppin, and H. Smith. 2020. Radionuclides from the Fukushima Daiichi Nuclear Power Plant in terrestrial systems. Nature Reviews Earth & Environment 1:644–660.

Oshita, S. 2013. Radioactive Nuclides in Vegetables and Soil Resulting from Low-Level Radioactive Fallout After the Fukushima Daiichi Nuclear Power Plant Accident: Case Studies in Tokyo and Fukushima. Pages 61–72 *in* T. M. Nakanishi and K. Tanoi, editors. Agricultural Implications of the Fukushima Nuclear Accident. Springer Japan, Tokyo.

Pederson, S. L., M. C. Li Puma, J. M. Hayes, K. Okuda, C. M. Reilly, J. C. Beasley, L. C. Li Puma, T. G. Hinton, T. E. Johnson, and K. S. Freeman. 2020. Effects of chronic low-dose radiation on cataract prevalence and characterization in wild boar (Sus scrofa) from Fukushima, Japan. Scientific Reports 10:4055.

Povinec, P., K. Hirose, and M. Aoyama. 2013. Fukushima Accident: Radioactivity Impact on the Environment. Elsevier, Waltham, MA.

Reisz, J. A., N. Bansal, J. Qian, W. Zhao, and C. M. Furdui. 2014. Effects of Ionizing Radiation on Biological Molecules—Mechanisms of Damage and Emerging Methods of Detection. Antioxidants & Redox Signaling 21:260–292.

Sanada, Y., T. Sugita, Y. Nishizawa, A. Kondo, and T. Torii. 2014. The aerial radiation monitoring in Japan after the Fukushima Daiichi nuclear power plant accident. Progress in Nuclear Science and Technology 4:76–80.

Sanada, Y., and T. Torii. 2015. Aerial radiation monitoring around the Fukushima Dai-ichi nuclear power plant using an unmanned helicopter. Journal of Environmental Radioactivity 139:294–299.

Sato, K., K. Fujimoto, W. Dai, and M. Hunger. 2013. Molecular Mechanism of Heavily Adhesive Cs: Why Radioactive Cs is not Decontaminated from Soil. The Journal of Physical Chemistry C 117:14075–14080.

Schley, L., and T. J. Roper. 2003. Diet of wild boar Sus scrofa in Western Europe, with particular reference to consumption of agricultural crops. Mammal Review 33:43–56.

Strand, P., T. Aono, J. E. Brown, J. Garnier-Laplace, A. Hosseini, T. Sazykina, F. Steenhuisen, and J. Vives i Batlle. 2014. Assessment of Fukushima-Derived Radiation Doses and Effects on Wildlife in Japan. Environmental Science & Technology Letters 1:198–203.

Strand, P., S. Sundell-Bergman, J. E. Brown, and M. Dowdall. 2017. On the divergences in assessment of environmental impacts from ionising radiation following the Fukushima accident. Journal of Environmental Radioactivity 169–170:159–173.

Suchara, I., J. Sucharová, M. Holá, H. Pilátová, and P. Rulík. 2016. Long-term retention of 137Cs in three forest soil types with different soil properties. Journal of Environmental Radioactivity 158–159:102–113.

Takahashi, J., Y. Onda, D. Hihara, and K. Tamura. 2019. Six-year monitoring of the vertical distribution of radiocesium in three forest soils after the Fukushima Dai-ichi Nuclear Power Plant accident. Journal of Environmental Radioactivity 210:105811.

Takahashi, J., S. Wakabayashi, K. Tamura, and Y. Onda. 2018. Downward migration of radiocesium in an abandoned paddy soil after the Fukushima Dai-ichi Nuclear Power Plant accident. Journal of Environmental Radioactivity 182:157–164.

Tanaka, S. 2012. Accident at the Fukushima Dai-ichi Nuclear Power Stations of TEPCO — Outline & lessons learned—. Proceedings of the Japan Academy. Series B, Physical and Biological Sciences 88:471–484.

USEPA (U.S. Environmental Protection Agency). 1996. Soil Screening Guidance: User's Guide. EPA/540/R-96/018. United States Environmental Protection Agency Office of Soil Waste and Emergency Response, Washington, DC 20460.

Watanobe, T., N. Okumura, N. Ishiguro, M. Nakano, A. Matsui, M. Sahara, and M. Komatsu. 1999. Genetic relationship and distribution of the Japanese wild boar (Sus scrofa leucomystax) and Ryukyu wild boar (Sus scrofa riukiuanus) analysed by mitochondrial DNA. Molecular Ecology 8:1509–1512.

Whicker, F. W. 1997. Health impacts of large releases of radionuclides. Impacts on plant and animal populations. Ciba Foundation Symposium 203:74–84; discussion 84-93.

Yamashiro, H., Y. Abe, T. Fukuda, Y. Kino, I. Kawaguchi, Y. Kuwahara, M. Fukumoto, S. Takahashi, M. Suzuki, J. Kobayashi, E. Uematsu, B. Tong, T. Yamada, S. Yoshida, E. Sato, H. Shinoda, T. Sekine, E. Isogai, and M. Fukumoto. 2013. Effects of radioactive caesium on bull testes after the Fukushima nuclear plant accident. Scientific Reports 3:2850.

Yamashiro, H., Y. Abe, G. Hayashi, Y. Urushihara, Y. Kuwahara, M. Suzuki, J. Kobayashi, Y. Kino, T. Fukuda, B. Tong, S. Takino, Y. Sugano, S. Sugimura, T. Yamada, E. Isogai, and M. Fukumoto. 2015. Electron probe X-ray microanalysis of boar and inobuta testes after the Fukushima accident. Journal of Radiation Research 56 Suppl 1:i42-47.

CHAPTER 2

RESOURCE SELECTION AND ACTIVITY PATTERNS OF WILD BOAR IN AND AROUND THE FUKUSHIMA EXCLUSION ZONE

Introduction

Expanding anthropogenic activity has contributed to the destruction and degeneration of many of earth's ecosystems (Kennish 2001, Chen and Tang 2005, Carvajal et al. 2018, Lino et al. 2019, Babí Almenar et al. 2019, Bryan-Brown et al. 2020). Land previously available for wildlife has been transformed for human use, and much of the remaining habitat is fragmented to varying extents (Carvajal et al. 2018, Lino et al. 2019, Babí Almenar et al. 2019, Bryan-Brown et al. 2020). In addition to direct impacts of habitat loss, human activity can indirectly impact wildlife through environmental contamination, light and noise pollution, and numerous other mechanisms (Moore et al. 2000, Bernanke and Köhler 2009, Kight et al. 2012, Tennessen et al. 2014, La Sorte et al. 2017). Anthropogenic pressure, both direct and indirect, is an important factor in many local and global extinction events (Halley et al. 2016, Hirt et al. 2021). Further, anthropogenic pressure can drive wildlife to use different habitats or adjust activity patterns in response to a perceived-risk associated with human presence (Frid and Dill 2002, Ciuti et al. 2012, Lodberg-Holm et al. 2019). Examples of altered behaviors in human-modified landscapes include shifting activity patterns to be more nocturnal (Gaynor et al. 2018, Nickel et al. 2020, Li et al. 2022), utilizing lower-quality resources farther from human activity (Hornseth and Rempel 2016, Ritzel and Gallo 2020), and having smaller home ranges in urban areas than natural ones (O'Donnell and delBarco-Trillo, 2020). Evidence of wildlife responses to human land use change is widespread; however, there has been considerably less effort devoted to investigating

how wildlife and ecosystems respond to the removal of humans, data that are critical to illuminate spatio-temporal processes associated with ecosystem recovery following anthropogenic disturbance (Perino et al. 2019).

The act of converting an altered landscape back to a more natural state is referred to as rewilding (Lorimer et al. 2015, Perino et al. 2019). These areas may be selected on purpose, often for the conservation of large predators or keystone species (e.g., reintroduction of wolves, *Canis lupus*, to Yellowstone; reintroduction of European Bison, *Bison Bonasus*; ensuring connectivity among metapopulations), or they may be the natural consequence following the removal of humans due to military conflicts (e.g., Korean Demilitarized Zone), environmental contamination (e.g., Chernobyl Exclusion Zone, Fukushima Exclusion Zone), urban-rural migration and industrialization leading to abandoned agricultural land (Rudel et al. 2002, Gellrich and Zimmermann 2007), or other reasons. There is growing evidence of the resiliency of ecosystems following a decrease in human activity, as many species are able to respond rapidly at both population and individual levels following human abandonment. For example, a study investigating the response of elk (*Cervus elaphus*) to the removal of human disturbance during calving season found that the removal of simulated human disturbance was correlated with increased reproductive success (Shively et al. 2005). Similarly, the Korean demilitarized zone has become an important stopover for migrating white-naped cranes (*Grus vipio*) following reductions in human activity and development in the region (Higuchi et al. 1996), and many species within the Chernobyl nuclear exclusion zone experienced population growth following the evacuation of humans despite the high radiation levels present (Deryabina et al. 2015).

Like the Chernobyl disaster, the 2011 Fukushima Dai-ichi Nuclear Power Plant accident released large amounts of radionuclides into the surrounding landscape (Tanaka 2012) and

triggered a mass evacuation of humans from the area, forming the Fukushima Exclusion Zone (FEZ). Over time, as radiation levels have fallen, parts of the FEZ have been reopened for human resettlement (Ministry of the Environment 2018). However, approximately 340 km^2 remain restricted from human habitation due to unsafe radiation levels. Humans were evacuated from this area a decade ago, but the FEZ's wildlife remained and have experienced chronic radiation exposure and low levels of human activity ever since. While some species appear to have experienced negative effects due to radiation such as physical abnormalities (Hiyama et al. 2012) or decreased reproductive success (Murase et al. 2015), other studies have failed to find a correlation between increased radiation and numerous biological endpoints (Yamashiro et al. 2013, Abe et al. 2020, Pederson et al. 2020, Cunningham et al. 2021). In fact, like Chernobyl, populations of many wildlife species within the FEZ have increased following the evacuation of humans despite elevated radiation levels (Lyons et al. 2020). The Japanese wild boar (*Sus scrofa leucomystax*), in particular, appears to be benefiting from the formation of the FEZ, as populations are 3-4 times more abundant within the FEZ compared to the surrounding landscape (Lyons et al. 2020).

Wild boar are an extremely adaptable species, known for their ability to survive in a variety of habitats including highly modified agricultural and developed ecosystems (Long 2003, Schley and Roper 2003, Ballari and Barrios-García 2014, González-Crespo et al. 2018). This adaptability has been cited as one of the driving factors for *S. scrofa*'s success as an invasive species – allowing populations of wild *S. scrofa* to successfully establish populations in new areas and survive on every continent but Antarctica. Wild boar diets are primarily composed of plant matter (leaves, stems, fruits, mast), although smaller amounts of animal matter (small mammals, reptiles, eggs, invertebrates) are routinely consumed (Massei et al. 1996, Schley and

Roper 2003, Baubet et al. 2004, Ballari and Barrios-García 2014). Boar living near rural or urban areas can also take advantage of energy rich food like crops, discarded trash, or gardens. However, there is a trade-off between the nutrition that can be gained and the risks (i.e., culling, traffic, etc.) associated with approaching human settlements. Despite these risks, increasing numbers of wild boar have been seen in anthropogenic areas over recent decades, especially rural and suburban settlements (Cahill et al. 2012, VerCauteren et al. 2020) and have caused substantial property damage (Schley et al. 2008, Barrios-Garcia and Ballari 2012, Bobek et al. 2017). Like other populations, Japanese wild boar (hereafter – wild boar) are associated with human-wildlife conflicts (e.g., destroying crops and paddy fields, vehicle collisions) (Honda and Sugita 2007, Honda and Kawauchi 2011, Hioki and Inaba 2021). Within the FEZ, camera trap studies suggest that wild boar populations are increasing and potentially becoming more diurnal (Lyons et al. 2020, Gerke et al. 2022). As areas of the FEZ reopen and small groups of residents return, this lack of temporal and spatial avoidance could lead to increased human-wildlife conflict. To address the growing wild boar population within the FEZ and increasing potential for conflict, the Japanese government has implemented a professional trapping program to mitigate damages caused by wild boar within the FEZ.

Our goal in this study was to use GPS movement data to quantify the resource selection and activity patterns of wild boar in and around the FEZ, and, when possible, to examine the impact of sex and season on shifts in those behaviors. (1) We broadly hypothesized that, at both broad 2nd order (i.e., home range placement within population range) and fine 3rd order scales (i.e., selection of resources within home range), wild boar would utilize areas near historically selected resources like water, forests, and crops (Massei et al. 1996, Schley and Roper 2003, Thurfjell et al. 2009, Clontz et al. 2021, Kramer et al. 2022) and would also utilize urban spaces

due to the substantial reduction in human presence in the region and the benefits they provide despite being abandoned (e.g., abandoned fruit trees, shelter in abandon buildings). (2) During autumn and winter, we hypothesized that boar would select for deciduous forests within their home range more heavily than evergreen forests due to the high energy mast resources available. (3) During spring and summer, we hypothesized that high temperatures would drive wild boar to utilize areas close to water sources within their home range for thermoregulation measures. (4) Finally, we hypothesized that wild boar inside the FEZ would be more diurnal compared to those outside the FEZ.

Methods

Study Site

Our study occurred in and around the FEZ, an approximately 1150km^2 area extending northwest from the Fukushima Dai-ichi Nuclear Power Plant (37°25'15.3"N 141°01'57.1"E) on the eastern coast of Japan (Figure 2.1). The region is characterized by a humid subtropical climate (Köppen 1936, Peel et al. 2007). Spring and summer in the FEZ are warm and wet (average monthly temperature and precipitation: 19.6°C, 148.2mm) whereas fall and winter are considerably cooler and drier (7.5°C, 85.5mm) (Japan Meteorological Agency 2022). The Abukuma mountains bisect the FEZ, creating both mountainous and coastal habitats (Figure 2.1). Mountainous areas are characterized by rolling deciduous broadleaf, deciduous needleleaf, and evergreen needleleaf forests with scattered grassland and urban settlements. Coastal areas are much flatter and historically dominated by a mixture of urban settlements and paddy fields. Since the 2011 tsunami and subsequent human evacuation, the landscape within the FEZ has changed due to abandonment, with vegetation encroaching in residential and urban areas and former paddy and agricultural fields being overtaken by grass (Sekizawa et al. 2015, Ishihara and

Tadono 2017). Extensive efforts to manually reduce radiation levels have been made by removing contaminated top-soil and sediments and washing contaminated areas with water (Ministry of the Environment 2018). Due to these remediation efforts, as well as the natural decay and migration of radioisotopes in the system, many areas of the FEZ began reopening for human resettlement starting in 2014 (Figure 2.1), although only a small proportion of residents had returned at the time of the study (Ministry of the Environment 2018). Of the original FEZ, 340 km^2 remains closed to human resettlement as of 2022.

Some of our analyses also included boar from Miyagi (fall-winter: 3.8C, 101.7 mm | spring-summer: 17.6C, 157.8mm) and Iwate (fall-winter: 4.5C, 52.9mm | spring, summer: 17.9C, 140mm) prefectures (Figure 2.1). Similar to the FEZ, this landscape is characterized by forested rolling mountains. However, compared to the FEZ, urban areas and paddy fields were farther inland and thus the overall landscape composition was slightly different compared to the FEZ. Thus, boar from Miyagi and Iwate were excluded from our resource selection analysis, and only used in our activity analysis, because of these general landscape differences. Similarly, because the majority of boar in the FEZ were collared in coastal regions, we excluded boar in mountainous regions from our resource selection analysis.

Animal Handling and Data Processing

We captured 37 wild boar inside the FEZ (≥ 21.2 kg, 16 males, 21 females) in both coastal (34) and mountain (3) habitats between 2016 and 2020 using box live traps (Figure 2.1). An additional 4 wild boar were collared in Miyagi (n = 2) and Iwate (n = 2) prefectures between 2012 and 2019 and were only used in behavioral analyses. We anesthetized each individual with 5 mg/kg Zoletil (Virbac, Australia) and 0.1 mg/kg medotomine (Domitor) injected intramuscularly. Once sedated, we collected age, sex, and weight, and fit each individual with a

GPS radio collar (Vectronic Aerospace, Berlin Germany). During processing, a top-up dose was given every 10 to 15 minutes, and individuals were released at the capture site upon recovery. GPS collars were initially programmed to take locations every 15 (n = 20), 30 (n = 13), or 60 (n = 8) minutes, but were later resampled to 60 minutes (+/- 5 minutes) to standardize the data used in our analyses among individuals. Due to potential changes in behaviour directly following collaring, we excluded all locations collected within 48 hours of release. In addition, we removed any obvious incorrect GPS fixes including obvious outliers and locations farther away from the previous locations than a boar could feasibly travel during the sampling rate. There is no hard boundary to the FEZ, and thus boar can move in and out of the zone freely. To ensure we were capturing the resource selection of boar within the zone, we only included boar in resource selection analyses which had at least 95% of these resampled hourly points within the FEZ boundaries.

Resource Selection

Spatial Layers Preparation

Fukushima Exclusion Zone

We manually created a spatial polygon for the FEZ by digitizing an image of its boundaries (Prime Minister's Office of Japan 2013) in ArcGIS Pro (version 2.9.0). We further corrected the digitized borders by adjusting them to align with township boundaries (ESRI Japan https://www.esrij.com/products/japan-shp/ Population and Border Information). Throughout our study period, as parts of FEZ were reopened to settlement, we correspondingly adjusted the FEZs boundaries to reflect these changes in our analyses.

Environmental Covariates

We were interested in the resource selection of wild boar at two scales: 2nd order and 3rd order (Johnson 1980). We started with the same set of environmental covariates for each analysis, but the specific covariates used in model generation varied slightly between scales due to multicollinearity between environmental attributes at different scales (see below). We selected eight environmental covariates (distance to crops, distance to urban areas, distance to deciduous forests, distance to evergreen forests, distance to paddy fields, distance to water, distance to major roads, and distance to non-major roads) that we a priori anticipated could have the greatest potential influence on wild boar movements (Kodera et al. 2001, Ballari and Barrios-García 2014, Nemoto et al. 2020, Clontz et al. 2021). These eight environmental covariates were selected either because they (1) fulfill some essential need for survival including food (crops, paddy fields, deciduous forests), cover (deciduous forests, evergreen forests), or water; or (2) are tightly linked to human activity and thus their use may be influenced by the removal of humans from the FEZ landscape (urban areas, major and non-major roads, crops, and paddy fields). For each environmental covariate, we generated distance rasters in ArcGIS Pro (Version 2.9.0) and imported these rasters into R version 4.0.3 (R Core Team 2019) to determine the minimum distance from used and available locations to each resource.

To account for changes in landcover over the duration of this study, particularly given shifts in habitats due to the abandonment and subsequent repopulation of some areas (Ishihara & Tadono, 2017; Sekizawa et al., 2015), we used two temporally distinct land cover rasters developed by the Earth Observation Research Center at the Japan Aerospace Exploration Agency (JAXA) (30 x 30 m | 10 x 10 m resolution) (Japan Aerospace Exploration Agency 2018, 2021) to represent the study area's landscape between 2014-2016 and between 2018-2020. Both raster layers included crops, urban areas, deciduous broadleaf forests, deciduous needleleaf forests,

evergreen broadleaf forests, evergreen needleleaf forests, grassland, and paddy fields land cover types. To simplify our analyses, we combined evergreen broadleaf and evergreen needleleaf forest layers into a single layer, and similarly combined deciduous broadleaf and deciduous needleleaf forests. We also combined converted paddy fields with paddy fields (see below), to obtain an overall distance to paddy field.

Since the 2011 tsunami and subsequent evacuation, many abandoned paddy fields within the FEZ have experienced significant vegetation changes due to the lack of farming (Sekizawa et al. 2015, Ishihara and Tadono 2017). Many of these paddy fields have been overtaken by grass and as a result categorized as grassland on land cover rasters. Therefore, to include these abandoned paddy fields in our analysis, we first determined which grassland pixels in the 2014-2016 and 2018-2020 land cover rasters were converted paddy fields by comparing them to a pre-tsunami land cover layer (10 x 10 m resolution) (Japan Aerospace Exploration Agency 2016) and then used the minimum distance to either a converted or non-converted paddy field as distance to paddy field in our analyses.

It is unlikely that roads and water sources shifted spatially due their abandonment. Thus, we did not create separate temporal distance rasters for these covariates. The distance to water raster (30 x 30 m) was produced by combining rivers and lakes layers from the National Land Numeric Information Division of the Ministry of Land, Infrastructure, Transport, and Tourism of Japan (retrieved from https://nlftp.mlit.go.jp/ksj/index.html). We used a roads spatial layer downloaded from OpenStreetMap (OpenStreetMap contributors, 2021 retrieved from https://download.geofabrik.de/asia/japan.html on 7/22/2021) to generate individual distance rasters (30 x 30 m) for motorways, trunk, primary, secondary, tertiary, unclassified and residential roads. We later combined extracted distances into distance to major road (motorways,

trunk, and primary roads) and distance to non-major roads (secondary, tertiary, unclassified, and residential roads) in R.

Prior to model generation, we tested for multicollinearity between environmental covariates by calculating variance inflation factors (VIF) using the usdm R package version 1.1-18 (Naimi 2017) in R version 4.0.3 (R Core Team 2019) with a maximum linear correlation threshold of 0.7 and a VIF threshold of 10. Due to multicollinearity, we excluded distance to agriculture, evergreen forests, and minor roads from our 3rd order analysis and distance to agriculture and evergreen forests from our 2nd order analysis.

2nd Order Resource Selection

We assessed resource selection at a broad scale by comparing the resources available within a boars' home range to those available throughout the broader landscape. At the 2nd order scale, we defined used areas by generating a 95% autocorrelated kernel density home range for each wild boar (Fleming et al. 2015) that had more than 15 days of data, not including days already removed post-collaring using the ctmm package version 0.6.0 (Calabrese et al. 2016). This 15-day requirement was selected because it ensured that we had enough data to capture the true home size of range resident individuals, as was indicated by stability of empirical variograms.

We decided to use autocorrelated kernel density estimates (AKDE), as opposed to other home range estimates because AKDEs account for the autocorrelation that is present when an individual's locations are recorded frequently enough that each subsequent location is correlated with the previous location. We defined the available area for our 2nd order analysis using a minimum convex polygon (MCP) surrounding all coastal boar locations (Figure 2.1), buffered by

the mean diameter (2759m) of all 95% autocorrelated home range estimates. The MCP was generated using the mcp function from the adehabitatHR package (version 0.4-19).

We randomly sampled habitat attributes at 5,000 locations within each boar's home range (140,000 locations across all boar) and compared the attributes present at these 'used' locations to those extracted by randomly sampling 25,000 locations within the MCP. These numbers (i.e., 5000 used; 25,000 available) were selected after preliminary tests indicated they were large enough to sufficiently capture the true values of sampling scale-sensitive parameters (Northrup et al. 2013). Because we were specifically interested in evaluating resource selection differences between males and females, we did not use model selection and instead used a global model for both males and females to facilitate comparison between sexes using the same model structure. We generated generalized linear mixed models with the habitat attributes as fixed effects based on a training dataset containing 70% of used and available data. We then determined the performance of our models by computing and comparing the area under a receiver operating characteristic curve (AUC ROC) for both the training dataset and a testing dataset which contained the remaining 30 percent of data. We generated our models using the glmer function of the lme4 package (version 1.1-26) with a binomial response, Nelder Mead optimizer, and a nACQ of 0 and tested model performance using the pROC package in R version 4.0.3 (R Core Team 2019).

3rd Order Resource Selection

At a finer scale, we assess resource selection at recorded GPS locations relative to random locations within a boar's home range. For this analysis, we separated our detections based on sex and season. We did not include season in our 2nd order analysis because Japanese wild boar are not known to make large scale seasonal migrations, which would result in distinct

seasonal home ranges. However, it is possible that season does play a role in the selection of resources within a wild boars' home range. For example, forested areas or proximity to water may play a larger role in warmer months compared to cooler months. Therefore, we divided our detections into spring-summer (April to September) and autumn-winter (October-March) for this analysis.

We quantified the available habitat by randomly sampling 95% home ranges generated during the 2nd order analysis. Each home range was sampled such that there were 5 times more available locations relative to used GPS locations. We decided to use 5 times the number of used locations for available because preliminary analyses suggested this number was large enough to ensure we captured sampling-scale sensitive parameters (Northrup et al. 2013). We used habitats associated with recorded GPS locations for used locations. Similar to our 2nd order analysis, we did not use model selection and instead used a global model, which allowed us to compare our covariates across sexes and seasons. We generated 4 generalized linear mixed models (male:autumn-winter, male:spring-summer, female:autumn-winter, female:spring-summer) based on a training dataset consisting of 70% of used and available data, using the glmer function of the lme4 package (version 1.1-26) with a binomial response, Nelder Mead optimizer, and a nACQ of 0. We assessed model fit by determining the AUC ROC for both training and testing datasets using the pROC package (version 1.18.0) in R (version 4.0.3).

Behavioral Analysis

Hidden Markov Models (HMMs) can be used to predict underlying behavioral states by looking for patterns in the distance traveled between consecutive detections (step length) and changes in the direction traveled (turn angle). Previous research has shown that both sex (Clontz et al. 2021) and human disturbance (Doherty et al. 2021, Stabach et al. 2022) can alter step

lengths and/or total amount of movement an individual travels. Therefore, we separated our data into four categories: males inside the FEZ, males outside the FEZ, females inside the FEZ, and females outside the FEZ. For individuals that moved across the FEZ boundary during their tracking period, we separated their data into two discrete datasets reflecting movements inside and outside the FEZ. Step lengths and turn angles for consecutive steps were generated with the prepData function in the moveHMM package (version 1.7) (Michelot et al. 2016) and were used as the observations for our HMMs. For each dataset we ran 25 iterations of HMMs with different starting values for step-lengths and turn-angles. These starting values were randomly generated within pre-selected bounds based on observed step-lengths and turn-angles. All models assumed 3 behavioral states, a gamma distribution for step-lengths, and a wrapped Cauchy distribution for turn angles. Model fitting and state decoding were both done using the moveHMM package (Version 1.7) in R. We then selected the best model for each dataset based on likelihood and used the Viterbi algorithm to assign behavioral states for each GPS location. We then used Watson's two-sample test of homogeneity (Zar 1976) to test for differences in the temporal distribution of each state across sex and location relative to the FEZ. To run Watson's two-sample test of homogeneity we used the watson.two function in the CircStats package (version 0.2-6).

Results

We obtained GPS data for 34 collared wild boar within coastal areas of the FEZ between January 2016 and November 2020 which following hourly resampling, resulted in 89,278 cleaned GPS fixes (14 males, 20 females). Of these 34 boar, 2 (1 male, 1 female; 526 cleaned GPS fixes) did not have sufficient data to generate home ranges for 2nd or 3rd order resource selection analyses and were only included in behavioral analyses. An additional 4 boar (2 male, 2

female; 15885 cleaned GPS fixes) spent less than 95% of their time in the FEZ and were excluded from the resource selection analyses and only used for behavioral analyses. All 11 males included in our resource selection analysis had data crossing into autumn-winter but only 5 of them had spring-summer data. Fifteen females included in our resource selection analysis had data in autumn-winter and 7 had data in spring-summer. In total, data from 28 boar (11 males, 18 females; 72,867 cleaned GPS fixes) were used in our resource selection analyses.

For our behavioral analyses, we an additional 3,920 hourly fixes were obtained from three wild boar collared in the FEZ's mountain regions (2 males, 1 female), 1,835 from one female boar who left their coastal home range and established a new home range in the mountains, and 11,224 hourly fixes from four wild boar (3 males, 1 female) collared outside the FEZ in the Miyagi and Iwate prefectures between 2012 and 2019. In total, we used data from 41 boar (19 males, 22 females; 106,257 cleaned GPS fixes) in our behavioral analyses.

It should be noted that two wild boar (one collared inside the FEZ and one in Miyagi prefecture) experienced dispersal events during the tracking period. For these two individuals, we removed GPS locations recorded during dispersal events and treated pre- and post-dispersal as separate individuals; doing this ensured that unusual behavior during dispersal did not interfere with our temporal behavior analysis and that changes in resource availability did not interfere with our resource selection analyses.

2nd Order Resource Selection

At the 2nd order scale, the majority of our measured habitat attributes influenced the placement of wild boar (*Sus scrofa leucomystax*) home ranges within the landscape (Table 2.1, Figure 2.2). Both males and females established home ranges close to paddy fields, major roads, and deciduous forests (Table 2.1, Figure 2.2). Females selected to be close to urban spaces, but

males did not select to be closer to or farther from these areas (Table 2.1, Figure 2.2). Males selected to be farther from water sources, whereas females did not significantly select to be closer or farther from water sources (Table 2.1, Figure 2.2). The AUC ROCs for male and female training and testing data indicated adequate model fit given our data (male training: 0.7211, male testing: 0.7208, female training: 0.7686, female testing: 0.7643).

3rd Order Resource Selection

At a finer scale, across sexes and seasons, wild boar selected to use areas closer to paddy fields within their home ranges (Table 2.2, Figure 2.3). Similar to our 2nd order results, males selected to be closer to urban areas across seasons and farther from water in spring-summer (Table 2.2, Figure 2.3). Females also selected to be farther from water in autumn-winter, but selected to be close to water during spring-summer (Table 2.2, Figure 2.3). Females also selected to be closer to urban areas in spring-summer (Table 2.2, Figure 2.3). Females selected to be closer to deciduous forests across seasons and evergreen forests during spring-summer, but selected to be farther from evergreen forests in autumn-winter (Table 2.2, Figure 2.3). Males selected to be closer to evergreen forests across seasons and deciduous forests during spring-summer; but selected to be farther from deciduous forests during autumn-winter (Table 2.2, Figure 2.3). Males selected to be closer to minor roads across seasons and closer to major roads in spring-summer but selected to be farther from major roads in autumn-winter (Table 2.2, Figure 2.3). Females selected to be farther from both major and minor roads in across seasons (Table 2.2, Figure 2.3). The AUC ROC scores for our 3rd order models also indicated that they predicted use better than random chance (male autumn-winter training: 0.6450, testing: 0.6388; male spring-summer training: 0.6822, testing: 0.6857; female autumn-winter training: 0.6393, testing: 0.6457; female spring-summer training: 0.6599, testing: 0.6599).

Behavioral Analysis

Using separate HMMs, we were able to distinguish three behavioral states for both males and females inside and outside the FEZ (Table 2.3): resting (characterized by short step lengths and turn angles close to -π), foraging (characterized by slightly longer step lengths and turn angles close to - π), and traveling (characterized by long step lengths and turn angles close to π).

There were clear differences in temporal behavioral patterns for both males and females inside and outside the FEZ (Table 2.4, Figure 2.4). Both males and females inside the FEZ were more active during the day compared to their counterparts outside the zone, spending more time making intermediate steps indicative of foraging and less time resting (Figure 2.4). Within the FEZ, males spent slightly more time foraging than females (Figure 2.4). Outside the FEZ, both males and females spent most of the day resting, with females resting slightly more than males (Figure 2.4). Although traveling tends to follow similar temporal patterns both inside and outside of the FEZ, with most traveling occurring during the night (Figure 2.4), there are still significant (p-value < 0.05) differences in traveling patterns based on location and sex (Table 2.4). For example, females outside the FEZ spend less time traveling during the day compared to females inside and males outside the FEZ tend to travel later into the morning compared to females outside (Figure 2.4).

Discussion

Using GPS locations of wild boar, we investigated fine and broad scale resource selection and movement behavior in and around the Fukushima Exclusion Zone in Japan. We found that spatial scale, season, and sex all impacted resource selection of wild boar. Most notably, we found that although wild boar in and around the FEZ often utilize natural areas like deciduous and evergreen forests, they also often utilize anthropogenic spaces like urban areas and paddy

fields. While further studies would be necessary to quantify the extent to which this usage is a consequence of the reduction of human activity following evacuation, the extensive use of anthropogenic spaces by wild boar in our study suggests there is a high potential for conflict as areas are resettled by humans. Our results also suggest wild boar within the FEZ exhibit altered temporal patterns of activity, with boar inside the zone exhibiting more diurnal activity than those in areas with greater human activity, supporting previous research within the FEZ using remote cameras (Lyons et al. 2020).

Wild boar are among the most behaviorally plastic and generalist large mammals (Schley and Roper 2003, Keuling et al. 2009, Barrios-Garcia and Ballari 2012), with the ability to adapt to changes in their environment by adjusting their resource selection and/or temporal activity patterns to mitigate conflict. At a broad 2nd order scale, females selected to be close to urban areas. Although these abandoned urban areas do not have the same energy rich resources as non-abandoned spaces (i.e. food waste, backyard gardens, etc.), wild boar may still be attracted to the resources available in the absence of human use. For example, within the Chernobyl exclusion zone, abandoned structures have been shown to be used by Przewalski's horses and other wildlife for shelter (Schlichting et al. 2020). It is possible that wildlife within the FEZ may make similar use of abandoned buildings (Gerke et al. 2020). Other remnants of humans use such as orchards or fruit trees in gardens planted before the evacuation, may also play a role in providing food. Encroaching shrubs and trees around towns and houses also may be inadvertently increasing wild boar habitat and thus encouraging use of urban areas. At a finer scale, wild boar also selected to be close to anthropogenic areas in every sex-season category except for females in autumn-winter, during which females did not have a significant selection pattern concerning urban spaces. Within the FEZ, there are extensive year-round culling efforts to protect urban

areas from boar and other problematic species. It is possible that this culling has driven at least some of the females to select for urban areas less strongly, which would account for the absence of selection during autumn-winter when other resources, like masts, are available elsewhere. Males, on the other hand, may experience more pressure due to increased population sizes and be driven to use these abandoned but still risky areas due to their solitary nature.

Like urban areas, paddy fields also can be an energy rich resource, evidenced by the vast amount of rooting damage within paddy fields across Japan each year (Honda 2007, Honda and Sugita 2007, Matsumura et al. 2019). While rice may not be actively harvested within the FEZ, rooting is still a common occurrence in these abandoned fields, suggesting that even abandoned fields provide an energy rich alternative to more natural sources. This premise is further supported by our results, in which paddy fields were heavily selected for across scales, sexes, and seasons. In addition to being a food resource (Honda 2007, Honda and Sugita 2007, Lee and Lee 2014, Matsumura et al. 2019), rice paddies tend to be in lowland areas and, when flooded, can potentially provide boar with other sources of water for drinking and thermoregulation. Wild boar are poor thermoregulators and require frequent access to water for drinking and wallowing (Graves 1984, Huynh et al. 2005, Bracke 2011). Thus, it is likely that the apparent avoidance of lakes and rivers in our resource selection analyses by some wild boar could simply be explained by wild boar utilizing paddy fields or other fine-scale water resources within the FEZ, and thus not requiring larger sources of fresh water.

Wild boar also selected to be close to deciduous forests and/or evergreen forests at different scales, sexes, and seasons. This result supports many previous studies in which forests were found to play an important role in wild boar resource selection (Kodera et al. 2001, Ballari and Barrios-García 2014, Nemoto et al. 2020, Clontz et al. 2021). Deciduous forests provide

numerous benefits to wild boar, particularly through nutrition in the form of growing vegetation during spring-summer and high calorie mast during autumn-winter. Further, forests can provide cover for thermoregulation (Kramer et al. 2022) and rearing young (Fernández-Llario 2004). During winter months, thick evergreen forests may be better at providing thermoregulation cover compared to deciduous forests, which could explain why male wild boar selected for evergreen forests over deciduous forests during autumn-winter. It is possible that females may have been captured during years or in areas that had greater quantities of masts available, which could explain why they selected for deciduous forests but not evergreen forests during autumn-winter. However, we did not have access to records of mast quantities over our study period and could not confirm this.

There is little consistency in previous research concerning the behavioral response of wild boar to roads: some studies failed to find any impact of roads on boar movement (Frantz et al. 2012), others found that roads can act as barriers to movement (Lecis et al. 2022), and still others found that boar can respond positively or negatively to roads depending on sex, season, and location on the rural-urban gradient (Stillfried et al. 2017, Clontz et al. 2021). We found similar conflicting results in our analysis as there were few trends across scales, sexes, seasons, or road type. While this inconsistency makes it difficult to make conclusions about the importance of roads to wild boar, it does support the idea that roads may have both positive and negative impacts. This inconsistency may also be explained by the fact that boar are generalists and can easily take advantage of or ignore different resources depending on what else is available in their home range (Massei et al. 1996, Schley and Roper 2003, Ballari and Barrios-García 2014, Nemoto et al. 2020, Clontz et al. 2021).

Using HMMs, we were able to differentiate male and female movement tracks, both inside and outside the FEZ, into three distinct behavioral states. We found that, regardless of sex, wild boar tended to travel at night and rest during the day. This is likely, at least partially, a thermoregulatory behavior (Geiser 2010, Giroux et al. 2022) and allows boar to reduce exposure to the midday heat. However, compared to outside the zone, wild boar within the FEZ spent less time resting and more time foraging during the day. This supports previous camera trap research which suggests that wild boar inside the FEZ were more diurnal compared to their counterparts outside the zone (Lyons et al. 2020). Shifting to a more nocturnal activity pattern is often seen among animals living in areas with higher human presence (Gaynor et al. 2018, Li et al. 2022). Thus, within the zone, where human activity and conflicts with people have been reduced substantially, it is not surprising that wild boar may be modifying their behavior to be more active during the day.

Conclusion

Wild boar are one of the most behaviorally plastic large mammals, able to adapt to new environments by varying their use of space and time. As such, they are ideally suited to quickly respond to abrupt changes in their habitat, such as the removal of humans from a previously inhabited area. Supporting this conjecture, previous studies in the FEZ and Chernobyl have shown that, following the removal of humans, both areas saw a large increase in wild boar populations – suggesting that at a population level wild boar are taking advantage of the lack of people (Deryabina et al. 2015, Lyons et al. 2020). In this study, we expanded on previous research on wild boar in evacuated areas by investigating resource use and potential behavioral changes of boar within the FEZ. Understanding the spatial and temporal patterns of boar within the FEZ can provide insight into how a generalist species may utilize areas following rewilding

and can assist those preparing within the FEZ for resettlement. We found that, in addition to utilizing natural areas like deciduous and evergreen forests, wild boar also often used anthropogenic spaces like urban spaces and paddy fields. In addition, wild boar's shift to diurnal activity within the FEZ also indicates a usage of time periods previously occupied by humans. Collectively, our results suggest that a generalist species facing a rewilding event will utilize both natural and anthropogenic areas depending on the desirability of the resources available. From a management perspective, our results suggest boar select highly for paddy fields, and so these areas may be important to focus on in management plans. Furthermore, although not as highly or consistently selected for as paddy fields, many boar collared in our study extensively utilized urban areas, highlighting the potential for conflicts in areas containing property left by residents.

Acknowledgements

We would like to thank the various impacted towns for giving us permission to conduct the research, and the many people who worked in the field to trap and collar animals used in this study including but not limited to the members of the Japanese hunting associations for their willingness to give us access to their trapped animals, D. Anderson, S. Chinn, K. Cunningham, J. Hayes, H. Ishiniwa, M. LiPuma, H. Nagata, Y. Nemoto, and S. Pederson. We would also like to thank Dr. Michael Kohl for sharing his insight into resource selection studies. The High-Resolution Land Use and Land Cover Map Products used for this paper have been provided by ALOS/ALOS-2 of the Japan Aerospace Exploration Agency. Map data copyrighted OpenStreetMap contributors and available from https://www.openstreetmap.org. We would like to thank G. Wittemyer and J. Hepinstall-Cymerman for their guidance and feedback on this study. Finally, we would like to thank the Japanese Ministry of Education, Culture, Sports,

Science and Technology for obtaining and publishing data that are made publicly available. Funding for this study was provided by Colorado State University, Fukushima University, the Research Council of Norway through its Centres of Excellence funding scheme, project number 223268/F50., the University of Georgia, as well as the U.S. Department of Energy Office of Environmental Management under Award Number DE-EM0005228 to the University of Georgia Research Foundation.

References

Abe, Y., H. Yamashiro, Y. Kino, T. Oikawa, M. Suzuki, Y. Urushihara, Y. Kuwahara, M. Morimoto, J. Kobayashi, T. Sekine, T. Fukuda, E. Isogai, and M. Fukumoto. 2020. Analysis of Ovaries and Fertilities in Domestic Animals Affected by the Fukushima Daiichi Nuclear Power Plant Accident. Pages 113–123 *in* M. Fukumoto, editor. Low-Dose Radiation Effects on Animals and Ecosystems: Long-Term Study on the Fukushima Nuclear Accident. Springer, Singapore.

Babí Almenar, J., A. Bolowich, T. Elliot, D. Geneletti, G. Sonnemann, and B. Rugani. 2019. Assessing habitat loss, fragmentation and ecological connectivity in Luxembourg to support spatial planning. Landscape and Urban Planning 189:335–351.

Ballari, S. A., and M. N. Barrios-García. 2014. A review of wild boar Sus scrofa diet and factors affecting food selection in native and introduced ranges. Mammal Review 44:124–134.

Barrios-Garcia, M. N., and S. A. Ballari. 2012. Impact of wild boar (Sus scrofa) in its introduced and native range: a review. Biological Invasions 14:2283–2300.

Baubet, E., C. Bonenfant, S. Brandt. 2004. Diet of the wild boar in the French Alps. Galemys 16:101–113.

Bernanke, J., and H.-R. Köhler. 2009. The Impact of Environmental Chemicals on Wildlife Vertebrates. Pages 1–47 *in* D. M. Whitacre, editor. Reviews of Environmental Contamination and Toxicology. Springer, New York, NY.

Bobek, B., J. Furtek, J. Bobek, D. Merta, and M. Wojciuch-Ploskonka. 2017. Spatio-temporal characteristics of crop damage caused by wild boar in north-eastern Poland. Crop Protection 93:106–112.

Bracke, M. B. M. 2011. Review of wallowing in pigs: Description of the behaviour and its motivational basis. Applied Animal Behaviour Science 132:1–13.

Bryan-Brown, D. N., R. M. Connolly, D. R. Richards, F. Adame, D. A. Friess, and C. J. Brown. 2020. Global trends in mangrove forest fragmentation. Scientific Reports 10:7117.

Cahill, S., F. Llimona, L. Cabañeros, and F. Calomardo. 2012. Characteristics of wild boar (Sus scrofa) habituation to urban areas in the Collserola Natural Park (Barcelona) and comparison with other locations. Animal Biodiversity and Conservation 35:221–233.

Calabrese, J. M., C. H. Fleming, and E. Gurarie. 2016. ctmm: an r package for analyzing animal relocation data as a continuous-time stochastic process. Methods in Ecology and Evolution 7:1124–1132.

Carvajal, M. A., A. J. Alaniz, C. Smith-Ramírez, and K. E. Sieving. 2018. Assessing habitat loss and fragmentation and their effects on population viability of forest specialist birds: Linking biogeographical and population approaches. Diversity and Distributions 24:820–830.

Chen, Y., and H. Tang. 2005. Desertification in north China: background, anthropogenic impacts and failures in combating it. Land Degradation & Development 16:367–376.

Ciuti, S., J. M. Northrup, T. B. Muhly, S. Simi, M. Musiani, J. A. Pitt, and M. S. Boyce. 2012. Effects of Humans on Behaviour of Wildlife Exceed Those of Natural Predators in a Landscape of Fear. PLOS ONE 7:e50611.

Clontz, L. M., K. M. Pepin, K. C. VerCauteren, and J. C. Beasley. 2021. Behavioral state resource selection in invasive wild pigs in the Southeastern United States. Scientific Reports 11:6924.

Cunningham, K., T. G. Hinton, J. J. Luxton, A. Bordman, K. Okuda, L. E. Taylor, J. Hayes, H. C. Gerke, S. M. Chinn, D. Anderson, M. L. Laudenslager, T. Takase, Y. Nemoto, H. Ishiniwa, J. C. Beasley, and S. M. Bailey. 2021. Evaluation of DNA damage and stress in wildlife chronically exposed to low-dose, low-dose rate radiation from the Fukushima Dai-ichi Nuclear Power Plant accident. Environment International 155:106675.

Deryabina, T. G., S. V. Kuchmel, L. L. Nagorskaya, T. G. Hinton, J. C. Beasley, A. Lerebours, and J. T. Smith. 2015. Long-term census data reveal abundant wildlife populations at Chernobyl. Current Biology 25:R824–R826.

Doherty, T. S., G. C. Hays, and D. A. Driscoll. 2021. Human disturbance causes widespread disruption of animal movement. Nature Ecology & Evolution 5:513–519.

Fernández-Llario, P. 2004. Environmental correlates of nest site selection by wild boar Sus scrofa. Acta Theriologica 49:383–392.

Fleming, C. H., W. F. Fagan, T. Mueller, K. A. Olson, P. Leimgruber, and J. M. Calabrese. 2015. Rigorous home range estimation with movement data: a new autocorrelated kernel density estimator. Ecology 96:1182–1188.

Frantz, A. C., S. Bertouille, M. C. Eloy, A. Licoppe, F. Chaumont, and M. C. Flamand. 2012. Comparative landscape genetic analyses show a Belgian motorway to be a gene flow barrier for red deer (Cervus elaphus), but not wild boars (Sus scrofa). Molecular Ecology 21:3445–3457.

Frid, A., and L. M. Dill. 2002. Human-caused Disturbance Stimuli as a Form of Predation Risk. Ecology and Society 6:11.

Gaynor, K. M., C. E. Hojnowski, N. H. Carter, and J. S. Brashares. 2018. The influence of human disturbance on wildlife nocturnality. Science 360:1232–1235.

Geiser, F. 2010. Aestivation in Mammals and Birds. Pages 95–111 *in* C. Arturo Navas and J. E. Carvalho, editors. Aestivation: Molecular and Physiological Aspects. Springer, Berlin, Heidelberg.

Gellrich, M., and N. E. Zimmermann. 2007. Investigating the regional-scale pattern of agricultural land abandonment in the Swiss mountains: A spatial statistical modelling approach. Landscape and Urban Planning 79:65–76.

Gerke, H. C., T. G. Hinton, K. Okuda, and J. C. Beasley. 2022. Increased abundance of a common scavenger affects allocation of carrion but not efficiency of carcass removal in the Fukushima Exclusion Zone. Scientific Reports 12:8903.

Gerke, H. C., T. G. Hinton, T. Takase, D. Anderson, K. Nanba, and J. C. Beasley. 2020. Radiocesium concentrations and GPS-coupled dosimetry in Fukushima snakes. Science of The Total Environment 734:139389.

Giroux, A., Z. Ortega, A. Bertassoni, A. L. J. Desbiez, D. Kluyber, G. F. Massocato, G. DE Miranda, G. Mourão, L. Surita, N. Attias, R. de C. Bianchi, V. P. de O. Gasparotto, and L. G. R. Oliveira-Santos. 2022. The role of environmental temperature on movement patterns of giant anteaters. Integrative Zoology 17:285–296.

González-Crespo, C., E. Serrano, S. Cahill, R. Castillo-Contreras, L. Cabañeros, J. M. López-Martín, J. Roldán, S. Lavín, and J. R. López-Olvera. 2018. Stochastic assessment of management strategies for a Mediterranean peri-urban wild boar population. PLOS ONE 13:e0202289.

Graves, H. B. 1984. Behavior and Ecology of Wild and Feral Swine (Sus Scrofa). Journal of Animal Science 58:482–492.

Halley, J. M., N. Monokrousos, A. D. Mazaris, W. D. Newmark, and D. Vokou. 2016. Dynamics of extinction debt across five taxonomic groups. Nature Communications 7:12283.

Higuchi, H., K. Ozaki, G. Fujita, J. Minton, M. Ueta, M. Soma, and N. Mita. 1996. Satellite Tracking of White-Naped Crane Migration and the Importance of the Korean Demilitarized Zone. Conservation Biology 10:806–812.

Hioki, A., and R. Inaba. 2021. Occupational Fatalities Due to Mammal-Related Accidents in Japan, 2000–2019. Wilderness & Environmental Medicine 32:19–26.

Hirt, M. R., A. D. Barnes, A. Gentile, L. J. Pollock, B. Rosenbaum, W. Thuiller, M. A. Tucker, and U. Brose. 2021. Environmental and anthropogenic constraints on animal space use drive extinction risk worldwide. Ecology Letters 24:2576–2585.

Hiyama, A., C. Nohara, S. Kinjo, W. Taira, S. Gima, A. Tanahara, and J. M. Otaki. 2012. The biological impacts of the Fukushima nuclear accident on the pale grass blue butterfly. Scientific Reports 2:570.

Honda, T. 2007. Factors Affecting Crop Damage by Wild Boar: The Analysis Using Census Data of Agriculture and Forestry. Journal of the Japanese Forest Society 89:249–252.

Honda, T., and N. Kawauchi. 2011. Methods for Constructing a Wild Boar Relative-Density Map to Resolve Human-Wild Boar Conflicts. Mammal Study 36:79–85.

Honda, T., and M. Sugita. 2007. Environmental factors affecting damage by wild boars (Sus scrofa) to rice fields in Yamanashi Prefecture, central Japan. Mammal Study 32:173–176.

Hornseth, M. L., and R. S. Rempel. 2016. Seasonal resource selection of woodland caribou (Rangifer tarandus caribou) across a gradient of anthropogenic disturbance. Canadian Journal of Zoology 94:79–93.

Huynh, T. T. T., A. J. A. Aarnink, W. J. J. Gerrits, M. J. H. Heetkamp, T. T. Canh, H. A. M. Spoolder, B. Kemp, and M. W. A. Verstegen. 2005. Thermal behaviour of growing pigs in response to high temperature and humidity. Applied Animal Behaviour Science 91:1–16.

Ishihara, M., and T. Tadono. 2017. Land cover changes induced by the great east Japan earthquake in 2011. Scientific Reports 7:45769.

Japan Aerospace Exploration Agency. 2016, September. High-Resolution Land Use and Land Cover Map of Japan [2006 - 2011] (Version 16.09). Japan Aerospace Exploration Agency.

Japan Aerospace Exploration Agency. 2018, March. High-Resolution Land Use and Land Cover Map of Japan [2014 - 2016] (Version 18.03). Japan Aerospace Exploration Agency.

Japan Aerospace Exploration Agency. 2021, March. High-Resolution Land Use and Land Cover Map of Japan [2018 - 2020] (Version 21.03). Japan Aerospace Exploration Agency.

Japan Meteorological Agency. 2022, July 31. Past Weather Data Search - Namie. https://www.data.jma.go.jp/obd/stats/etrn/index.php?prec_no=36&block_no=0295&year=&month=&day=&view=.

Johnson, D. H. 1980. The Comparison of Usage and Availability Measurements for Evaluating Resource Preference. Ecology 61:65–71.

Kennish, M. J. 2001. Coastal Salt Marsh Systems in the U.S.: A Review of Anthropogenic Impacts. Journal of Coastal Research 17:731–748.

Keuling, O., N. Stier, and M. Roth. 2009. Commuting, shifting or remaining? Mammalian Biology 74:145–152.

Kight, C. R., M. S. Saha, and J. P. Swaddle. 2012. Anthropogenic noise is associated with reductions in the productivity of breeding Eastern Bluebirds (Sialia sialis). Ecological Applications 22:1989–1996.

Kodera, Y., N. Kanzaki, Y. Kaneko, and K. Tokida. 2001. Habitat selection of Japanese wild boar in Iwami district, Shimane Prefecture, western Japan. Wildlife Conservation Japan 6:119–129.

Köppen, W. 1936. Das geographische System der Klimate, Handbuch der Klimatologie. Borntraeger, Berlin.

Kramer, C. J., M. R. Boudreau, R. S. Miller, R. Powers, K. C. VerCauteren, and R. K. Brook. 2022. Summer habitat use and movements of invasive wild pigs (Sus scrofa) in Canadian agro-ecosystems. Canadian Journal of Zoology 100:494–506.

La Sorte, F. A., D. Fink, J. J. Buler, A. Farnsworth, and S. A. Cabrera-Cruz. 2017. Seasonal associations with urban light pollution for nocturnally migrating bird populations. Global Change Biology 23:4609–4619.

Lecis, R., O. Dondina, V. Orioli, D. Biosa, A. Canu, G. Fabbri, L. Iacolina, A. Cossu, L. Bani, M. Apollonio, and M. Scandura. 2022. Main roads and land cover shaped the genetic structure of a Mediterranean island wild boar population. Ecology and Evolution 12:e8804.

Lee, S.-M., and W.-S. Lee. 2014. Diet of The Wild boar (Sus scrofa) in Agricultural Land of Geochang, Gyeongnam Province, Korea. Journal of Korean Society of Forest Science 103:307–312.

Li, X., W. Hu, W. V. Bleisch, Q. Li, H. Wang, W. Lu, J. Sun, F. Zhang, B. Ti, and X. Jiang. 2022. Functional diversity loss and change in nocturnal behavior of mammals under anthropogenic disturbance. Conservation Biology 36:e13839.

Lino, A., C. Fonseca, D. Rojas, E. Fischer, and M. J. R. Pereira. 2019. A meta-analysis of the effects of habitat loss and fragmentation on genetic diversity in mammals. Mammalian Biology 94:69–76.

Lodberg-Holm, H. K., H. W. Gelink, A. G. Hertel, J. E. Swenson, M. Domevscik, and S. M. J. G. Steyaert. 2019. A human-induced landscape of fear influences foraging behavior of brown bears. Basic and Applied Ecology 35:18–27.

Long, J. L. 2003. Introduced Mammals of the World : Their History, Distribution, and Influence. CSIRO Publishing, Cambridge, MA.

Lorimer, J., C. Sandom, P. Jepson, C. Doughty, M. Barua, and K. J. Kirby. 2015. Rewilding: Science, Practice, and Politics. Annual Review of Environment and Resources 40:39–62.

Lyons, P. C., K. Okuda, M. T. Hamilton, T. G. Hinton, and J. C. Beasley. 2020. Rewilding of Fukushima's human evacuation zone. Frontiers in Ecology and the Environment 18:127–134.

Massei, G., P. Genov, and B. Staines. 1996. Diet, food availability and reproduction of wild boar in a Mediterranean coastal area.

Matsumura, H., T. Kawana, K. Sekiyama, T. Otani, S. Uematsu, M. Saito, and M. Hiroshi. 2019. Extension of protective fencing is not connected to reduction of paddy damage by wild boars. Wildlife and Human Society 7:23–31.

Michelot, T., R. Langrock, and T. Patterson. 2016. moveHMM: An R package for the analysis of animal movement data. Methods in Ecology and Evolution 7:1308–1315.

Ministry of the Environment. 2018. Decontamination Projects for Radioactive Contamination Discharged by Tokyo Electric Power Company Fukushima Daiichi Nuclear Power Station Accident. Editorial Committee for the Paper on Decontamination Projects http://josen.env.go.jp/en/policy_document/pdf/decontamination_report1807_01.pdf

Moore, M. V., S. M. Pierce, H. M. Walsh, S. K. Kvalvik, and J. D. Lim. 2000. Urban light pollution alters the diel vertical migration of *Daphnia*. SIL Proceedings, 1922-2010 27:779–782.

Murase, K., J. Murase, R. Horie, and K. Endo. 2015. Effects of the Fukushima Daiichi nuclear accident on goshawk reproduction. Scientific Reports 5:9405.

Naimi, B. 2017, June 25. Uncertainty Analysis for Species Distribution Models. CRAN.

Nemoto, Y., H. Oomachi, R. Saito, R. Kumada, M. Sasaki, and S. Takatsuki. 2020. Effects of 137Cs contamination after the TEPCO Fukushima Dai-ichi Nuclear Power Station accident on food and habitat of wild boar in Fukushima Prefecture. Journal of Environmental Radioactivity 225:106342.

Nickel, B. A., J. P. Suraci, M. L. Allen, and C. C. Wilmers. 2020. Human presence and human footprint have non-equivalent effects on wildlife spatiotemporal habitat use. Biological Conservation 241:108383.

Northrup, J. M., M. B. Hooten, C. R. Anderson Jr., and G. Wittemyer. 2013. Practical guidance on characterizing availability in resource selection functions under a use–availability design. Ecology 94:1456–1463.

O'Donnell, K., and J. delBarco-Trillo. 2020. Changes in the home range sizes of terrestrial vertebrates in response to urban disturbance: a meta-analysis. Journal of Urban Ecology 6:juaa014.

Pederson, S. L., M. C. Li Puma, J. M. Hayes, K. Okuda, C. M. Reilly, J. C. Beasley, L. C. Li Puma, T. G. Hinton, T. E. Johnson, and K. S. Freeman. 2020. Effects of chronic low-dose radiation on cataract prevalence and characterization in wild boar (Sus scrofa) from Fukushima, Japan. Scientific Reports 10:4055.

Peel, M. C., B. L. Finlayson, and T. A. McMahon. 2007. Updated world map of the Ko¨ppen-Geiger climate classification. Hydrol. Earth Syst. Sci.:12.

Perino, A., H. M. Pereira, L. M. Navarro, N. Fernández, J. M. Bullock, S. Ceauşu, A. Cortés-Avizanda, R. van Klink, T. Kuemmerle, A. Lomba, G. Pe'er, T. Plieninger, J. M. R. Benayas, C. J. Sandom, J.-C. Svenning, and H. C. Wheeler. 2019. Rewilding complex ecosystems. Science 364.

Prime Minister's Office of Japan. 2013, August 8. 避難指示区域の概念図. http://www.kantei.go.jp/saigai/pdf/20130808gainenzu.pdf

R Core Team. 2019. R: A Language and Environment for Statistical Computing. R, R Foundation for Statistical Computing, Vienna.

Ritzel, K., and T. Gallo. 2020. Behavior Change in Urban Mammals: A Systematic Review. Frontiers in Ecology and Evolution 8.

Rudel, T. K., D. Bates, and R. Machinguiashi. 2002. A Tropical Forest Transition? Agricultural Change, Out-migration, and Secondary Forests in the Ecuadorian Amazon. Annals of the Association of American Geographers 92:87–102.

Schley, L., M. Dufrêne, A. Krier, and A. C. Frantz. 2008. Patterns of crop damage by wild boar (Sus scrofa)in Luxembourg over a 10-year period. European Journal of Wildlife Research 54:589.

Schley, L., and T. J. Roper. 2003. Diet of wild boar Sus scrofa in Western Europe, with particular reference to consumption of agricultural crops. Mammal Review 33:43–56.

Schlichting, P. E., V. Dombrovski, and J. C. Beasley. 2020. Use of abandoned structures by Przewalski's wild horses and other wildlife in the Chernobyl Exclusion Zone. Mammal Research 65:161–165.

Sekizawa, R., K. Ichii, and M. Kondo. 2015. Satellite-based detection of evacuation-induced land cover changes following the Fukushima Daiichi nuclear disaster. Remote Sensing Letters 6:824–833.

Shively, K. J., A. W. Alldredge, and G. E. Phillips. 2005. Elk Reproductive Response to Removal of Calving Season Disturbance by Humans. The Journal of Wildlife Management 69:1073–1080.

Stabach, J. A., L. F. Hughey, R. D. Crego, C. H. Fleming, J. G. C. Hopcraft, P. Leimgruber, T. A. Morrison, J. O. Ogutu, R. S. Reid, J. S. Worden, and R. B. Boone. 2022. Increasing Anthropogenic Disturbance Restricts Wildebeest Movement Across East African Grazing Systems. Frontiers in Ecology and Evolution 10.

Stillfried, M., P. Gras, K. Börner, F. Göritz, J. Painer, K. Röllig, M. Wenzler, H. Hofer, S. Ortmann, and S. Kramer-Schadt. 2017. Secrets of Success in a Landscape of Fear: Urban Wild Boar Adjust Risk Perception and Tolerate Disturbance. Frontiers in Ecology and Evolution 5.

Tanaka, S. 2012. Accident at the Fukushima Dai-ichi Nuclear Power Stations of TEPCO — Outline & lessons learned—. Proceedings of the Japan Academy. Series B, Physical and Biological Sciences 88:471–484.

Tennessen, J. B., S. E. Parks, and T. Langkilde. 2014. Traffic noise causes physiological stress and impairs breeding migration behaviour in frogs. Conservation Physiology 2:cou032.

Thurfjell, H., J. P. Ball, P.-A. Åhlén, P. Kornacher, H. Dettki, and K. Sjöberg. 2009. Habitat use and spatial patterns of wild boar Sus scrofa (L.): agricultural fields and edges. European Journal of Wildlife Research 55:517–523.

VerCauteren, K., J. Beasley, S. Ditchkoff, J. Mayer, G. Roloff, and B. Strickland. 2020. Invasive Wild Pigs in North America: Ecology, Impacts, and Management. CRC Press.

Yamashiro, H., Y. Abe, T. Fukuda, Y. Kino, I. Kawaguchi, Y. Kuwahara, M. Fukumoto, S. Takahashi, M. Suzuki, J. Kobayashi, E. Uematsu, B. Tong, T. Yamada, S. Yoshida, E. Sato, H. Shinoda, T. Sekine, E. Isogai, and M. Fukumoto. 2013. Effects of radioactive caesium on bull testes after the Fukushima nuclear plant accident. Scientific Reports 3:2850.

Zar, J. H. 1976. Watson's nonparametric two-sample test. Behavior Research Methods & Instrumentation 8:513–513.

Table 2.1. Fixed-effect coefficients of 2nd order resource selection models generated to compare the distance to habitat covariates of interest at used and available locations for male and female wild boar (*Sus scrofa leucomystax*) collared inside of the Fukushima Exclusion Zone between 2016 and 2020

	Male					**Female**				
	Estimate	SE	z value	Pr(>|z|)		Estimate	SE	z value	Pr(|z|)	
Water (km)	1.264	0.026	48.372	< 2e-16	***	0.034	0.024	1.434	0.151	
Deciduous (km)	-1.106	0.046	-24.250	< 2e-16	***	-4.852	0.056	-86.689	<2e-16	***
Paddy (km)	-2.546	0.033	-76.658	< 2e-16	***	-2.880	0.036	-80.075	<2e-16	***
Urban (km)	-0.033	0.019	-1.732	0.083	.	-1.311	0.021	-63.669	<2e-16	***
Major Roads (km)	-0.101	0.009	-11.841	< 2e-16	***	-0.219	0.008	-27.405	<2e-16	***

*** indicates $p < 0.001$, * indicates $p < 0.05$, . indicates < 0.1

Table 2.2. Selection coefficients for 3rd order resource selection models generated to compare the distance to habitat covariates of interest at used and available locations for male and female wild boar (*Sus scrofa leucomystax*) collared in the Fukushima Exclusion Zone between 2016 and 2020. Each model was based on data separated by sex and by season (Autumn-Winter: October-March | Spring-Summer: April – September).

	Male Spring-Summer					**Female Spring-Summer**				
	Estimate	Std. Error	z value	Pr(>|z|)		Estimate	Std. Error	z value	Pr(>|z|)	
Water (km)	0.740	0.074	10.058	< 2e-16	***	-0.169	0.063	-2.696	0.007	**
Deciduous (km)	-5.532	0.368	-15.029	< 2e-16	***	-5.658	0.247	-22.903	< 2e-16	***
Evergreen (km)	-1.187	0.325	-3.657	0.000	***	-1.143	0.243	-4.703	0.000	***
Paddy (km)	-2.537	0.156	-16.261	< 2e-16	***	-5.691	0.153	-37.309	< 2e-16	***
Urban (km)	-1.611	0.135	-11.895	< 2e-16	***	-2.835	0.146	-19.480	< 2e-16	***
Minor Road (km)	-1.751	0.158	-11.066	< 2e-16	***	0.519	0.142	3.654	0.000	***
Major Road (km)	-0.249	0.025	-9.955	< 2e-16	***	0.207	0.049	4.190	0.000	***
	Male Autumn-Winter					**Female Autumn-Winter**				
Water (km)	0.092	0.051	1.802	0.072	.	0.588	0.052	11.344	< 2e-16	***
Deciduous (km)	1.423	0.137	10.364	<2e-16	***	-3.049	0.150	-20.347	< 2e-16	***
Evergreen (km)	-5.591	0.194	-28.902	<2e-16	***	1.978	0.135	14.660	< 2e-16	***
Paddy (km)	-2.042	0.088	-23.295	<2e-16	***	-3.335	0.109	-30.746	< 2e-16	***
Urban (km)	-0.883	0.077	-11.463	<2e-16	***	-0.147	0.075	-1.955	0.051	.
Minor Road (km)	-1.416	0.103	-13.734	<2e-16	***	0.562	0.113	4.974	0.000	***
Major Road (km)	0.311	0.016	19.731	<2e-16	***	0.135	0.035	3.824	0.000	***

*** indicates p < 0.001, * indicates p < 0.05, . indicates < 0.1

Table 2.3. Mean step lengths and turn angles for three separate behavioral states of male and female wild boar (*Sus scrofa*) inside and outside of the Fukushima Exclusion Zone (2012-2020) as determined using hidden Markov models.

	Traveling		**Foraging**		**Resting**	
Step Length Parameters	Mean	SD	Mean	SD	Mean	SD
Male Inside	251.043	235.422	34.489	23.506	9.770	7.178
Male Outside	208.557	193.068	29.341	18.221	9.297	6.053
Female Inside	159.520	140.307	35.888	21.204	11.378	8.097
Female Outside	206.473	189.773	60.452	37.283	15.834	11.240

	Traveling		**Foraging**		**Resting**	
Turn Angle Parameters	Mean	Concentration	Mean	Concentration	Mean	Concentration
Male Inside	0.017	0.154	-3.061	0.344	-3.042	0.205
Male Outside	0.073	0.217	-3.066	0.371	3.139	0.273
Female Inside	0.052	0.130	-3.080	0.363	-3.054	0.186
Female Outside	-0.052	0.198	3.040	0.281	-2.969	0.214

Table 2.4. P-values from Watson's two-sample test of homogeneity comparing distributions of resting, foraging, and traveling behaviors between males inside the Fukushima Exclusion Zone (FEZ), males outside the FEZ, females inside the FEZ, and females outside the FEZ. These distributions were based on locational data collected from wild boar (*Sus scrofa leucomystax*) collared in Tohoku, Japan between 2012 and 2022. Each consecutive location was assigned a behavioral state based on a previously generated hidden Markov model.

Resting	Male Inside FEZ	Male Outside FEZ	Female Inside FEZ	Female Outside FEZ
Male - Inside FEZ	X			
Male - Outside FEZ	< 0.001	X		
Female - Inside FEZ	> 0.100	< 0.001	X	
Female - Outside FEZ	< 0.001	< 0.001	< 0.001	X

Foraging	Male Inside FEZ	Male Outside FEZ	Female Inside FEZ	Female Outside FEZ
Male - Inside FEZ	X			
Male - Outside FEZ	< 0.001	X		
Female - Inside FEZ	< 0.050	< 0.001	X	
Female - Outside FEZ	< 0.001	< 0.001	< 0.001	X

Traveling	Male Inside FEZ	Male Outside FEZ	Female Inside FEZ	Female Outside FEZ
Male - Inside FEZ	X			
Male - Outside FEZ	< 0.001	X		
Female - Inside FEZ	< 0.001	< 0.001	X	
Female - Outside FEZ	< 0.001	< 0.001	< 0.001	X

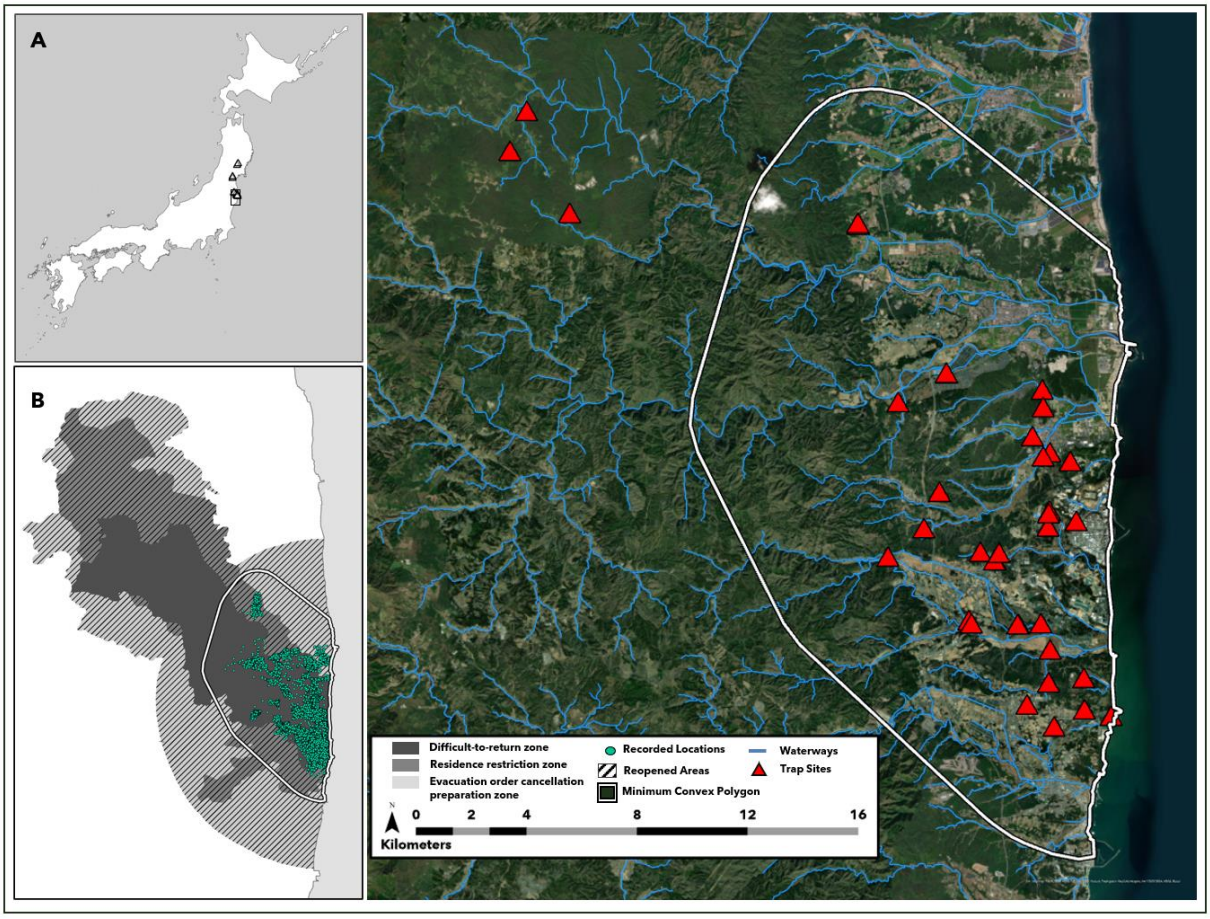

Figure 2.1. Capture sites of 41 wild boar (*Sus scrofa leucomystax*). (A) Capture sites relative to the entire country: including locations of captures in Fukushima, Miyagi, and Iwate prefectures, (B) wild boar GPS locations used in resource selection analysis relative to the boundary of the Fukushima Exclusion Zone (FEZ) with areas of the FEZ that have been opened since initial formation hashed out, (C) Satellite image of the study area for the resource selection analysis with rivers and a minimum complex polygon of coastal boar locations displayed.

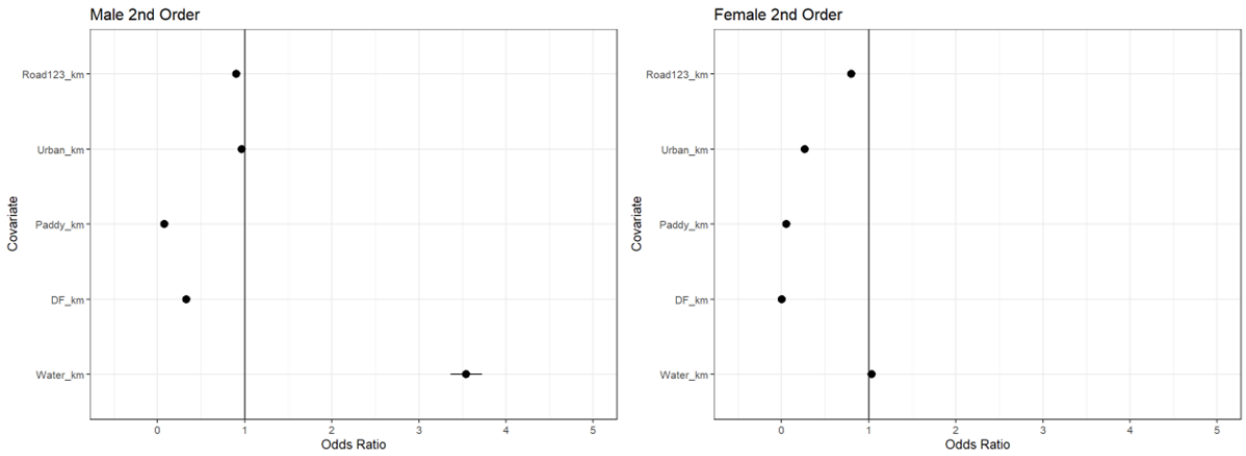

Figure 2.2. Predictive odds ratios with 95% confidence intervals based on 2nd order resource selection models for male and female wild boar (*Sus scrofa leucomystax*) collared in the Fukushima Exclusion Zone between 2016 to 2020.

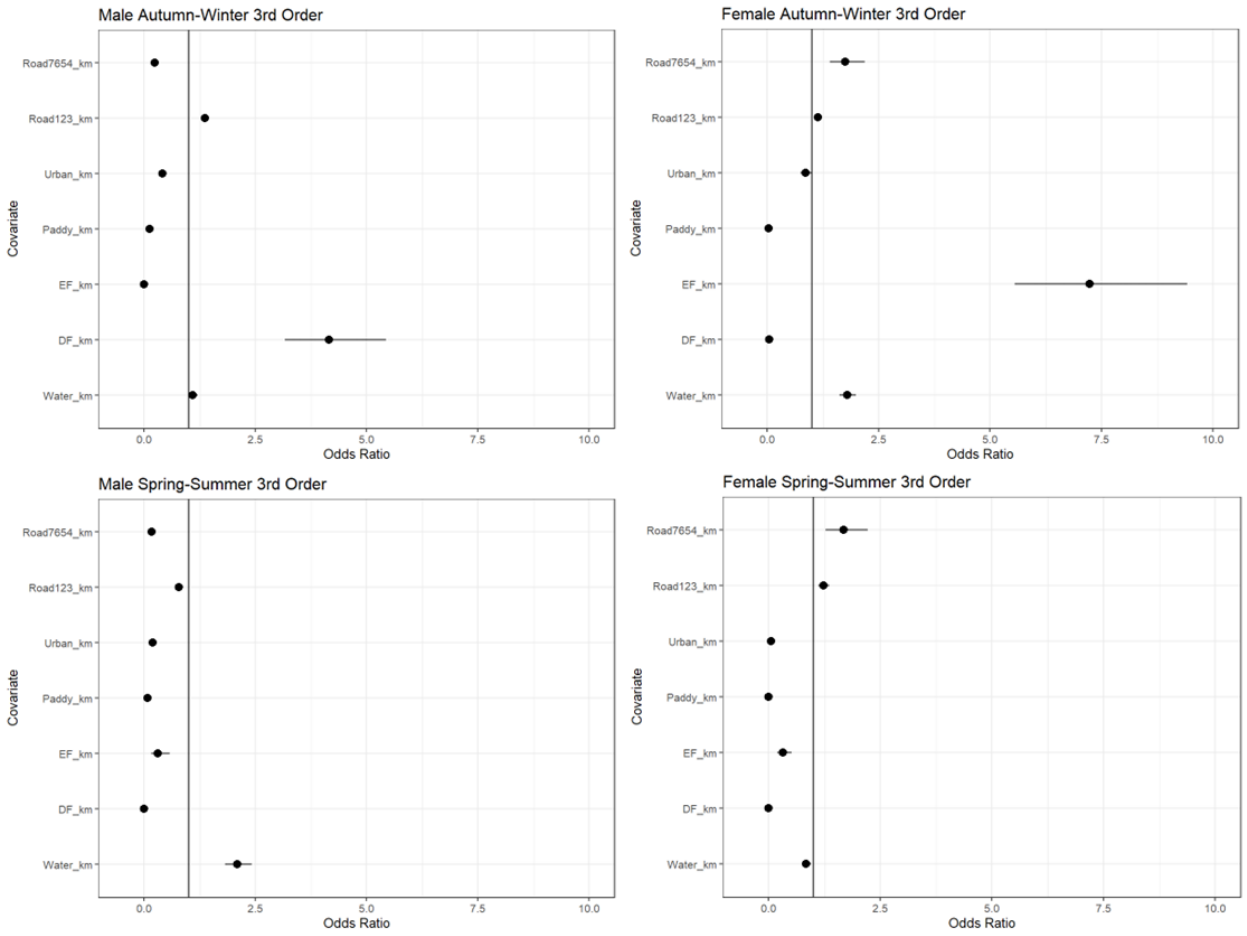

Figure 2.3. Predictive odds ratios with 95% confidence intervals based on 3nd order resource selection models for male and female wild boar (*Sus scrofa leucomystax*) collared in the Fukushima Exclusion Zone between 2016 to 2020.

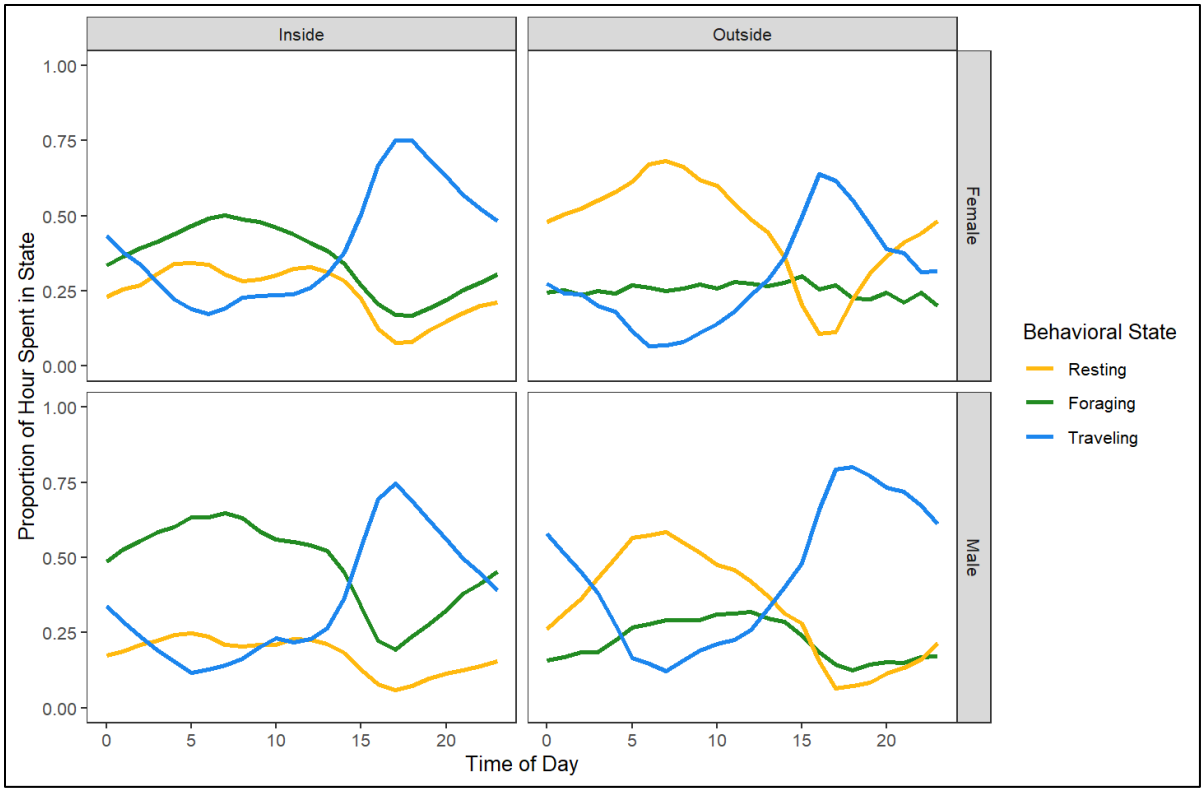

Figure 2.4. Proportion of time of day spent in one of three behavioral states (resting, foraging, and traveling) as determined by a three-state Markov model of wild boar (*Sus scrofa leucomystax*) collared in Tohoku, Japan between 2012 and 2022. Data were divided by location relative to the Fukushima Exclusion Zone (inside or outside) and by sex prior to model generation.

CHAPTER 3

THE IMPACT OF SAMPLING SCALE: A COMPARISON OF METHODS ESTIMATING CONTAMINANT EXPOSURE IN FREE-RANGING WILDLIFE

Introduction

Environmental contamination is a pervasive global problem for both human and environmental health (Boyd 2010, Kim et al. 2015, Manisalidis et al. 2020, Hassaan and El Nemr 2020, Landrigan et al. 2020). The impact of environmental contaminants is often tied to the level at which it is encountered (Arkhipov et al. 1994, Aunan and Pan 2004, Hu et al. 2021, Filippini et al. 2022). Thus, determining contaminant exposure is a fundamental step of ecological risk assessments and is also important in the development of precise dose-effect relationships for exposed biota (USEPA 1996, DOE 2002, 2019, Stark et al. 2017). However, our ability to predict an organism's exposure is at least partially limited by (1) our ability to effectively capture the spatially heterogeneous contaminant levels found across the entire impacted area and (2) our ability to predict how organisms utilize the contaminated area and thus to what level they interact with and are exposed to contamination (Hinton et al. 2013). The level of detail required to generate estimates and the accuracy required from estimated exposures is often quite different depending on whether it is needed for an ecological risk assessment or a research-oriented dose-effect study (USEPA 1996, Suter II et al. 2000, DOE 2002, 2019).

Ecological risk assessors can often avoid the challenge of obtaining detailed exposure information through a stepped approach, in which assessments are performed in successively more rigorous tiers (Suter II et al. 2000). Simple screening-level tiers are used initially, in which simulations of contaminant exposure are generated from conservative input values that purposely

maximize estimates of biota exposure (USEPA 1992, DOE 2002, 2019). The rationale is that if conservative inputs result in simulated exposures less than an approved bench-mark value, then the risk assessor is confident that harmful effects will not be observed in animals exposed to lesser, but unknown exposures. A fundamental assumption of exposure studies is that organisms move randomly throughout an area (USEPA 1996). Thus, contaminant exposure is assumed to be equal to the average contaminant concentration across a usage area (USEPA 1996). However, because it is difficult to ensure that the true contaminant concentration is captured using random survey methods, maximal contaminant levels are often used in exposure modeling during screening steps (USEPA 1996, DOE 2002, 2019). Further, if a population's area of use is larger than the contaminated area, the estimated average contaminant value across an entire contaminated area is thought to be sufficiently conservative for exposure estimates (DOE 2002). However, for large contamination events like the Chernobyl and Fukushima Daiichi Nuclear Power Plant (FDNPP) accidents, it is possible that entire groups of individuals, if not entire populations, spend all their time within the highly contaminated exclusion zones and thus averaging across the contaminated area may not consistently be conservative. Further, it should be noted that organisms almost never move randomly across a landscape and instead are driven by a complex combination of factors (e.g., resources, predators, anthropogenic activity; Laundré et al. 2001, Kay et al. 2017, McNitt et al. 2020, Taubmann et al. 2021, Clontz et al. 2021). Therefore, it is possible that coarse random sampling of the landscape may fail to sample the actual habitat used by an organism and may thereby not adequately capture actual exposure rates.

In contrast, research-oriented exposure studies typically seek realistic, rather than conservative, exposure data so that the uncertainties of derived dose-effect relationships are reduced and a greater confidence in results can be achieved (Bouville et al. 2014). However,

dose-effect relationships derived from chronic exposure to contaminants are rare (Sanchez et al. 2010, Stark et al. 2017). Even when dose-effect relationships are studied, the results are often controversial due to the use of inadequate exposure data (Strand et al. 2014, 2017). The ability to accurately track chronic contaminant exposure is limited by the technical and logistic challenges of placing monitors on wildlife. While wildlife monitors do exist for some contaminants (Hinton et al. 2015, Aramrun et al. 2019), the additional funding and effort required to deploy them makes their use unfeasible for many studies. Thus, even when realistic dose-effect relationships are warranted, many studies rely on simple surveys conducted at or near study sites (i.e., trap sites, transects; Nelson Beyer et al. 1985, Beyer and Stafford 1993, Møller and Mousseau 2009, Lehmann et al. 2016). Although these surveys allow exposures to be estimated easily, the use of these simple methods points to a potentially fallible assumption in exposure science – that an estimate made using minimal data can adequately capture the exposure of wildlife moving through and interacting with a complex contaminated landscape. Research is needed to determine what scale of contaminant data, as well as what scale of animal movement data, combine to effectively produce usable dose-effect relationships from model simulations of chronic exposures to contaminants. Furthermore, the role of fine-scale exposure and whether such heterogeneity needs to be accounted for while estimating exposure is largely unknown.

Determining the impact of fine-scale heterogeneity in contaminant distribution on estimates of contaminant exposure requires knowledge of the true fine-scale distribution of contaminants. However, given limited manpower and funding, assessors may be unable to conduct extensive enough surveys to obtain fine scale knowledge of contaminant distributions. These surveys are made more difficult by the fact that many terrestrial and aquatic contaminants must be measured directly through collection and analysis of field samples (Selid et al. 2009, Li

et al. 2019, Jin et al. 2020). However, some types of radiation from radioactive contamination can be measured remotely with instrumentation (e.g., dosimeters, scintillation detectors) carried by an individual (Andoh et al. 2019), motor vehicle (Andoh et al. 2015), or helicopter (Sanada and Torii 2015). Thus, extensive surveys of radioactive contamination can be conducted with relatively little manpower (Sanada et al. 2019). This ease of survey makes radioactive contamination uniquely suited to answering questions about the impact of fine-scale heterogeneity on external exposure.

The FDNPP accident in 2011 resulted in the deposition of a large amount of radioactive contamination onto the surrounding landscape. Among the radionuclides released were ^{134}Cs and ^{137}Cs, both of which were released in large enough quantities (~13 PBq each; Chino et al. 2011, Kato et al. 2019) and with long enough half-life (2.1 and 30.2 y, respectively) that they continued contributing substantial gamma emissions even after many of the other emitted radionuclides had decayed (Povinec et al. 2013a, Chartin et al. 2013, Nabeshi et al. 2015, Xu et al. 2016, Johansen et al. 2021). Due to uneven radionuclide fallout during the initial disaster (Morino et al. 2013, Draxler et al. 2015), varying rates at which cesium migrates through the landscape (depending on slope, soil clay content, erosion, precipitation, and land cover; Zhang et al. 1994, Fujii et al. 2014, Onda et al. 2020) and focused remediation efforts around abandoned towns (Ministry of the Environment 2018), the contaminated area surrounding the FDNPP is a heterogeneous patchwork of varying activity levels of radionuclides. This heterogeneity may be further amplified by shifting weather patterns between wet and dry seasons, as soil moisture may interfere with gamma emissions and thus alter measured surface dose rates (IAEA 2003, Ajayi et al. 2015). Therefore, it is likely that the exposure encountered by an individual is highly

dependent on their location and that fine-scale movements through small patches of high radiation may affect the overall dose received by an individual.

Due to the extent of the accident, and concerns for human health, the landscape surrounding the FDNPP has been extensively surveyed using multiple survey methods representing broad differences in sampling scale (Sanada and Torii 2015, Andoh et al. 2015, 2019). These differences in sample scale make the Fukushima Exclusion Zone (FEZ) ideal for testing the impact which accounting for fine scale heterogeneity has on the conservativeness (relative to ecological risk analyses) and realism (relative to accurate dose-effect research) of modeled simulated exposure predictions, both in terms of scale of contaminant heterogeneity itself and of how wildlife utilize the landscape.

This study explores the utility of several approaches for predicting an organism's exposure to radiation. At its core, each approach is based on a combination of (1) some method of capturing the spatial distribution of contamination with (2) some method for estimating an organism's spatial movement patterns. Specifically, we are interested in the extent to which finer sampling of contaminant distribution and increasing the complexity of models predicting an organism's movement have on the (1) conservativeness and (2) realism of exposure estimates. We do this by comparing the actual external radiation exposures, collected using GPS-coupled contaminant monitors deployed on Japanese wild boar (*Sus scrofa leucomystax*) within the FEZ, with estimates of exposures made by combining contaminant surveys that vary in how finely they map contaminant distribution with increasingly more complex methods for tracking and predicting an organism's movement. We predicted that (1) estimates made using conservative model inputs, such as the maximum contaminant levels within a reasonable distance to a known location, would produce conservative estimates of external exposure, (2) the average

contaminant concentration across the entire FEZ would not produce conservative estimates of exposure experienced by boar living solely within the contaminated areas, and (3) finer scale contaminant maps combined with more precise locational overlays would generate the most realistic radiation estimates of external exposure encountered by an individual.

Methods

M1 Study Area

In 2011, the combined damage from a massive earthquake and tsunami led to the meltdown of reactors at the FDNPP on the eastern coast of Japan. The FDNPP disaster released large amounts of radionuclides into the ocean and surrounding terrestrial environment (Tanaka 2012), with the highest land contaminant concentrations falling to the northwest of the plant – stretching from the Pacific Ocean towards the Abukuma mountains. The radioactive fallout resulted in the evacuation of 1,150 km^2, forming the FEZ. Since 2011, dose rates have dropped across the FEZ due to both natural processes such as the radioactive decay (half-life ^{134}Cs: 2.1 years, ^{137}Cs: 30.2 years) and the migration of radionuclides into deeper soil layers, as well as remediation efforts (Mikami et al. 2019). However, dose rates have not fallen evenly across the FEZ: remediation efforts are systematically focused around cities (Ministry of the Environment 2018) and natural processes such as radionuclide migration are dependent on localized external factors such as precipitation, land cover, slope and soil type (Zhang et al. 1994, Fujii et al. 2014, Onda et al. 2020).

Near the coast, the FEZ is predominantly composed of a mixture of urban spaces and paddy fields, interspersed with evergreen and deciduous forests along areas of higher elevation. Following abandonment, most paddy fields have slowly transitioned and are now largely composed of grass. Further inland, the FEZ is characterized by rolling mountains composed of a

mixture of evergreen and deciduous forests. Forested areas received the bulk of terrestrial fallout from the FDNPP disaster (Kato et al. 2019). The FEZ has a humid subtropical climate (Köppen, 1936; Peel et al., 2007) with warm summers (study period average 22°C; Japan Meteorological Agency 2022) and cool winters (study period average 5°C; Japan Meteorological Agency 2022). This area is also characterized by a wet season between June and September (average 192 mm precipitation) with drier months the rest of the year (average 76 mm precipitation).

The combination of both initial deposition patterns and variable dose rate reduction have resulted in a heterogeneous patchwork of radiation levels throughout the FEZ. Due to this reduction in dose rates, as of 2020 70% of the FEZ has reopened to the public, while a 350 km^2 area remains officially evacuated (Ministry of Economy, Trade and Industry 2020). We used the original 1,150 km^2 area as our study area because it is the terrestrial area which had, or were suspected to have, the highest radiation levels in the weeks following the disaster. Thus, this area is representative of a boundary which might be used by risk assessors or other parties interested in estimating exposure in a conservative manner. We used a polygon, which was previously generated for a separate study based on an image of the FEZ's boundary (Prime Minister's Office of Japan 2013), to set the boundaries of our contaminant maps.

M2 Trapping and Collaring Information

Hunters captured Japanese wild boar (hereafter: boar) using box live traps within the FEZ between early 2016 and 2018 and gave us access to the boar to be used in this study. Each boar was anesthetized using 5 mg Zoletil and 0.1 mg Domitor per estimated kg mass of animal. While anesthetized, we recorded sex, age, and weight. For a subset of 6 capture locations, we also collected ambient dose rates ($\mu Sv\ h^{-1}$) measured at 1 m above the ground surface with a NaI (TI) scintillation survey meter (Hitachi TCS-172, Tokyo Japan). We then fitted each individual with a

GPS-coupled contaminant monitor. These GPS-coupled contaminant monitors (980 g) allowed for both (1) GPS tracking in harsh field conditions via the GlobalStar satellite array (Vectronic Aerospace, Berlin Germany) and (2) measurements of external exposure to radiation via electronic dosimeters (Mirion Technologies, Atlanta Georgia). Animal locations and external doses from radiation were obtained hourly. These monitors were developed, calibrated, and field tested in a previous study on wild pigs (Hinton et al. 2015) and have been used on wolves (*Canis lupus*) in Chernobyl (Hinton et al. 2019). All captured boar were released at the capture site after processing. Boar capture and processing were done in compliance with the Animal Use Committees of Fukushima University and the University of Georgia, IACUC A2015 05-004-Y3-A6.

M3 Generation of Contaminant Maps

M3.1 Selection of MEXT Surveys

The Ministry of Education, Culture, Sports, Science, and Technology (MEXT) has conducted numerous monitoring surveys with a variety of methods in order to track the dose rates and contaminant concentrations across the area surrounding the FDNPP (Sanada et al. 2014, Saito et al. 2015, Sanada and Torii 2015, Andoh et al. 2015, 2019). In this study, we selected the three surveys that we felt were representative of the type of surveys used in previous contaminant exposure studies and/or that had the greatest potential to adequately capture fine-scale contaminant heterogeneity within our study area. Namely, we used (1) a soil survey from 2011 which we sub-sampled to only include samples near the FEZ, these samples were taken on average 1277 ± 554 m apart and were subsequently kriged (Methods M3.2.1) to a resolution of 550m; (2) a coarser annual soil survey (sub-sampled to near the FEZ; average nearest neighbor distance 3719 ± 854 m), which we subsequently interpolated (Methods M3.2.2) to a 550m

resolution using inverse distance weighting (hereafter: IDW); and (3) annual aerial surveys from which contamination levels were mapped to a resolution of 275 m.

Soil surveys historically have been used to map radionuclides in terrestrial systems, especially when concerned with wildlife that burrow into or live on the ground. However, while small scale contamination events may be directly mapped using soil surveys, for landscape level events – including the FDNPP disaster – the manpower required to comprehensively sample the entire region would be enormous. As a result, both soil surveys used in our study are quite coarse (average nearest neighbor distances 1277 m and 3719 m) when compared to airborne surveys (average nearest neighbor distance 20 to 225 m for unmanned and manned surveys respectively). In this study, we use mathematical models (i.e., IDW, kriging) to interpolate between sparse sampling points and generate contaminant maps covering the FEZ. However, even with interpolation, contaminant maps made from these soil surveys may fail to capture the fine scale heterogeneity seen within the FEZ. In addition, these soil surveys focus on inhabitable areas (Saito et al. 2015) and thus may fail to survey habitats occupied by wildlife but not humans. Furthermore, soil surveys focus on only one potential contaminant reservoir (i.e., the soil column) and thus may fail to capture contaminants present elsewhere in an ecosystem such as contaminants captured on or absorbed into trees (Koizumi et al. 2013, Nishikiori et al. 2015, Ota and Koarashi 2022).

Compared to soil surveys, flyover surveys can return dose rates from a larger region, at a finer spatial scale, and require relatively little manpower. In addition to capturing dose rates exuding from non-soil deposition locations, flyover surveys also have the advantage that they can survey locations that would be difficult to reach in person. However, flyover surveys provide estimates for dose rates at 1 m above the surface (Sanada et al. 2014, Sanada and Torii 2015) and

thus, may not adequately capture the radiation exposure of a terrestrial organism living close to and interacting with soils contaminated with radionuclides.

M3.2 Generation of Soil Contaminant Maps

M3.2.1 Generation of Soil Contaminant Maps Based on 2011 Soil Survey

Following the 2011 accident, the MEXT conducted a relatively extensive soil survey of radionuclide deposition densities ($Bq \cdot m^{-2}$) consisting of 2,200 locations across eastern portions of Fukushima, Miyagi, Yamagata, Tochigi, and Ibaraki prefectures (Saito et al. 2015). We subset the data to only include including locations inside or within 5 kilometers of the FEZ boundary (365 survey locations). Survey sites ranged from 13 to 3842 m away from their nearest neighbor, with an average nearest neighbor distance of 1277 m. At each survey location, the average deposition density from 5 soil samples taken within a 3 x 3 m square were used as a measure of radionuclide concentration (Onda et al. 2015). A depth of 5 cm was used for each soil sample because the majority of contaminants remained in the soil surface layers in the months following the disaster (Onda et al. 2015). Although this survey also recorded the deposition densities of other radionuclides, we focused on ^{134}Cs and ^{137}Cs because they were deposited with great enough quantity and with long enough half-lives that the effects of other radionuclides during our study period were negligible compared to these two (Povinec et al. 2013a, Nabeshi et al. 2015, Xu et al. 2016, Johansen et al. 2021).

For our analysis, we later replaced the average deposition densities where radiocesium was not detected with one-half the limit of detection or one-half the minimum deposition density recorded for each nuclide. The reason for replacing these deposition densities with one-half the limit of detection or minimum detected deposition density, as opposed to replacing with 0, is two-fold. First, deposition densities of ^{134}Cs and ^{137}Cs followed more of a lognormal distribution

than a normal one. Taking the logarithm of deposition densities can transform this lognormal distribution to a more normal one. However, it is impossible to take the log of 0. Thus, using a very small non-zero number allows us to transform deposition densities to a more normal distribution in future steps without having to remove these not-detection datapoints. Second, just because ^{134}Cs and ^{137}Cs were not detected does not necessarily mean that these nuclides were absent from the soil sample. It is possible that both nuclides were present, but at a density lower than that which could be detected. One method of accounting for these extremely low but present deposition densities is to replace not-detected deposition densities with a value greater than 0 but less than the limit of detection.

The 2011 soil survey locations were close enough that we were able to generate an interpolated map using kriging. Due to spatial non-stationarity of deposited cesium (i.e., the mean and variation of deposited cesium changes across space), we used regression kriging. The following process for regression kriging was completed separately with ^{134}Cs and ^{137}Cs deposition densities because we needed separate radionuclide activity concentrations to generate specific dose conversion coefficients that could be used to convert soil radionuclide concentrations into estimated exposures in a later step. We started by transforming the recorded deposition densities to a logarithmic scale. We then fit 8 generalized linear models selected *a priori* with combinations of covariates we thought might affect deposition density: (1) distance from the nuclear power plant to the survey location, (2) angle between the nuclear power plant and the survey location broken into its orthonormal components (x and y), (3) elevation of the survey location, and (4) an interaction term between elevation and angle. The elevation data used for this paper have been provided by Earth Observation Research Center of the Japan Aerospace Exploration Agency (EORC 2019). We generated residuals for each survey location by

subtracting values predicted using the best fit model (i.e., the model with the lowest AIC) from the logarithm of the actual deposition density measured in 2011, for both ^{134}Cs and ^{137}Cs. Model generation was performed using the glm function in the R stats package (version 4.0.3). It should be noted that more complex models for simulating plume direction and deposition following the FDNPP disaster can be found in the literature (Sugiyama et al. 2012, Woo 2013, Povinec et al. 2013b, Kitayama et al. 2018, Fang et al. 2022). However, we decided to use generalized linear models because our aim was to generate a model that could be produced by an individual without extensive modeling experience and without extensive knowledge of the true layout of radionuclides. Finally, we generated two kriged surfaces of residuals using Ordinary kriging with a spherical model and no assumption of anisotropy via the geostatistical wizard in ArcGIS Pro (version 2.9.0).

We assessed how well the kriged surface worked as a predictive model for locations with unknown residuals by using leave-one-out cross validation using ArcGIS Pro with input locations (version 2.9.0). Specifically, we used cross-validation to check that (1) the predicted values were close to the actual residual inputs and that (2) we minimized smoothing (i.e., the underestimation of variability in the dataset). In leave-one-out cross validation, an interpolation model's parameters were estimated using all known data points (i.e., residuals). One at a time, a single residual was removed and the remaining residuals were combined with this interpolation model to predict the removed value. This process was repeated for all survey locations. In essence, leave-one-out cross validation simulates the process of predicting a value at an unknown locations. Thus, this validation method gave us an idea of how well our kriged surface predicts the residuals at locations that had no actual survey point.

We exported the kriged surfaces as maps with a 550 m resolution; this resolution was selected because it was less than half the average distance between nearest neighbors (Hengl 2006) but still larger than the minimum distance between nearest neighbors. In other words, kriging allowed us to estimate a resolution smaller than the average nearest neighbor distance between soil sampling locations. When exported, these maps represented a predictive map of the residuals which may be present between the log of actual ^{134}Cs and ^{137}Cs deposition densities and those that can be predicted using the best fit generalized linear model discussed previously. We imported each residual map back into R, and back transformed these kriged residual surfaces to maps of deposition densities, and decay corrected them to our survey years (2015-2018) using physical half-lifes (^{134}Cs: 2.1 years, ^{137}Cs: 30.2 years). Finally, we used a soil density map (see below section M3.2.3) to convert these layers from $Bq \cdot m^{-2}$ to $Bq \cdot kg^{-1}$ and extracted the area within the FEZ to form our final contamination maps for ^{134}Cs and ^{137}Cs during each study year (Figure 3.2).

M3.2.2 Generation of Soil Contaminant Maps Based on Yearly Soil Surveys

Since the FDNPP disaster, the Nuclear Regulation Authority and MEXT have conducted yearly surveys every fall to quantify surface deposition densities of gamma-emitting radionuclides ($Bq \cdot m^{-2}$) of regions contaminated by the FDNPP disaster (sampling depth 5 cm) or areas adjacent (Saito and Onda 2015). The contaminated area was divided into 5 km^2 squares, with one survey location per cell provided the area was inhabitable (Saito and Onda 2015). As a result, these yearly soil surveys are even more coarse than the 2011 soil survey. The MEXT surveys typically relied on portable germanium semiconductor detectors to take measurements *in situ* but also used fixed germanium semiconductors in areas with high dose rates. Like the 2011 survey, we focused on ^{134}Cs and ^{137}Cs deposition densities and ignored all other radionuclides.

For our study, we included all soil sample data within 5 km of the FEZ boundaries taken between 2015 and 2018. There were no survey locations where ^{134}Cs or ^{137}Cs was not detected. Due to the scarcity of the data, we were unable to properly fit a kriged surface and instead used interpolated distance weighting (IDW) to generate a yearly deposition density map for both ^{134}Cs and ^{137}Cs for the area inside the FEZ for each of our study years (2015-2018). To parallel the maps produced from 2011 soil surveys, the pixel resolution for this map was 550 m x 550 m. We combined these estimated values with our patched and resampled soil density maps, discussed in section M3.2.3 below, to convert our deposition densities from $Bq \cdot m^{-2}$ to $Bq \cdot kg^{-1}$ for our final maps.

M3.2.3 Generation of Soil Density Map

The ERICA modeling tool (version 2.0; Brown et al. 2016) can simulate external radiation exposures to wildlife using Dose Conversion Coefficients (DCCs) based on soil radioactivity concentrations ($Bq \cdot kg^{-1}$). The ERICA tool is discussed in more detail in section M5. Contamination data from maps made using the MEXT soil surveys report activity concentrations as radioactivity per area ($Bq \cdot m^{-2}$) and must be converted to radioactivity per mass to be usable in ERICA. This conversion is relatively easy if provided with sampling depth and soil density. Therefore, we downloaded a mean soil density map from soilgrids.org around our study area (Longitude: 140.0300 to 142.0300 Degrees, Latitude: 36.4649 to 38.4649 Degrees, Resolution: ~250m; Poggio et al. 2021) with the same soil sampling depth as the MEXT surveys (0-5cm). While this map provided almost continuous coverage of non-urban areas, many urban spaces did not have a recorded soil density. The compaction of urban soils can lead to an increase of soil bulk density compared to its natural state (Gliński and Lipiec 1990), thus we used the maximum soil density recorded within each city boundary to patch missing soil

densities within those city limits. City boundaries were obtained from a shapefile generated by the OCHA Regional Office for Asia and the Pacific (OCHA-ROAP 2019). This patched map was used directly to provide soil densities when converting point soil samples, such as for the nearest sample method, because it maintained the source's original fine scale resolution. However, for converting entire soil maps (such as those used when estimating average activity levels across an entire home range), this fine scale soil density map was resampled using bilinear interpolation to match the resolution (550m) of the produced soil contamination maps produced throughout this study. Resampling and interpolation of the contaminant map was done in ArcGIS Pro (version 2.9.0).

M3.3 Generation of Airborne Contaminant Maps

Every year, in the fall, the MEXT conducts two helicopter surveys over the area contaminated by the FDNPP accident: one manned survey covering the area within 80 km of the FDNPP (Sanada et al. 2014, 2019) and one unmanned survey within 5 km of the reactor (Sanada and Torii 2015, Sanada et al. 2016). The manned survey used a helicopter which flew approximately 150-300 m off the ground (Sanada et al. 2014) and used NaI scintillators to detect the level of gamma rays once a second (~225m apart for survey points used in this study; Sanada et al. 2019). The measurements reported represent the average gamma rays within a 150-300 m radius of the helicopter at ground level (Sanada et al. 2014). An air dose at 1 m above the ground surface was later estimated using these detected values (Sanada et al. 2014, 2019). The unmanned survey used $LaBr_3$:Ce scintillators to detect gamma rays every second (~20m apart for survey points used in this study) along a typical flight altitude of 80 m (Sanada and Torii 2015). Each reported sample represented the average of gamma rays detected across an 80 m radius at ground level (Sanada and Torii 2015). Like the manned survey, detected values were later used

to calculate air dose rates ($\mu Sv \cdot h^{-1}$) at 1 m (Sanada and Torii 2015). We used both surveys to generate a single continuous contaminant map with a resolution of 275 m in ArcGIS Pro (version 2.9.0) by assigning the mean of all survey locations within each map's pixel to that pixel. Neither of the airborne surveys took measurements directly over the nuclear power plant. We patched this area using inverse distance weighting interpolation. Finally, we extracted the area within the FEZ to generate our final yearly airborne contamination maps.

M4 Extraction of Data Based on Boar Locations

Depending on the availability of resources, species of interest, and effort put into collecting and analyzing locational data for biota, approximations of the total area used by an individual animal can be generated with variable levels of confidence. To test the effect of increased knowledge of animal movements on the conservativeness and realism of estimated radiation dose, we created simulations using three levels of collected locational data: no known locations, one known location (i.e., trap site), and many locations collected using a GPS collar.

M4.1 No Available Locational Data External Exposure Estimates

To simulate a scenario that has no known location data about a species of interest, we generated averages of mapped soil activity and airborne external dose across the entire study area. To do this, we overlayed the FEZ on contaminant maps closest, temporally, to the period in which each boar was collared. For maps generated using soil surveys, we extracted the average soil activity ($Bq \cdot kg^{-1}$) within the FEZ boundaries. We then converted this soil activity level into an estimate of external exposure ($\mu Gy \cdot h^{-1}$) using the ERICA assessment tool (version 2.0) in a process described in detail in section M5. For maps generated based on airborne surveys, we directly converted the averaged the extracted external dose ($\mu Sv \cdot h^{-1}$) extracted across the entire FEZ to external exposure ($\mu Gy \cdot h^{-1}$) in a 1:1 conversion.

M4.2 One Known Location External Exposure Estimates

M4.2.1 External Exposure Estimated from Dose Rate at Trap Site

We then simulated a scenario in which a dosimeter was used to take a single dose measurement at a trap site or other point of interest. To do this, we used the dosimeter reading recorded at 6 trap sites and for the remaining boar (n=10) without a trap site dose measurement we estimated an hourly dose rate by using the first hourly exposure (μGy) recorded by the collar. To ensure that anesthesia was properly reversed, all boar stayed at the trap site, with their GPS-coupled dosimeter collars turned on, for several hours prior to their release. Thus, early dose rate signals from the collars are valid measurements of contaminant exposure at the trap site. Because the collar also picks up internal exposure, we converted this first hourly record to an external exposure by subtracting the internal exposure previously collected from the individual itself or inferred from other boar trapped near the trap site.

M4.2.2 External Exposure Estimated from Nearest Survey Location to Trap Site

Next, we used the dose from the nearest soil survey location to each trap site, to simulate a scenario in which external exposure is estimated using nearby survey locations directly. For each survey type (i.e., yearly soil surveys, dose corrected 2011 survey, airborne surveys) we used the survey year that was closest temporally to the period in which each boar was collared. For soil surveys, we converted the point survey location from $Bq \cdot m^{-2}$ to $Bq \cdot kg^{-1}$ using the fine-scale patched soil density map, as opposed to the resampled soil density map. This soil activity concentration was then converted into an external dose estimate using the process discussed in section M5. We directly used the nearest airborne survey point as an external dose estimate for each boar.

M4.2.3 External Exposure Estimated from Highest Exposure Near Trap Site

Previous wild boar studies seeking a conservative estimate for external radiation exposure, and not having GPS-dosimeters on animals, generated a maximum plausible lifetime dose by using the highest contamination value within 5 kilometers of a boar's trap site (e.g., Pederson et al. 2020). To simulate this, we generated a circle with a radius of 5 kilometers, centered on each trap site, and overlayed it on the contaminant maps closest temporally to the period in which a boar was collared. Five kilometers was previously selected because it was thought to be large enough to encompass a boar's actual home range. We extracted the highest soil activity level for each radionuclide and airborne dose rate within this 5 km radius as the maximum plausible exposure for each individual. This soil activity level ($Bq \cdot kg^{-1}$) was converted to an external exposure estimate ($\mu Gy \cdot h^{-1}$) using the process described in section M5. Airborne dose rates ($\mu Sv \cdot h^{-1}$) were converted directly to external exposure estimates ($\mu Gy \cdot h^{-1}$) in a 1:1 conversion.

M4.2.4 External Exposure Estimated from Presumptive Home Range

We expanded upon the previous method, in which one known location was available, and simulated a situation in which basic home range attributes (such as typical size) is also known. For this scenario, we used a home range with an area of 1.1 km^2 based on the average of previously published home range sizes for Japanese wild boar (Kodera et al., 2001). We overlayed this plausible home range on each temporally appropriate contaminant map and extracted an average soil activity level and airborne external exposure across this area. The average soil activity ($Bq \cdot kg^{-1}$) was used to generate an external exposure estimate ($\mu Gy \cdot h^{-1}$) as described in section M5. The average airborne dose rates ($\mu Sv \cdot h^{-1}$) were directly converted (1:1) to external exposure estimates ($\mu Gy \cdot h^{-1}$).

M4.3 Multiple Known Locations External Exposure Estimates

Finally, we simulated studies in which individual animals were collared with GPS devices that track locations at routine (e.g., hourly) intervals. Like estimates made using one known location, we used several methods to convert GPS locations into estimates of spatial use by individual boar: estimating exposure using a 99% home range, 50% core area, weighted home range, and rasterized probability mass function (hereafter: rPMF). It should be noted that for each of these estimates we excluded the first 48 hours of data to prevent any changes in behavior caused by collaring from influencing our results.

M4.3.1 External Exposure Estimates Based on 99% Home Range or 50% Core Area

The 99% home range and 50% core area both represent scenarios in which isopleths are generated using GPS locations (i.e., equal utilization across the use area is assumed). We generated 99% and 50% autocorrelated kernel density estimates for each wild boar (Fleming et al. 2015) based on recorded GPS locations using the ctmm package version 0.6.0 (Calabrese et al. 2016). We overlayed these isopleths on the contaminant maps closest temporally to the period in which a boar was collared and extracted an average soil activity and average airborne dose rate. We converted the average soil activity ($Bq \cdot kg^{-1}$) to an external exposure ($\mu Gy \cdot h^{-1}$) using the process described in section M5. The average airborne dose rate ($\mu Sv \cdot h^{-1}$) was used directly as an estimate of external exposure ($\mu Gy \cdot h^{-1}$).

M4.3.2 External Exposure Estimates Based on Weighted Home Range or Rasterized Probability Mass Function

The weighted home range and rPMF both represent scenarios in which unequal usage of a home range are accounted for. These options may be more optimal for individuals dealing with study species with large home ranges but small core areas. In the case of the weighted home

range, the external exposure within the core area represents approximately 50.5% of the estimate exposure regardless if it takes up 50.5% of the 99% home range. In the case of the rPMF, each pixel of the soil and airborne contamination maps is weighted corresponding to the likelihood a boar spent time in it.

To generate a weighted home range, we separated the 99% home range into the area inside and outside of the 50% core area and found averages of soil activity and airborne activity in both respective areas. We then generated a weighted average of soil activity and airborne external exposure using the following equation: weighted average = ($average_{inside}$ * 50/99) + ($average_{outside}$ * 49/99). We used a denominator of 99 rather than 100 because we used a 99% home range instead of one accounting for 100% usage.

To generate a rPMF, we regenerated utilization distributions using autocorrelated kernel density estimates with the ctmm package (version 0.6.0). However, for this analysis we set the resolution and grid size to match that of the soil and airborne maps such that each pixel within the rPMF would align with the raster contamination maps. We exported these utilization distributions using the raster function of the raster package (version 3.5-2) specifying that the PMF distribution function should be used. Specifying PMF when exporting a raster ensures that the exported value of each map pixel is the total probability of usage within that pixel. We then overlayed the rPMF on the temporally appropriate contaminant map and summed the product of the exported probability with the soil activity or airborne external exposure to generate fine scale weighted averages. Weighted averages of soil activity levels ($Bq \cdot kg^{-1}$) were converted to external exposure estimates ($\mu Gy \cdot h^{-1}$) using the process outlined in section M5. Weighted averages of airborne dose rates ($\mu Sv \cdot h^{-1}$) were used directly as estimates of external exposure ($\mu Gy \cdot h^{-1}$).

M5 Exposure Simulation with the ERICA Tool

The ERICA Tool (Larsson 2008, Brown et al. 2016) is software designed to assist with tiered risk assessments through the simulation of dose rates encountered by biota when provided nuclide specific activity concentrations. In this study, we used ERICA (version 2.0, Tier 2 Assessment) to convert previously estimated soil activity levels ($Bq \cdot kg^{-1}$) into external exposure estimates ($\mu Gy \cdot h^{-1}$). In addition to our initial soil activity estimates, this process also required details regarding the typical size of boar and soil moisture.

M5.1 Generation of Model Organism in ERICA

The ERICA Tool uses elliptical organisms in its simulations of exposure. In this study, we used two sizes of ellipsoids to model our collared boar: large (75 kg, 1.3 m in length, 0.5 m width, 0.5 m height) and small (45 kg, 1.0 m length, 0.4 m width, and 0.4 m height). We used the first large ellipsoid to estimate exposures for collared boar whose weights were greater than or equal to 60 kg and the second small ellipsoid for collared boar whose weights were less than 60 kg. We specified within ERICA that these model organisms were terrestrial, spending all their time on the ground.

M5.2 Generation of Soil Dryness Metric for Individual Boar

Soil moisture attenuates radionuclide gamma emissions (Ajayi et al. 2015) coming from the soil column, thus reducing external exposure to biota. Accounting for this attenuation may improve the realism in estimating external exposure from soil activity data. We obtained soil moisture data within the FEZ and calculated average monthly soil moistures across the FEZ (JAXA JPMAP System 2017) by averaging city specific monthly soil data based on the proportion of the FEZ each city takes up. Because soil moisture varies by month, especially between the dry and wet season, we calculated a unique soil moisture metric for each boar based

on the period in which it was monitored. We calculated this metric by averaging the previously calculated FEZ monthly average across all months a boar was collared. Finally, because the ERICA tool specifically requests soil dryness percentage, as opposed to soil moisture, we quantified soil dryness by subtracting this soil moisture metric from 100.

M5.3 Conversion of Average Soil Activity Concentration to External Dose

Alongside organism size and soil dryness, we inputted our previously estimated ^{134}Cs and ^{137}Cs soil activity levels (section M4) into ERICA. We then recorded the reported radionuclide specific external doses. These external doses were subsequently combined in R to produce a single external exposure estimate for each boar given a specific method.

M6 Comparison to Actual

Finally, we compared external exposures ($\mu Gy \cdot h^{-1}$) estimated from the various contaminant mapping and animal use regimes to the average hourly external exposure empirically measured by the GPS-dosimeters for each boar over their monitoring period. In the case of methods that used no known location or one known location, we used the entire collar period to calculate this average actual exposure. However, for methods relying on GPS collar data we excluded the first 2-3 days post-collaring of recorded exposure rates such that they matched the dataset used in generating home ranges and rPMFs. For each method used to estimate external exposure (i.e., each type of locational overlay and contaminant map combination or manual survey conducted), we used a one tailed paired t-test to determine if estimated external exposures were significantly greater than actual external exposures (alpha = 0.05). To compare how realistic the results produced by each method were, we calculated a coefficient of determination (R^2) based on a linear model between predicted and actual external

exposures. We considered $R^2 \geq 0.75$ to be strongly correlated, 0.50-0.74 to be moderate, and 0.25-0.49 to be weakly correlated.

Results

R1 Trapping and Collaring

We collared 16 wild boar (4 males, 12 females) within the FEZ between January 2016 and October 2018. After removing the first two days of locations post-collaring, we had 22,830 GPS fixes for use in GPS overlays. Each boar was collared for an average of 68.5 ± 49.6 days.

R2 Soil and Airborne Contaminant Maps

R2.1 Contaminant Maps Based on 2011 Soil Survey

Of the 8 generalized linear models tested to predict deposition densities of ^{134}Cs and ^{137}Cs, we found that the best model included all possible covariates: distance to FDNPP, elevation, angle to FDNPP, and an interaction between elevation and angle (Table 3.1). Using the residuals generated based on these models, we were able to fit kriged maps based on 2011 data with adequate cross-validation results (Figure 3.1, Table 3.2). Once complete, the decay corrected contaminant maps predicted that the highest levels of radiation extended to the northwest of the FDNPP (Figure 3.2) and that both ^{134}Cs and ^{137}Cs decayed each year over our study period (Table 3.3).

R2.2 Contaminant Maps Based on Yearly Soil Surveys

Similar to the contaminant maps made from the 2011 survey, the contaminant maps based on a yearly soil also predicted that the highest levels of radiation would be encountered to the north of the FDNPP (Figure 3.2). However, unlike the decay corrected contaminant maps, predicted radionuclide concentration did not always decrease across our survey years (Table 3.3).

R2.3 Contaminant Maps Based on Airborne Surveys

We also found the contaminant maps based on airborne surveys predicted the highest levels of terrestrial radiation would be encountered to the northwest of the FDNPP. Like the decay corrected contaminant maps, average dose rates decreased across our survey years (Table 3.3).

R3 Comparison of Predicted to Actual External Exposures

R3.1 No Available Location External Exposure Estimates

Regardless of which contaminant map was used, averaging the external exposure across the entire FEZ rarely resulted in a conservative nor a realistic estimate of external exposure. In fact, this method only produced conservative estimates for two boar, in which all contaminant maps produced estimated external exposures greater than the actual exposures. In all other cases, the estimated value was less than the actual exposure. Similarly, this method was unable to consistently estimate realistic external exposures (R^2 ranging from 0 to 0.03) (Figure 3.3).

R3.2 One Known Location External Exposure Estimates

Of the one known location methods (i.e., sample at trap site, nearest survey location, presumptive home range, and maximum external exposure within 5km of the trap site), only finding the maximum dose within a 5km radius of the trap site resulted in a consistently conservative estimate. Furthermore, this conservativeness was maintained regardless of which contamination map was used. Although this method also produced weak correlations between the estimated and actual exposures when overlayed on kriged 2011 soil contaminant maps (R^2 = 0.37), there was virtually no correlation using the other two contaminant maps (i.e., R^2 0.05 and 0.07) (Figure 3.3).

The remaining methods failed to produce consistently conservative estimates, but several methods produced estimates that may be adequate in terms of accuracy depending on the goals of a study. The presumptive home range was the most consistently realistic among the methods evaluated: producing R^2 values indicating moderate correlations when overlayed on an airborne contaminant map ($R^2 = 0.62$) and weak correlations using the decay corrected kriged soil contaminant map ($R^2 = 0.46$) (Figure 3.3). The nearest survey location also produced moderate correlations when the airborne contaminant map was used ($R^2 = 0.58$) but failed to produce reliable correlations when the other two contaminant maps were used ($R^2 = 0.01$ and 0.03) (Figure 3.3). In general, the contaminant map created using the coarse yearly soil surveys performed poorly (R^2 between 0.01 and 0.07) (Figure 3.3). Finally, estimates of external exposure based on measurements at the trap site were poorly correlated to actual exposures ($R^2 = 0.17$) (Figure 3.3).

R3.3 Multiple Known Locations External Exposure Estimates

The most consistently realistic methods for producing external exposure estimates were overlays based on actual GPS data combined with the fine scale airborne contamination maps, all of which produced strong (99% home range $R^2 = 0.78$, weighted home range $R^2 = 0.87$, rPMF $R^2 = 0.89$, 50% home range $R^2 = 0.91$) correlations between estimated and actual exposures (Figure 3.3). Estimates based on the decay corrected kriged contamination maps also may be adequate for some studies with three methods producing moderate correlations (weighted home range $R^2 = 0.5$, rPMF $R^2 = 0.54$, 50% home range $R^2 = 0.56$) and one method producing a weak correlation (99% home range $R^2 = 0.44$) (Figure 3.3). Like the one location methods, the estimates based on yearly soil data failed to produce consistently realistic estimates (99% home range $R^2 = 0.05$, weighted home range $R^2 = 0.05$, rPMF $R^2 = 0.05$, 50% home range $R^2 = 0.06$) (Figure 3.3).

Discussion

Predicting contaminant exposure is an important part of risk assessments and dose-effect research. However, contaminants rarely, if ever, deposit in simple and easy to predict patterns. Instead, contaminant deposition and eventual migration through a landscape generates a patchwork of variable contaminant concentrations. As a result, exposure is highly location dependent and, consequently, predicting exposure levels requires knowledge of both the spatial distribution of contaminants and an ability to predict how an organism might utilize the contaminated area. Using GPS-coupled contaminant monitors attached to wild boar within the FEZ, coupled with simulated exposures derived from varying complexities and sampling scale, here we demonstrate that, in general, more extensive sampling of both contaminants and animal locations result in the most realistic estimates of exposure. Perhaps more importantly, we found that one of the most commonly used methods for estimating external exposure (i.e., using dose rate at a trap site; e.g., Møller and Mousseau 2009, 2013, Lehmann et al. 2016) failed to produce realistic estimates. Contrastingly, our results revealed that conservative estimates did not require extensive knowledge about the true distribution of contaminants or of an organism's actual movements. In fact, conservative estimates of radiation exposure were obtained with relatively little effort, requiring only one known location and a survey which captured at least some areas of higher radiation but could be relatively coarse in and of itself. Collectively, these results indicate that fine-scale heterogeneity plays a role in the actual extent of contaminant exposure an individual encounters, and thus accounting for this heterogeneity is important in dose-effect studies, but that coarser surveys can be used if conservative and not realistic estimates are desired.

Conservative estimates of exposure are important for screening tiers in risk assessments. It is generally assumed that using conservative inputs in contaminant exposure models will result in conservative estimates suitable for those tiers (USEPA 1996, DOE 2019). Therefore, it is not surprising that using maximum external exposures within 5-kilometers of the trap site, we were able to consistently generate conservative estimates. Interestingly, we were able to use the maximum external exposure to generate a conservative estimate regardless of which contaminant map was used and relying on only one known boar location. This result suggests the maximum external exposure method is less sensitive to fine scale heterogeneity and local movement decisions. Provided a large enough radius is used, in our case one that is large enough to encapsulate an individual's home range, and a survey is extensive enough to capture some areas of high external exposure, a conservative estimate can be generated with minimal effort and with scarce datasets.

Contrastingly, we found that using average dose rates and contamination levels across the FEZ did not conservatively estimate the exposure of boar collared within the zone. In fact, estimates made using the average across FEZ tended to underestimate exposure rates, similar to observations by Hinton et al. (2019) for wolves in Chernobyl. A large portion of this underestimation is likely due to sampling bias, due to boar being collared in coastal regions of the FEZ, closest to the damaged reactor, where external exposures are higher than the FEZ average. However, despite this sampling bias, we still felt the lack of conservative estimates using this method should be discussed, especially as it pertains to previous suggestions for generating conservative estimates (DOE 2002, 2019). Specifically, that using an average across a contaminated region should generally give a conservative estimate of exposure (DOE 2019). This suggestion assumes that an individual or population's area of use only overlaps partially

with a contaminated area and will thus also overlap with uncontaminated areas (DOE 2019). However, in our study, the majority of collared boar remained completely within the FEZ and thus may rarely if ever encounter areas with almost no contaminants. Thus, we suggest that the method of using average values across a contaminated area to generate a conservative estimate is not suitable in scenarios where the contaminated area is big enough to contain an individual's entire home range or an entire population, depending on whether an individual or a population is the unit of concern. Instead, we suggest relying on more conservative estimates of exposure, such as using the maximum contaminant level within a reasonable distance to the trap site.

Unlike screening tiers, which rely on conservative estimates, dose-effect studies require accurate knowledge of an individual's received dose. We found that finer scale airborne contaminant surveys combined with GPS collar data resulted in the most realistic estimates of external exposure. Further, as shown by the low R^2 values for all estimates made using the coarse yearly soil surveys, failing to capture finer scale contaminant heterogeneity resulted in poor estimates of exposure even if one accurately captured an individual's movement patterns. However, when contaminant heterogeneity was accounted for, better estimates of an organism's movements generally resulted in better estimates of exposure. Among the GPS overlays on an airborne map, those that accounted for high use areas (50% core area, weighted home ranges, rasterized probability mass functions) were slightly more realistic than simply using a 99% isopleth alone. This supports a previous study in Chernobyl in which area-weighted exposure estimates made using core and 99% usage range were highly correlated with actual external exposure (Hinton et al. 2019). Together, this suggests that capturing both fine scale heterogeneity of contaminants on a landscape and accurately capturing specific areas of higher use by wildlife is important in achieving accurate external exposure estimates.

While using GPS tracking data to estimate habitat use is ideal, it is implausible in many studies. Thus, many studies in radioecology instead use point locations such as a trap site, camera trap, or even the town in which an individual was collected (Hiyama et al. 2012, Akimoto 2014, Boratyński et al. 2014, Murase et al. 2015). Therefore, understanding the extent to which point locations can be used in generating precise dose-effect relationships is important to validating previous studies and in determining methodology needed to achieve goals of future studies. Among the estimates produced using one known location, using a presumptive home range was the most consistently realistic method, producing both a moderate correlation using airborne contamination maps and a weak correlation using the decay corrected kriged contaminant map based on 2011 soil samples (average nearest neighbor: 1277m). Like the 99% isopleth generated using GPS data, this method does not focus on areas of core use but instead on areas of potential use. This is likely why, like GPS overlays, a presumptive home range generates reasonable external exposure estimates using both airborne contaminant maps and decay corrected kriged contaminant maps. However, unlike the 99% home range which at least captures broad selection of resources by wildlife within the landscape, the presumptive home range method does not make any assumptions about the likelihood of use beyond whether it is within a 1.1km^2 circle around a known trap site and thus is not as realistic as GPS estimates. It is possible that further accounting for areas of suspected desirability (Pastorok et al. 1996, Johnson 2002), such as those having desirable resources, may further increase the realism of these presumptive home range estimates. Although wild boar are generalists, preferences for certain resources still occur. For example, wild boar in and around the FEZ generally prefer areas near urban spaces, paddy fields, and deciduous forests at both coarse and fine spatial scales (Chapter 2). Considering previous literature about how contaminant levels can vary by land cover,

accounting for preferences of certain areas and accurately capturing external exposures within those high-use areas likely increases accuracy.

Finally, we found that using dose rate at or near the trap site did not correlate with actual external exposure. This result supports previous skepticism directed towards dose-effect studies which have relied on dose rates estimated from trap site locations (Møller and Mousseau 2009, 2013, Lehmann et al. 2016). However, previous research also indicates that point ambient dose rates may be adequate for estimating exposure to animals with small home ranges (Gerke et al. 2020). This suggests that there may be a lower limit to the scale at which fine-scale contaminant heterogeneity has a significant impact on contaminant exposure. However, more research would be needed to know the exact scale-of-effect. Until more research is conducted, we suggest that those interested in obtaining a realistic exposure use the average of multiple measurements across an animal's presumptive or actual home range rather than single point measurements.

Conclusion

Contamination rarely, if ever, falls in broad and simple patterns and instead deposits to form fine scale heterogeneous patchworks across the landscape. Therefore, although our study was focused on radioactive contamination, we feel that our results have broader implications for other types of contaminants introduced into the environment. Specifically, our results have implications for future research seeking to generate conservative and realistic estimates of exposure following contamination events. In this study we show that accounting for fine scale heterogeneity in exposure estimates greatly increases the estimate's realism. Therefore, when a realistic estimate is desired, we suggest using finer scale contaminant surveys as much as possible. We also recommend using home ranges, whether presumptive or actual, to estimate wildlife locations within produced contaminant maps and avoiding using single point

measurements like ambient dose at trap site. Conservative estimates, on the other hand, require far less effort and likely can be achieved with much more coarse surveys by using inputs which assume maximal exposures. Contrastingly, estimates made using the average contaminant level across the FEZ did not generate conservative estimates, suggesting this method should not be used when an organism spends all its time within a contaminated area.

Acknowledgements

We would like to thank all the impacted towns who allowed us to conduct research within their boundaries. Further, we would like to thank those who worked in the field to trap and collar the boar used in this study. This includes, but is not limited to, members of the Japanese hunting association, D. Anderson, S. Chinn, K. Cunningham, J. Hayes, H. Ishiniwa, M. LiPuma, H. Nagata, Y. Nemoto, and S. Pederson. We would like to thank Dr. Hepinstall-Cymerman, whose insight was invaluable during steps involving kriging in ArcGIS Pro. We would like to thank G. Wittemyer and J. Hepinstall-Cymerman for their guidance and feedback of this study. Funding for this study was provided by Colorado University, Fukushima University, the Research Council of Norway Centres of Excellence (project number 223268/F50), the University of Georgia, and the U.S. Department of Energy Office of Environmental Management (award number DE-EM0005228). The soil moisture data that was used in this paper was supplied by the JPMAP System, Japan Aerospace Exploration Agency (JAXA).

References

Ajayi, N., D. Abajingin, and O. Olowomofe. 2015. Soil Moisture and its Effect on Gamma Radiation Level at the Air Ground Interface. European Journal of Basic and Applied Sciences 2:72–77.

Akimoto, S. 2014. Morphological abnormalities in gall-forming aphids in a radiation-contaminated area near Fukushima Daiichi: selective impact of fallout? Ecology and Evolution 4:355–369.

Andoh, M., Y. Nakahara, S. Tsuda, T. Yoshida, N. Matsuda, F. Takahashi, S. Mikami, N. Kinouchi, T. Sato, M. Tanigaki, K. Takamiya, N. Sato, R. Okumura, Y. Uchihori, and K. Saito. 2015. Measurement of air dose rates over a wide area around the Fukushima Dai-ichi Nuclear Power Plant through a series of car-borne surveys. Journal of Environmental Radioactivity 139:266–280.

Andoh, M., H. Yamamoto, T. Kanno, and K. Saito. 2019. Measurement of ambient dose equivalent rates by walk survey around Fukushima Dai-ichi Nuclear Power Plant using KURAMA-II until 2016. Journal of Environmental Radioactivity 210:105812.

Aramrun, K., N. A. Beresford, L. Skuterud, T. H. Hevrøy, J. Drefvelin, K. Bennett, C. Yurosko, P. Phruksarojanakun, J. Esoa, M. Yongprawat, A. Siegenthaler, R. Fawkes, W. Tumnoi, and M. D. Wood. 2019. Measuring the radiation exposure of Norwegian reindeer under field conditions. The Science of the Total Environment 687:1337–1343.

Arkhipov, N. P., N. D. Kuchma, S. Askbrant, P. S. Pasternak, and V. V. Musica. 1994. Acute and long-term effects of irradiation on pine (Pinus silvestris) strands post-Chernobyl. The Science of the Total Environment 157:383–386.

Aunan, K., and X.-C. Pan. 2004. Exposure-response functions for health effects of ambient air pollution applicable for China – a meta-analysis. Science of The Total Environment 329:3–16.

Beyer, W. N., and C. Stafford. 1993. Survey and evaluation of contaminants in earthworms and in soils derived from dredged material at confined disposal facilities in the Great Lakes Region. Environmental Monitoring and Assessment 24:151–165.

Boratyński, Z., P. Lehmann, T. Mappes, T. A. Mousseau, and A. P. Møller. 2014. Increased radiation from Chernobyl decreases the expression of red colouration in natural populations of bank voles (Myodes glareolus). Scientific Reports 4:7141.

Bouville, A., M. S. Linet, M. Hatch, K. Mabuchi, and S. L. Simon. 2014. Guidelines for Exposure Assessment in Health Risk Studies Following a Nuclear Reactor Accident. Environmental Health Perspectives 122:1–5.

Boyd, R. S. 2010. Heavy Metal Pollutants and Chemical Ecology: Exploring New Frontiers. Journal of Chemical Ecology 36:46–58.

Brown, J. E., B. Alfonso, R. Avila, N. A. Beresford, D. Copplestone, and A. Hosseini. 2016. A new version of the ERICA tool to facilitate impact assessments of radioactivity on wild plants and animals. Journal of Environmental Radioactivity 153:141–148.

Chartin, C., O. Evrard, Y. Onda, J. Patin, I. Lefèvre, C. Ottlé, S. Ayrault, H. Lepage, and P. Bonté. 2013. Tracking the early dispersion of contaminated sediment along rivers draining the Fukushima radioactive pollution plume. Anthropocene 1:23–34.

Chino, M., H. Nakayama, H. Nagai, H. Terdada, G. Katata, and H. Yamazawa. 2011. Preliminary Estimation of Release Amounts of 131I and 137Cs Accidentally Discharged from the Fukushima Daiichi Nuclear Power Plant into the Atmosphere. Journal of Nuclear Science and Technology 48:1129–1134.

Clontz, L. M., K. M. Pepin, K. C. VerCauteren, and J. C. Beasley. 2021. Behavioral state resource selection in invasive wild pigs in the Southeastern United States. Scientific Reports 11:6924.

DOE (U.S. Department of Energy). 2002. A Graded Approach for Evaluating Radiation Doses to Aquatic and Terrestrial Biota. DOE-STD-1153-2002. Standard, U.S. Department of Energy, Washington, DC 20585.

DOE (U.S. Department of Energy). 2019. A Graded Approach for Evaluating Radiation Doses to Aquatic and Terrestrial Biota. DOE-STD-1153-2019. U.S. Department of Energy, Washington, DC 20585.

Draxler, R., D. Arnold, M. Chino, S. Galmarini, M. Hort, A. Jones, S. Leadbetter, A. Malo, C. Maurer, G. Rolph, K. Saito, R. Servranckx, T. Shimbori, E. Solazzo, and G. Wotawa. 2015. World Meteorological Organization's model simulations of the radionuclide dispersion and deposition from the Fukushima Daiichi nuclear power plant accident. Journal of Environmental Radioactivity 139:172–184.

EORC (Earth Observation Research Center), 2019, March 15. ALOS Global Digital Surface Model "ALOS World 3D - 30m (AW3D30)." Japan Aerospace Exploration Agency.

Fang, S., S. Zhuang, D. Goto, X. Hu, L. Sheng, and S. Huang. 2022. Coupled modeling of in- and below-cloud wet deposition for atmospheric 137Cs transport following the Fukushima Daiichi accident using WRF-Chem: A self-consistent evaluation of 25 scheme combinations. Environment International 158:106882.

Filippini, T., L. A. Wise, and M. Vinceti. 2022. Cadmium exposure and risk of diabetes and prediabetes: A systematic review and dose-response meta-analysis. Environment International 158:106920.

Fujii, K., S. Ikeda, A. Akama, M. Komatsu, M. Takahashi, and S. Kaneko. 2014. Vertical migration of radiocesium and clay mineral composition in five forest soils contaminated by the Fukushima nuclear accident. Soil Science and Plant Nutrition 60:751–764.

Gerke, H. C., T. G. Hinton, T. Takase, D. Anderson, K. Nanba, and J. C. Beasley. 2020. Radiocesium concentrations and GPS-coupled dosimetry in Fukushima snakes. Science of The Total Environment 734:139389.

Gliński, J., and J. Lipiec. 1990. Soil Physical Conditions and Plant Roots. CRC Press, Boca Raton.

Hassaan, M. A., and A. El Nemr. 2020. Pesticides pollution: Classifications, human health impact, extraction and treatment techniques. The Egyptian Journal of Aquatic Research 46:207–220.

Hengl, T. 2006. Finding the right pixel size. Computers & Geosciences 32:1283–1298.

Hinton, T. G., M. E. Byrne, S. Webster, and J. C. Beasley. 2015. Quantifying the spatial and temporal variation in dose from external exposure to radiation: a new tool for use on free-ranging wildlife. Journal of Environmental Radioactivity 145:58–65.

Hinton, T. G., M. E. Byrne, S. C. Webster, C. N. Love, D. Broggio, F. Trompier, D. Shamovich, S. Horloogin, S. L. Lance, J. Brown, M. Dowdall, and J. C. Beasley. 2019. GPS-coupled contaminant monitors on free-ranging Chernobyl wolves challenge a fundamental assumption in exposure assessments. Environment International 133:105152.

Hinton, T. G., J. Garnier-Laplace, H. Vandenhove, M. Dowdall, C. Adam-Guillermin, F. Alonzo, C. Barnett, K. Beaugelin-Seiller, N. A. Beresford, C. Bradshaw, J. Brown, F. Eyrolle, L. Fevrier, J.-C. Gariel, R. Gilbin, T. Hertel-Aas, N. Horemans, B. J. Howard, T. Ikäheimonen, J. C. Mora, D. Oughton, A. Real, B. Salbu, M. Simon-Cornu, M. Steiner, L. Sweeck, and J. Vives i Batlle. 2013. An invitation to contribute to a strategic research agenda in radioecology. Journal of Environmental Radioactivity 115:73–82.

Hiyama, A., C. Nohara, S. Kinjo, W. Taira, S. Gima, A. Tanahara, and J. M. Otaki. 2012. The biological impacts of the Fukushima nuclear accident on the pale grass blue butterfly. Scientific Reports 2:570.

Hu, X. F., M. Lowe, and H. M. Chan. 2021. Mercury exposure, cardiovascular disease, and mortality: A systematic review and dose-response meta-analysis. Environmental Research 193:110538.

IAEA (International Atomic Energy Agency). 2003. Guidelines for radioelement mapping using gamma ray spectrometry data. International Atomic Energy Agency, Vienna, Austria.

Japan Meteorological Agency. 2022, July 31. Past Weather Data Search - Namie. https://www.data.jma.go.jp/obd/stats/etrn/index.php?prec_no=36&block_no=0295&year=&month=&day=&view=.

Jin, M., H. Yuan, B. Liu, J. Peng, L. Xu, and D. Yang. 2020. Review of the distribution and detection methods of heavy metals in the environment. Analytical Methods 12:5747–5766.

Johansen, M. P., D. Anderson, D. Child, M. A. C. Hotchkis, H. Tsukada, K. Okuda, and T. G. Hinton. 2021. Differentiating Fukushima and Nagasaki plutonium from global fallout using 241Pu/239Pu atom ratios: Pu vs. Cs uptake and dose to biota. Science of The Total Environment 754:141890.

Johnson, A. R. 2002. Landscape Ecotoxicology and Assessment of Risk at Multiple Scales. Human and Ecological Risk Assessment: An International Journal 8:127–146.

JAXA JPMAP System (Japan Aerospace Exploration Agency's Public-health Monitor and Analysis Platform System). 2017. Soil Moisture Contents [AMSR-E/AMSR-2]. https://www.jpmap-jaxa.jp/jpmap/en/.

Kato, H., Y. Onda, X. Gao, Y. Sanada, and K. Saito. 2019. Reconstruction of a Fukushima accident-derived radiocesium fallout map for environmental transfer studies. Journal of Environmental Radioactivity 210:105996.

Kay, S. L., J. W. Fischer, A. J. Monaghan, J. C. Beasley, R. Boughton, T. A. Campbell, S. M. Cooper, S. S. Ditchkoff, S. B. Hartley, J. C. Kilgo, S. M. Wisely, A. C. Wyckoff, K. C. VerCauteren, and K. M. Pepin. 2017. Quantifying drivers of wild pig movement across multiple spatial and temporal scales. Movement Ecology 5:14.

Kim, K.-H., E. Kabir, and S. Kabir. 2015. A review on the human health impact of airborne particulate matter. Environment International 74:136–143.

Kitayama, K., Y. Morino, M. Takigawa, T. Nakajima, H. Hayami, H. Nagai, H. Terada, K. Saito, T. Shimbori, M. Kajino, T. T. Sekiyama, D. Didier, A. Mathieu, D. Quélo, T. Ohara, H. Tsuruta, Y. Oura, M. Ebihara, Y. Moriguchi, and T. Shibata. 2018. Atmospheric Modeling of 137Cs Plumes From the Fukushima Daiichi Nuclear Power Plant—Evaluation of the Model Intercomparison Data of the Science Council of Japan. Journal of Geophysical Research: Atmospheres 123:7754–7770.

Koizumi, A., T. Niisoe, K. H. Harada, Y. Fujii, A. Adachi, T. Hitomi, and H. Ishikawa. 2013. 137Cs Trapped by Biomass within 20 km of the Fukushima Daiichi Nuclear Power Plant. Environmental Science & Technology 47:9612–9618.

Landrigan, P. J., J. J. Stegeman, L. E. Fleming, D. Allemand, D. M. Anderson, L. C. Backer, F. Brucker-Davis, N. Chevalier, L. Corra, D. Czerucka, M.-Y. D. Bottein, B. Demeneix, M. Depledge, D. D. Deheyn, C. J. Dorman, P. Fénichel, S. Fisher, F. Gaill, F. Galgani, W. H. Gaze, L. Giuliano, P. Grandjean, M. E. Hahn, A. Hamdoun, P. Hess, B. Judson, A. Laborde, J. McGlade, J. Mu, A. Mustapha, M. Neira, R. T. Noble, M. L. Pedrotti, C. Reddy, J. Rocklöv, U. M. Scharler, H. Shanmugam, G. Taghian, J. A. J. M. van de Water, L. Vezzulli, P. Weihe, A. Zeka, H. Raps, and P. Rampal. 2020. Human Health and Ocean Pollution. Annals of Global Health 86:151.

Larsson, C.-M. 2008. An overview of the ERICA Integrated Approach to the assessment and management of environmental risks from ionising contaminants. Journal of environmental radioactivity 99:1364–70.

Laundré, J. W., L. Hernández, and K. B. Altendorf. 2001. Wolves, elk, and bison: reestablishing the “landscape of fear” in Yellowstone National Park, U.S.A. Canadian Journal of Zoology 79:1401–1409.

Lehmann, P., Z. Boratyński, T. Mappes, T. A. Mousseau, and A. P. Møller. 2016. Fitness costs of increased cataract frequency and cumulative radiation dose in natural mammalian populations from Chernobyl. Scientific Reports 6:19974.

Li, C., K. Zhou, W. Qin, C. Tian, M. Qi, X. Yan, and W. Han. 2019. A Review on Heavy Metals Contamination in Soil: Effects, Sources, and Remediation Techniques. Soil and Sediment Contamination: An International Journal 28:380–394.

Manisalidis, I., E. Stavropoulou, A. Stavropoulos, and E. Bezirtzoglou. 2020. Environmental and Health Impacts of Air Pollution: A Review. Frontiers in Public Health 8.

McNitt, D. C., R. S. Alonso, M. J. Cherry, M. L. Fies, and M. J. Kelly. 2020. Influence of forest disturbance on bobcat resource selection in the central Appalachians. Forest Ecology and Management 465:118066.

Mikami, S., H. Tanaka, H. Matsuda, S. Sato, Y. Hoshide, N. Okuda, T. Suzuki, R. Sakamoto, M. Andoh, and K. Saito. 2019. The deposition densities of radiocesium and the air dose rates in undisturbed fields around the Fukushima Dai-ichi nuclear power plant; their temporal changes for five years after the accident. Journal of Environmental Radioactivity 210:105941.

Ministry of Economy, Trade and Industry. 2020, March 10. 避難指示区域の概念図と各区域の人口及び世帯数について（2020年3月10日). https://www.meti.go.jp/earthquake/nuclear/kinkyu/hinanshiji/2020/200310hinannshijigainennzu_population.pdf.

Ministry of the Environment. 2018. Decontamination Projects for Radioactive Contamination Discharged by Tokyo Electric Power Company Fukushima Daiichi Nuclear Power Station Accident. Editorial Committee for the Paper on Decontamination Projects http://josen.env.go.jp/en/policy_document/pdf/decontamination_report1807_01.pdf

Møller, A. P., and T. A. Mousseau. 2009. Reduced abundance of insects and spiders linked to radiation at Chernobyl 20 years after the accident. Biology Letters 5:356–359.

Møller, A. P., and T. A. Mousseau. 2013. Assessing effects of radiation on abundance of mammals and predator–prey interactions in Chernobyl using tracks in the snow. Ecological Indicators 26:112–116.

Morino, Y., T. Ohara, M. Watanabe, S. Hayashi, and M. Nishizawa. 2013. Episode Analysis of Deposition of Radiocesium from the Fukushima Daiichi Nuclear Power Plant Accident. Environmental Science & Technology 47:2314–2322.

Murase, K., J. Murase, R. Horie, and K. Endo. 2015. Effects of the Fukushima Daiichi nuclear accident on goshawk reproduction. Scientific Reports 5:9405.

Nabeshi, H., T. Tsutsumi, Y. Uekusa, A. Hachisuka, R. Matsuda, and R. Teshima. 2015. Surveillance of Strontium-90 in Foods after the Fukushima Daiichi Nuclear Power Plant Accident. Shokuhin Eiseigaku Zasshi. Journal of the Food Hygienic Society of Japan 56:133–143.

Nishikiori, T., M. Watanabe, M. K. Koshikawa, T. Takamatsu, Y. Ishii, S. Ito, A. Takenaka, K. Watanabe, and S. Hayashi. 2015. Uptake and translocation of radiocesium in cedar leaves following the Fukushima nuclear accident. Science of The Total Environment 502:611–616.

Nelson Beyer, W., O. H. Pattee, L. Sileo, D. J. Hoffman, and B. M. Mulhern. 1985. Metal contamination in wildlife living near two zinc smelters. Environmental Pollution Series A, Ecological and Biological 38:63–86.

OCHA-ROAP (United Nations Office for the Coordination of Humanitarian Affairs Regional Office for Asia and the Pacific). 2019, December 19. Japan - Subnational Administrative Boundaries. https://data.humdata.org/dataset/cod-ab-jpn?.

Onda, Y., H. Kato, M. Hoshi, Y. Takahashi, and M.-L. Nguyen. 2015. Soil sampling and analytical strategies for mapping fallout in nuclear emergencies based on the Fukushima Dai-ichi Nuclear Power Plant accident. Journal of Environmental Radioactivity 139:300–307.

Onda, Y., K. Taniguchi, K. Yoshimura, H. Kato, J. Takahashi, Y. Wakiyama, F. Coppin, and H. Smith. 2020. Radionuclides from the Fukushima Daiichi Nuclear Power Plant in terrestrial systems. Nature Reviews Earth & Environment 1:644–660.

Ota, M., and J. Koarashi. 2022. Contamination processes of tree components in Japanese forest ecosystems affected by the Fukushima Daiichi Nuclear Power Plant accident 137Cs fallout. Science of The Total Environment 816:151587.

Pastorok, R. A., R. D. Nielsen, and M. K. Butcher. 1996. Future directions in modeling wildlife exposure to toxic chemicals. Human and Ecological Risk Assessment: An International Journal 2:570–579.

Pederson, S. L., M. C. Li Puma, J. M. Hayes, K. Okuda, C. M. Reilly, J. C. Beasley, L. C. Li Puma, T. G. Hinton, T. E. Johnson, and K. S. Freeman. 2020. Effects of chronic low-dose radiation on cataract prevalence and characterization in wild boar (Sus scrofa) from Fukushima, Japan. Scientific Reports 10:4055.

Poggio, L., L. M. de Sousa, N. H. Batjes, G. B. M. Heuvelink, B. Kempen, E. Ribeiro, and D. Rossiter. 2021. SoilGrids 2.0: producing soil information for the globe with quantified spatial uncertainty. SOIL 7:217–240.

Povinec, P., K. Hirose, and M. Aoyama. 2013a. Fukushima Accident: Radioactivity Impact on the Environment. Elsevier Inc., Waltham, MA.

Povinec, P. P., M. Gera, K. Holý, K. Hirose, G. Lujaniené, M. Nakano, W. Plastino, I. Sýkora, J. Bartok, and M. Gažák. 2013b. Dispersion of Fukushima radionuclides in the global atmosphere and the ocean. Applied Radiation and Isotopes 81:383–392.

Prime Minister's Office of Japan. 2013, August 8. 避難指示区域の概念図. http://www.kantei.go.jp/saigai/pdf/20130808gainenzu.pdf

R Core Team. 2019. R: A Language and Environment for Statistical Computing. R, R Foundation for Statistical Computing, Vienna.

Saito, K., and Y. Onda. 2015. Outline of the national mapping projects implemented after the Fukushima accident. Journal of Environmental Radioactivity 139:240–249.

Saito, K., I. Tanihata, M. Fujiwara, T. Saito, S. Shimoura, T. Otsuka, Y. Onda, M. Hoshi, Y. Ikeuchi, F. Takahashi, N. Kinouchi, J. Saegusa, A. Seki, H. Takemiya, and T. Shibata. 2015. Detailed deposition density maps constructed by large-scale soil sampling for gamma-ray emitting radioactive nuclides from the Fukushima Dai-ichi Nuclear Power Plant accident. Journal of Environmental Radioactivity 139:308–319.

Sanada, Y., T. Orita, and T. Torii. 2016. Temporal variation of dose rate distribution around the Fukushima Daiichi nuclear power station using unmanned helicopter. Applied Radiation and Isotopes 118:308–316.

Sanada, Y., T. Sugita, Y. Nishizawa, A. Kondo, and T. Torii. 2014. The aerial radiation monitoring in Japan after the Fukushima Daiichi nuclear power plant accident. Progress in Nuclear Science and Technology 4:76–80.

Sanada, Y., and T. Torii. 2015. Aerial radiation monitoring around the Fukushima Dai-ichi nuclear power plant using an unmanned helicopter. Journal of Environmental Radioactivity 139:294–299.

Sanada, Y., Y. Urabe, M. Sasaki, K. Ochi, and T. Torii. 2019. Evaluation of ecological half-life of dose rate based on airborne radiation monitoring following the Fukushima Dai-ichi nuclear power plant accident. Journal of Environmental Radioactivity 210:105816.

Sanchez, Y. A., K. Deener, E. C. Hubal, C. Knowlton, D. Reif, and D. Segal. 2010. Research needs for community-based risk assessment: findings from a multi-disciplinary workshop. Journal of Exposure Science & Environmental Epidemiology 20:186–195.

Selid, P. D., H. Xu, E. M. Collins, M. Striped Face-Collins, and J. X. Zhao. 2009. Sensing Mercury for Biomedical and Environmental Monitoring. Sensors 9:5446–5459.

Stark, K., J. M. Goméz-Ros, J. Vives i Batlle, E. Lindbo Hansen, K. Beaugelin-Seiller, L. A. Kapustka, M. D. Wood, C. Bradshaw, A. Real, C. McGuire, and T. G. Hinton. 2017. Dose assessment in environmental radiological protection: State of the art and perspectives. Journal of Environmental Radioactivity 175–176:105–114.

Strand, P., T. Aono, J. E. Brown, J. Garnier-Laplace, A. Hosseini, T. Sazykina, F. Steenhuisen, and J. Vives i Batlle. 2014. Assessment of Fukushima-Derived Radiation Doses and Effects on Wildlife in Japan. Environmental Science & Technology Letters 1:198–203.

Strand, P., S. Sundell-Bergman, J. E. Brown, and M. Dowdall. 2017. On the divergences in assessment of environmental impacts from ionising radiation following the Fukushima accident. Journal of Environmental Radioactivity 169–170:159–173.

Sugiyama, G., J. Nasstrom, B. Pobanz, K. Foster, M. Simpson, P. Vogt, F. Aluzzi, and S. Homann. 2012. Atmospheric Dispersion Modeling: Challenges of the Fukushima Daiichi Response. Health Physics 102:493–508.

Suter II, G. W., R. A. Efroymson, B. E. Sample, and D. S. Jones. 2000. Ecological Risk Assessment for Contaminated Sites. CRC Press.

Tanaka, S. 2012. Accident at the Fukushima Dai-ichi Nuclear Power Stations of TEPCO — Outline & lessons learned—. Proceedings of the Japan Academy. Series B, Physical and Biological Sciences 88:471–484.

Taubmann, J., J.-L. Kämmerle, H. Andrén, V. Braunisch, I. Storch, W. Fiedler, R. Suchant, and J. Coppes. 2021. Wind energy facilities affect resource selection of capercaillie Tetrao urogallus. Wildlife Biology 2021:wlb.00737.

USEPA (U.S. Environmental Protection Agency). 1992. Supplemental guidance to RAGS: calculating the concentration term. Intermittent Bulletin. Publication 9285.7-081. U.S. Environmental Protection Agency, Office of Solid Waste and Emergency Response, Washington, DC.

USEPA (U.S. Environmental Protection Agency). 1996. Soil Screening Guidance: User's Guide. EPA/540/R-96/018. United States Environmental Protection Agency Office of Soil Waste and Emergency Response, Washington, DC 20460.

Woo, T. H. 2013. Atmospheric modeling of radioactive material dispersion and health risk in Fukushima Daiichi nuclear power plants accident. Annals of Nuclear Energy 53:197–201.

Xu, S., L. Zhang, S. P. H. T. Freeman, X. Hou, A. Watanabe, D. C. W. Sanderson, A. Cresswell, and K. Yamaguchi. 2016. Iodine isotopes in precipitation: Four-year time series variations before and after 2011 Fukushima nuclear accident. Journal of Environmental Radioactivity 155–156:38–45.

Zhang, X., T. A. Quine, D. E. Walling, and Z. Li. 1994. Application of the Caesium-137 Technique in a Study of Soil Erosion on Gully Slopes in a Yuan Area of the Loess Plateau near Xifeng, Gansu Province, China. Geografiska Annaler. Series A, Physical Geography 76:103–120.

Table 3.1 Model selection for the distribution of the logarithm of 2011 deposition densities of ^{134}Cs and ^{137}Cs within 5 kilometers of the Fukushima Exclusion Zone with calculated Akaike Information Criterion values.

	Cesium 134		**Cesium 137**	
Model	AIC	ΔAIC	AIC	ΔAIC
$\log_{10}$(deposition density)~distance to FDNPP + cos(angle to FDNPP) + sin(angle to FDNPP) + elevation + cos(angle to FDNPP):elevation + sin(angle to FDNPP):elevation	**358.50**	**0.00**	**360.73**	**0.00**
$\log_{10}$(deposition density)~distance to FDNPP + cos(angle to FDNPP) + sin(angle to FDNPP) + elevation	582.24	223.75	585.60	224.88
$\log_{10}$(deposition density)~ distance to FDNPP + elevation	604.95	246.45	608.85	248.13
$\log_{10}$(deposition density)~cos(angle to FDNPP) + sin(angle to FDNPP) + elevation	597.77	239.27	602.80	242.07
$\log_{10}$(deposition density)~cos(angle to FDNPP) + sin(angle to FDNPP) + distance to FDNPP	580.31	221.81	583.64	222.91
$\log_{10}$(deposition density)~ cos(angle to FDNPP) + sin(angle to FDNPP)	608.28	249.78	613.73	253.01
$\log_{10}$(deposition density)~elevation	616.26	257.76	620.98	260.26
$\log_{10}$(deposition density)~distance to FDNPP	605.30	246.80	609.02	248.30

Table 3.2 Leave one out cross validation statistics generated by ArcGIS Pro (version 2.9.0) following regression kriging of residuals generated from a generalized linear model of 2011 deposition densities of ^{134}Cs and ^{137}Cs within 5 kilometers of the Fukushima Exclusion Zone.

Statistics	**Cesium 134**	**Cesium 137**
Mean Error	-0.002	-0.002
Root Mean Square	0.315	0.313
Mean Standardized	-0.004	-0.005
Root Mean Square Standardized	0.974	0.967
Average Standard Error	0.325	0.326

Table 3.3 Average activity concentrations and dose rates within the FEZ generated from contaminant maps based on 3 different types of surveys conducted by the Ministry of Education, Culture, Sports, Science, and Technology (MEXT). Surveys include (1) a soil survey conducted in 2011 and subsequently kriged to a resolution of 550, (2) a yearly soil survey interpolated to a resolution of 550 using inverse distance weighting, and (3) yearly airborne surveys.

Study Year	**2011 Soil Survey** Activity Concentration ($kBq \cdot kg^{-1}$)		**Yearly Soil Survey** Activity Concentration ($kBq \cdot kg^{-1}$)		**Yearly Airborne Survey** Average Dose Rate ($\mu Sv \cdot h^{-1}$)
	Cesium 134	Cesium 137	Cesium 134	Cesium 137	Combined Dose Rates
2015	3.40	14.4	3.16	13.3	2.37
2016	2.43	14.1	2.32	13.7	1.90
2017	1.74	13.8	2.41	18.2	1.72
2018	1.24	13.5	1.70	17.7	1.51

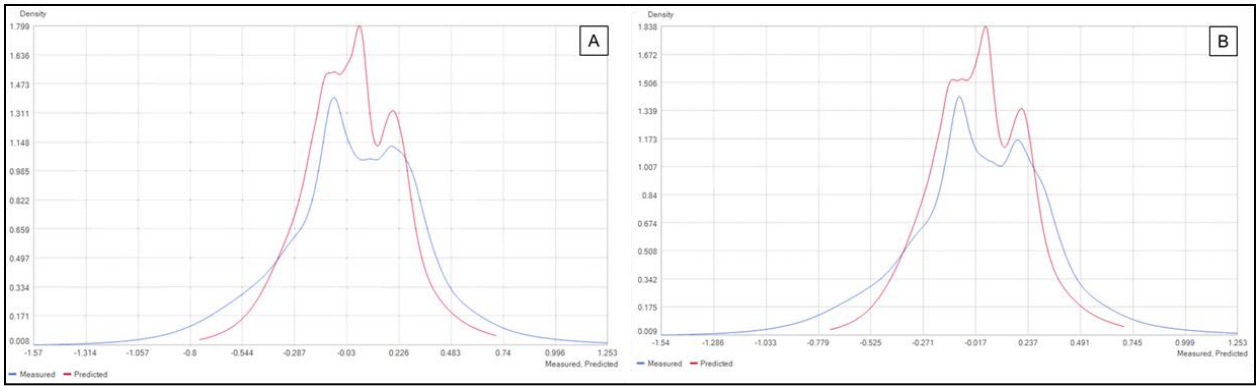

Figure 3.1 Distribution of measured (blue) compared to predicted (red) residuals following leave-one-out cross validation of two kriged surfaces produced using regression kriging by ArcGIS Pro (version 2.9.0); each residual is the difference between 2011 deposition densities of ^{134}Cs and ^{137}Cs within 5 kilometers of the Fukushima Exclusion Zone and those predicted using two generalized linear models.

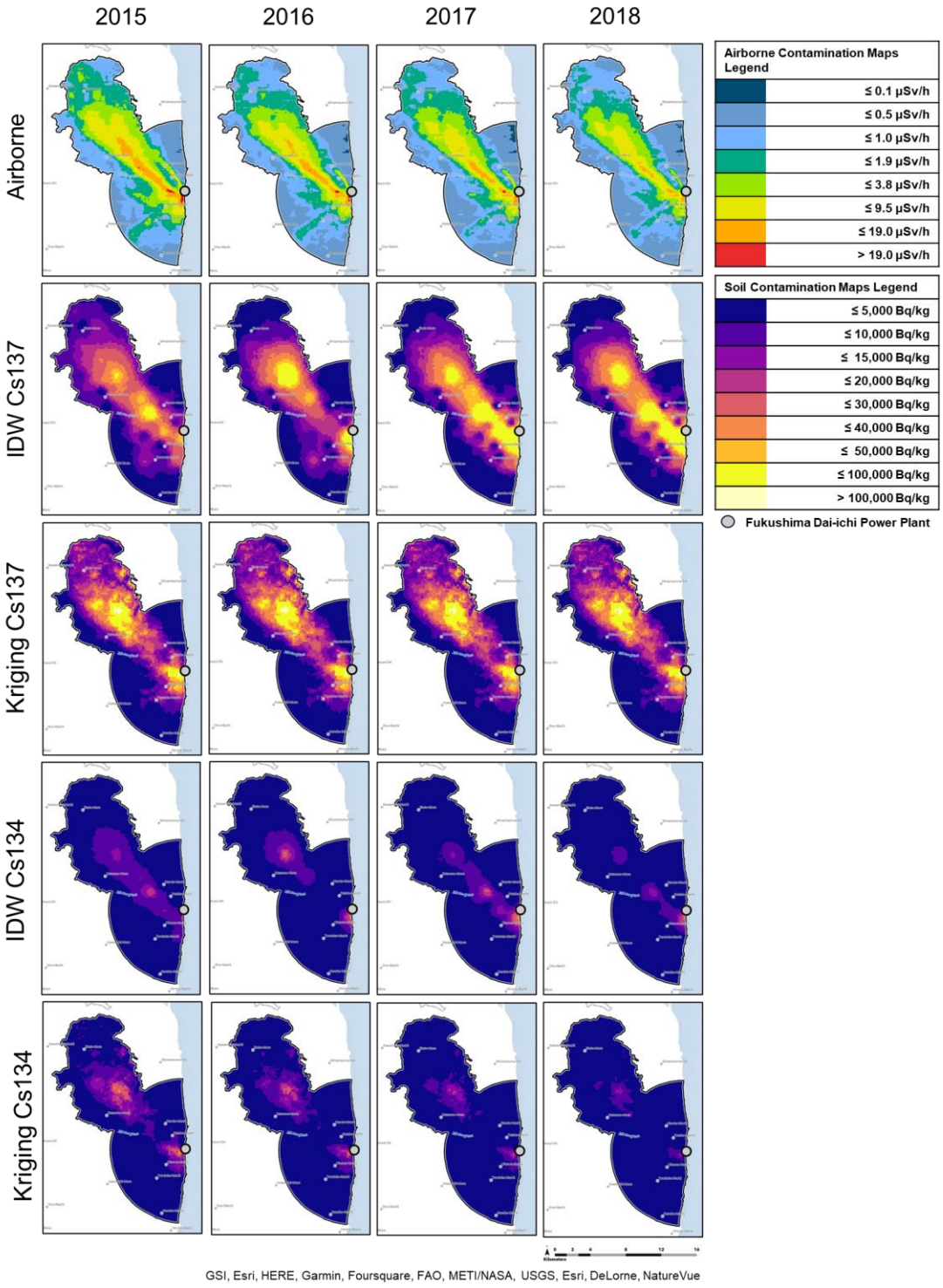

Figure 3.2 Dose rates and radioactive contamination within the Fukushima Exclusion Zone generated using three types of surveys across four study years: yearly airborne surveys conducted by the Ministry of Education, Culture, Sports, Science, and Technology (MEXT), yearly soil surveys conducted by MEXT and interpolated using inverse distance weighting (IDW), and a kriged and decay corrected soil survey conducted by MEXT in 2011.

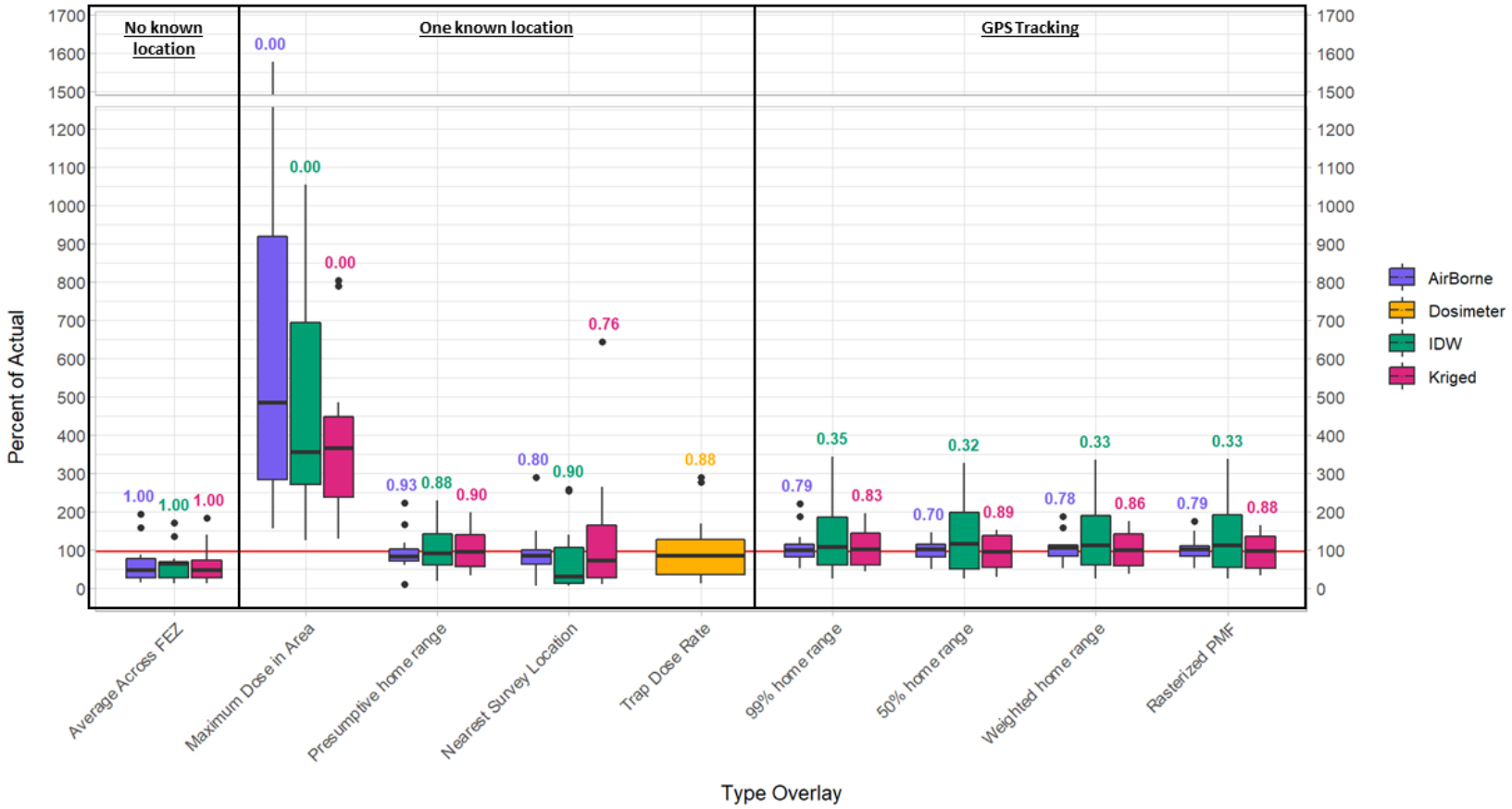

Figure 3.3 Visualization of the conservativeness of methods for estimating external exposure. Box-plot of the percent of actual external exposure each external exposure estimate represents, estimates over 100 represent a conservative estimate. Box upper and lower boundaries correspond to 25th and 75th percentiles. Upper and lower whiskers correspond to the largest and lowest values within 1.5 * inter-quartile range of the box boundaries. Outliers are plotted as points. Numbers above each boxplot represent the p-values from a paired one tailed t-test where the null hypothesis is that estimated external exposures will be less than or equal to the actual exposures and the alternative hypothesis is that estimated external exposures are greater than actual exposures.

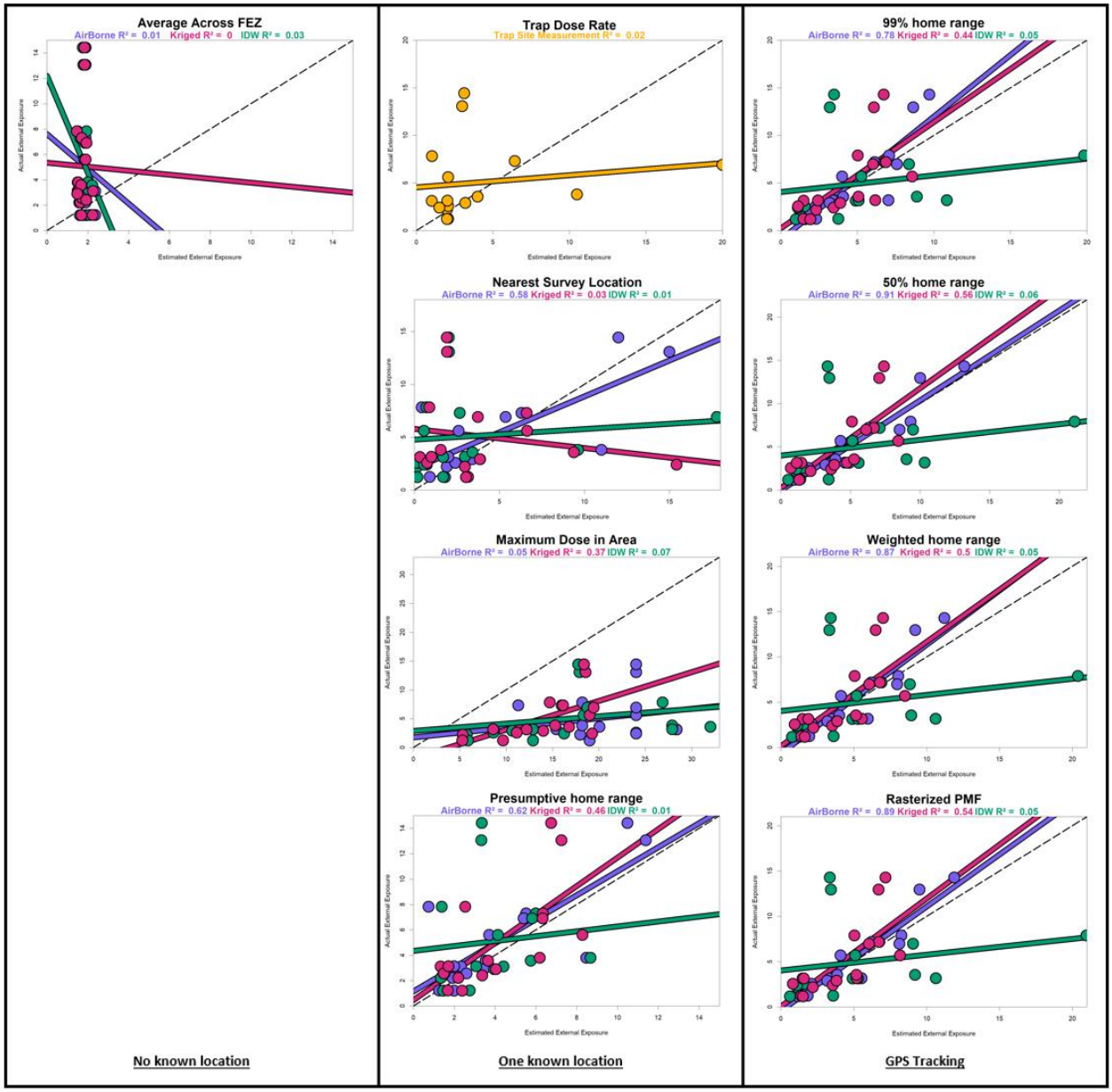

Figure 3.4 Visualization of the realism of different methods for estimating external exposure. Regression plots of estimated external exposures ($\mu Gy \cdot h^{-1}$), generated using 9 different methods of estimating external exposure, compared to actual external exposures (obtained from GPS-monitors on individual boar) with corresponding coefficients of determination.

CHAPTER 4

CONCLUSIONS

Understanding if and how contamination events impact wildlife is an important aspect of both risk assessments and of monitoring ecosystem health. In the case of the Fukushima Dai-ichi Nuclear Power Plant accident, these impacts are not limited to those caused directly by contaminants but also by the removal of humans from a large section of land for an extended period. Thus, the FEZ provides an opportunity to study how wildlife respond to both contaminant exposure and a rewilding event. In this thesis, I quantified resource selection of wild boar within the FEZ, with a sub-focus on how wild boar are utilizing abandoned anthropogenic spaces. I also used a combination of GPS data and radiological surveys to assess various methods of estimating external radiation exposure, with an emphasis on examining how differences in sampling scale may impact the realism and conservativeness of external exposure estimates. Results from this thesis have direct implications for both those working within the FEZ to prepare areas for resettlement and those interested in obtaining estimates of contaminant exposure and conducting risk assessment surveys for free ranging wildlife across the globe.

In Chapter 2, I investigated the resource selection of wild boar in and around the Fukushima Exclusion Zone. I generated 95% home ranges for 34 wild boar based on autocorrelated kernel density estimates. I compared resources available within those home ranges to those available in a buffered MCP surrounding recorded GPS collar locations (2^{nd} order resource selection) and to those overlapping the actual GPS collar locations (3^{rd} order resource selection). Overall, I found that, in addition to using natural areas like forests, wild boar living in and around the FEZ also utilized anthropogenic areas like urban spaces and paddy fields. Specifically, I observed that paddy fields and deciduous forests were selected for across scales,

sex, and seasons. This supports previous literature in which paddy fields (Honda 2007, Honda and Sugita 2007) and mast from deciduous forests (Groot Bruinderink et al. 1994, Jędrzejewska et al. 1997, Schley and Roper 2003) were shown to provide desirable food resources for wild boar. Deciduous forests also provide cover for both thermoregulation (Kramer et al. 2022) and rearing young (Fernández-Llario 2004). Anthropogenic areas, on the other hand, were selected at both broad and fine scales during spring-summer across sexes and by males during autumn-winter. It is possible that these abandoned anthropogenic areas may provide food in the form of unmanaged orchards or gardens or shelter in the form of abandoned buildings and encroaching shrubland. Together these results have implications for managers preparing the FEZ for resettlement. In particular, the extensive use of former urban areas by wild boar highlights a likely source of human-wildlife conflicts as areas are reopened for resettlement by humans.

In chapter 2, I also investigated temporal trends in boar movement behavior and how those trends differed from wild boar outside the FEZ boundary. I generated Hidden Markov Models and assigned each consecutive location a behavioral state (resting, foraging, traveling). I then compared the frequency distribution of each behavioral state through time. I found that boar within the FEZ were more diurnal than those outside the zone. This supports previous literature in which boar within the FEZ were found to be more diurnal through the use of camera traps (Lyons et al. 2020). Together, these resource selection and temporal behavioral results suggest that wild boar within the FEZ are using the anthropogenic areas made available by the evacuation of humans and have become more diurnal in the absence of human presence.

In chapter 3, I investigated the utility of several methods for estimating external radiation exposure encountered by Japanese wild boar trapped and collared within the FEZ. Varying scales of contaminant heterogeneity were quantified using contaminant maps based on one of three

types of surveys: (1) a fine-scale airborne survey, (2) a coarse but yearly soil survey interpolated using inverse distance weighting, and (3) a moderately extensive soil survey from 2011 interpolated using regression kriging and subsequently decay corrected to the study years. These contaminant surveys were combined with locational overlays based on three levels of known boar locations: (1) no known location, (2) one known location, or (3) many known GPS locations. I predicted that (1) conservative external estimates would be produced when purposefully using maximal model inputs, (2) the average contaminant concentration across the FEZ would not be conservative, and that (3) fine scale contaminant maps combined with more realistic locational overlays would generate the most realistic estimates of radiation exposure.

Supporting prediction 1, I found that the only method which was consistently conservative was the maximum external exposure within a 5-kilometer radius of the trap site. Interestingly, this method was conservative regardless of which contaminant map was used. This result has implications for conducting risk assessments, which utilize conservative estimates of exposure in screening steps (USEPA 1996, DOE 2002, 2019), and suggests that conservative estimates are less sensitive to fine scale contaminant heterogeneity than realistic estimates. This result also supports previous research, which used a similar method to estimate maximum lifetime dose (Pederson et al. 2020).

Supporting prediction 2, I found that using the average contamination level across the contaminated area (i.e., the FEZ) was not a conservative method of estimating exposure. Instead, exposure was generally underestimated using this method. This result supports previous research conducted in Chernobyl, in which the area-weighted mean soil activity density across the Polessie State Radiation Ecology Reserve underestimated the average external exposure of wolves collared with GPS-coupled contaminant monitors within the reserve (Hinton et al. 2019).

This result suggests that the average contamination level across the contaminated area may not be conservative, especially if the contamination event was large enough to encompass entire home-ranges or entire populations, depending on whether the individual or population is the unit of concern.

Supporting prediction 3, I found that that the most realistic estimates of radiation exposure by wild boar were produced by combining locational overlays generated from GPS tracking data with fine-scale airborne contaminant maps. Similarly, I found that methods with only a fine-scale contaminant map or a realistic locational overlay did not perform as well as those with both. For example, contaminant maps made using the coarse yearly soil survey rarely produced estimates which correlated with actual exposures, even when combined with the most realistic GPS locational overlays. Further, locational overlays made without utilizing an individual's tracking data produced less realistic exposure estimates, even when combined with fine-scale airborne surveys; although it should be noted that presumptive home ranges performed well enough to be useable for some dose-effect studies. For example, one of the most common methods for estimating exposure (i.e., dose rate at trap site; Møller and Mousseau 2009, 2013, Lehmann et al. 2016) did not correlate with actual exposure. Together, these results suggest that both fine-scale contaminant heterogeneity and an organism's movement patterns play an important role in determining the actual contaminants they encounter.

Conclusions And Take-Aways

The FEZ, and analogous areas like the Chernobyl Exclusion Zone, provide unique opportunities to explore the intersection of spatial ecology and contaminant exposure science. As re-wilding in these areas continue, it will be increasingly important to understand the impact of re-wilding and of chronic radiation exposure on the species residing within the zone. Such

information is vital for refining effective management techniques and for monitoring wildlife health within contaminated landscapes.

My results suggest that highly adaptable species, like wild boar, may respond to rewilding by utilizing both natural and abandoned anthropogenic areas, depending on the desirability of available resources. Similarly, these species may adjust their temporal activity to use time periods previously occupied by humans. Such information is vital within the FEZ for refining effective management techniques. The confirmation that wild boar use anthropogenic areas extensively highlights potential management concerns in both the protection of property currently abandoned and of potential conflicts in newly resettled areas. Further, Chapter 2's results that boar strongly select for both deciduous forests and paddy fields may assist managers interested in management of the overall FEZ boar population, and not just those utilizing towns, by providing information about areas where trapping would be most optimal.

Results from my research also suggest that fine scale contaminant heterogeneity plays a significant role in determining the actual exposure an organism encounters. Thus, more realistic exposure estimates may be generated by accounting for the fine scale heterogeneity an organism might encounter through both more extensive contaminant surveys and through more realistic models of an organism's spatial usage (i.e., home range, core area, presumptive home range, etc.). Conservative estimates, on the other hand, seem to be much less susceptible to the impacts of fine scale heterogeneity and can be generated with significantly less information about both an organism's location and contaminant distribution. Thus, initial risk assessments following a contamination event can be conducted with significantly less work than would be needed for dose-effect studies.

Collectively, the findings of this thesis have implications for both managers currently working in the FEZ as well as individuals interested in obtaining conservative or realistic exposure estimates. Further, these chapters expand on previously published literature about the intersection of spatial and radioecology, presenting opportunities to further explore the intersection of these areas of science in more detail in the future. For example, future research could further integrate fine-scale movement behavior and resource selection of organisms to further increase the realism of exposure estimates.

References

DOE (U.S. Department of Energy). 2002. A Graded Approach for Evaluating Radiation Doses to Aquatic and Terrestrial Biota. DOE-STD-1153-2002. Standard, U.S. Department of Energy, Washington, DC 20585.

DOE (U.S. Department of Energy). 2019. A Graded Approach for Evaluating Radiation Doses to Aquatic and Terrestrial Biota. DOE-STD-1153-2019. U.S. Department of Energy, Washington, DC 20585.

Fernández-Llario, P. 2004. Environmental correlates of nest site selection by wild boar Sus scrofa. Acta Theriologica 49:383–392.

Groot Bruinderink, G. W. T. A., E. Hazebroek, and H. Van Der Voot. 1994. Diet and condition of wild boar, Sus scrofu scrofu, without supplementary feeding. Journal of Zoology 233:631–648.

Hinton, T. G., M. E. Byrne, S. C. Webster, C. N. Love, D. Broggio, F. Trompier, D. Shamovich, S. Horloogin, S. L. Lance, J. Brown, M. Dowdall, and J. C. Beasley. 2019. GPS-coupled contaminant monitors on free-ranging Chernobyl wolves challenge a fundamental assumption in exposure assessments. Environment International 133:105152.

Honda, T. 2007. Factors Affecting Crop Damage by Wild Boar: The Analysis Using Census Data of Agriculture and Forestry. Journal of the Japanese Forest Society 89:249–252.

Honda, T., and M. Sugita. 2007. Environmental factors affecting damage by wild boars (Sus scrofa) to rice fields in Yamanashi Prefecture, central Japan. Mammal Study 32:173–176.

Jędrzejewska, B., W. Jędrzejewski, A. N. Bunevich, L. Miłkowski, and Z. A. Krasiński. 1997. Factors shaping population densities and increase rates of ungulates in Bialowieza Primeval Forest (Poland and Belarus) in the 19th and 20th centuries. Acta Theriologica 42:399–451.

Kramer, C. J., M. R. Boudreau, R. S. Miller, R. Powers, K. C. VerCauteren, and R. K. Brook. 2022. Summer habitat use and movements of invasive wild pigs (Sus scrofa) in Canadian agro-ecosystems. Canadian Journal of Zoology 100:494–506.

Lehmann, P., Z. Boratyński, T. Mappes, T. A. Mousseau, and A. P. Møller. 2016. Fitness costs of increased cataract frequency and cumulative radiation dose in natural mammalian populations from Chernobyl. Scientific Reports 6:19974.

Lyons, P. C., K. Okuda, M. T. Hamilton, T. G. Hinton, and J. C. Beasley. 2020. Rewilding of Fukushima's human evacuation zone. Frontiers in Ecology and the Environment 18:127–134.

Møller, A. P., and T. A. Mousseau. 2009. Reduced abundance of insects and spiders linked to radiation at Chernobyl 20 years after the accident. Biology Letters 5:356–359.

Møller, A. P., and T. A. Mousseau. 2013. Assessing effects of radiation on abundance of mammals and predator–prey interactions in Chernobyl using tracks in the snow. Ecological Indicators 26:112–116.

Pederson, S. L., M. C. Li Puma, J. M. Hayes, K. Okuda, C. M. Reilly, J. C. Beasley, L. C. Li Puma, T. G. Hinton, T. E. Johnson, and K. S. Freeman. 2020. Effects of chronic low-dose radiation on cataract prevalence and characterization in wild boar (Sus scrofa) from Fukushima, Japan. Scientific Reports 10:4055.

Schley, L., and T. J. Roper. 2003. Diet of wild boar Sus scrofa in Western Europe, with particular reference to consumption of agricultural crops. Mammal Review 33:43–56.

USEPA (U.S. Environmental Protection Agency). 1996. Soil Screening Guidance: User's Guide. EPA/540/R-96/018. United States Environmental Protection Agency Office of Soil Waste and Emergency Response, Washington, DC 20460.